

**EMERGENT GRAVITY PHENOMENA IN ACCRETING
ASTROPHYSICAL SYSTEMS**

By
SATADAL DATTA
PHYS08201205004

Harish-Chandra Research Institute, Allahabad

A thesis submitted to the
Board of Studies in Physical Sciences
In partial fulfillment of requirements
for the Degree of
DOCTOR OF PHILOSOPHY
of
HOMI BHABHA NATIONAL INSTITUTE



October, 2019

Homi Bhabha National Institute¹

Recommendations of the Viva Voce Committee

As members of the Viva Voce Committee, we certify that we have read the dissertation prepared by Satadal Datta entitled "Emergent Gravity Phenomena in Accreting Astrophysical Systems" and recommend that it may be accepted as fulfilling the thesis requirement for the award of Degree of Doctor of Philosophy.

Chairman - Prof. Pinaki Majumdar

Date:



20/1/20

Guide /Convener - Prof. Tapas Kumar Das

Date:



20/1/2020

Co-Guide -

Date:



20/1/2020

Examiner - Prof. Jayanta K. Bhattacharjee

Date:



20/01/2020

Member 1 - Prof. Ujjwal Sen

Date:

Member 2 - Prof. Santosh Kumar Rai

Date:



20/1/2020

Member 3 - Prof. S. Naik

Date:



20/1/20

Final approval and acceptance of this thesis is contingent upon the candidate's submission of the final copies of the thesis to HBNI.

I/We hereby certify that I/we have read this thesis prepared under my/our direction and recommend that it may be accepted as fulfilling the thesis requirement.

Date: 20.01.2020

Place: Prayagraj



Prof. Tapas Kumar Das
Guide

¹ This page is to be included only for final submission after successful completion of viva voce.

STATEMENT BY AUTHOR

This dissertation has been submitted in partial fulfillment of requirements for an advanced degree at Homi Bhabha National Institute (HBNI) and is deposited in the Library to be made available to borrowers under rules of the HBNI.

Brief quotations from this dissertation are allowable without special permission, provided that accurate acknowledgement of source is made. Requests for permission for extended quotation from or reproduction of this manuscript in whole or in part may be granted by the Competent Authority of HBNI when in his or her judgment the proposed use of the material is in the interests of scholarship. In all other instances, however, permission must be obtained from the author.



Satadal Datta

DECLARATION

I, hereby declare that the investigation presented in the thesis has been carried out by me. The work is original and has not been submitted earlier as a whole or in part for a degree / diploma at this or any other Institution / University.



Satadal Datta

List of Publications arising from the thesis

Journal

1. “Bondi flow revisited”, Satadal Datta, *Astrophysics and Space Science*, **2016**, *361*, 1-15.
2. “Acoustic geometry obtained through the perturbation of Bernoulli’s constant”, Satadal Datta, Md. Arif Shaikh and Tapas Kumar Das, *New Astronomy*, **2018**, *63*, 65-74.

Preprint

1. “Lagrangian Description in the context of Emergent Spacetime”, Satadal Datta and Tapas Kumar Das, *arXiv:1910.06768 [gr-qc]*, **2019**.
2. “Instabilities in nonrelativistic spherically symmetric self-gravitating accretion”, Satadal Datta, *arXiv:1902.00359 [astro-ph.HE]*, **2019**.

Conferences

1. “Bondi Flow Revisited”, XXXV Meeting of Astronomical Society of India (ASI), India (<http://astronsoc.in/asi2017/>), 6th-10th March, 2017. (Poster Presentation).
2. “Acoustic geometry obtained through the perturbation of the Bernoulli’s constant”, 29th meeting of the Indian Association for General Relativity and Gravitation (IAGRG), India ([http://www.iitg.ernet.in/18th-20th May, 2017](http://www.iitg.ernet.in/18th-20th%20May%202017/)) (Poster Presentation).
3. “Analogue tachyon in Jeans Cloud”, XXXVI Meeting of Astronomical Society of India (ASI), India (<http://astronsoc.in/asi2018/>), February, 2018 (Poster Presentation).
4. Attended, International Workshop on Bose-Einstein Condensation and related phenomena (IWBECP), March 2018.

Others

1. "Acoustic Analogue of Gravitational Wave", Satadal Datta, *Phys. Rev. D*, **2018**, 98, 1-17.

2. "Analogue tachyon in Jeans Cloud", Satadal Datta, *arXiv:1707.03284 [astro-ph.HE]*, **2017**.

3. "Amplitude death by delay induced in system of two coupled Van der Pol Oscillators", Satadal Datta, *arXiv:1709.09909 [nlin.CD]*, **2017**.

4. "A parametric model to study mass radius relationship of stars", Safiqul Islam, Satadal Datta and Tapas Kumar Das, *Pramana J-Phys*, **2019**, 92, 1-15.

5. "Bifurcations of a Van der Pol Oscillator in a double well", Satadal Datta, *arXiv:1709.10126 [nlin.CD]*, **2017**.



Satadal Datta

DEDICATION

*Dedicated to my parents Narayan Chandra Datta and Madhumita Datta,
my sister Rimjhim,
my Physics teacher Prof. Tilak Sinha,
my very good friend Arijit da,
my inspiration Lionel Messi and my favourite modern composer Ludovico Einaudi*

ACKNOWLEDGEMENTS

I would like to express my gratitude to my PhD supervisor, Prof. Tapas Kumar Das. I am very thankful to him for introducing me to the very interesting topic of Physics, analogue gravity in the context of accretion astrophysics. It is also worth mentioning that he has given me immense freedom to learn and explore new topics of Physics which are even disconnected to the subject of my PhD topic. Thus, I can strongly say that due to him, I have got some real taste of doing research in Physics. Other than academics, in several occasions, he has even helped me personally as a friend, I am immensely grateful to him. I am thankful to my PhD supervisor's amazing daughter Bobo for making me nostalgic about my school days and making some busy days colourful with her jolly presence. I am very thankful to the Professors who have sincerely taken classes during the course work. Prof. Rajesh Gopakumar taught us Classical Mechanics, that was a wonderful course to follow, I enjoyed that thoroughly. I would like to sincerely thank Prof. Arun K. Pati, Prof. Jayanta Kumar Bhattacharjee, Prof. G. Venketeswara Pai, Prof. Ashoke Sen for their wonderful courses. I would like to sincerely thank Prof. Pinaki Majumder, I learned a lot from him during the small project under the supervision of him. I am very thankful to Prof. Jayanta Kumar Bhattacharjee, I have really enjoyed working with him on Nonlinear Dynamics. I am very thankful to the colleagues in our Astrophysics group; Arif, Safiqul da, Pratik da, Susovan, Nandan da, Arpan da, Karan, Priti di. I am thankful to some visiting students in our group too. I thank Pratik da for his sincere advice in several occasions and for making some hours magnificent with his songs. Ohh what a magnificent voice he has! I am thankful to Hrishikesh, Pathikrit, Ishika, Priyanka, Soumyadeep, Sanhita, Sanchari, Subhadip, Sanya. I have learnt many things from them too.

About administration and technical section, I am thankful to Archana Ma'am, Sanjeev, Rachna Ma'am, Chandan, Ravi for sincerely helping me in several occasions.

I am very thankful to the mess workers, the guest house workers and the workers in the pantry. I specially thank to Shiv ji, he really cooks with passion. I am thankful to the security guards for making us feel safe in the campus. I am thankful to the members in electrical and engineering

section. I am thankful to all the gardeners for making the campus beautiful. For their immense hard work and labour, the campus looks so beautiful with flowers during Spring.

I am thankful to the students of Harsha school. I have enjoyed teaching them and I have learnt many things from them too.

Now it is the turn to thank my fellow HRI mates with whom I have spent some beautiful years of my life in HRI. When I joined HRI, that was the first time I was away from my home, away from my family. I was really sad and felt lonely in the beginning, but after sometime, I came to the realization that the institute was homely due to friendly atmosphere. This was only possible because of my friends (including batch mate, senior fellows, junior fellows and HRI residents). I can never forget them. Here the list goes on: Dibya da, Arijit da, Pallab da, Bibek da, Debasis da, Tarat da, Paromita di, Sudipto da, Soumyarup da, Jaya di, Gupto da, Jayita di, Titas, Arif, Juhi, Ankur, Bidisha, Harshant, Subhronel da, Nandan da, Sankha da, Hijbool, Arpan, Alam, Ratul (both Banerjee and Mahanta), Sohail, Sankha, Nirnoy, Susovan, Arnab, Arpan da, Saptarshi, Sreetama, Dipyaman, Subhojit, Masuda da, Sauri da, Aditya da, Yogesswar da, Manjuri di, Nilay da, Subho da, Swapno da, Sarif vai, Samiran da, Manikandan, Siddharth, Kasinath, Bhuwanesh, Pramod, Samrat, Kornikar, Tanmoy, Pradeep da, Mithun da. I have always appreciated and enjoyed the sense of humour of Dibya da. I have learnt a lot from my classmate Ankur. Titas is a funny guy and cool in problem solving, I have really enjoyed friendship with him. I have really enjoyed the midnight 'adda' and discussions in the institute guest house with Sudipto da, Jayita di, Debasis da, Subhronel da, Indrani di, Nirnoy, Sankha, Pallab da, Nilay da, Subho da, Alam vai. I have always enjoyed the short walk which I usually take after dinner with my close friends Dibya da, Sudipto da, Debasis da, Ritobrata, Jayita di, Arnab, Arpan da, Arijit da and the list goes on again! Very recently, while I was busy in writing my thesis, the Linux operating system in my laptop stopped working. Surprisingly, I did not have back up! It was completely my fault. Arijit da helped me in recovering the files and thus he literally saved the thesis! I have no words to express my gratitude to him. This is how my friends have always been there. I am thankful to them from my heart. I sincerely thank Arnab, Bhuwanesh, Arif; they have helped me during the submission of my synopsis documents. I thank Rachna Ma'am for helping me out with the official procedures regarding

thesis submission. I sincerely thank Jayita di for her advice on several occasions, she is truly inspiring. I am thankful to my table tennis fellows too; Arnab, Arpan da, Arijit da, Jayita di, Saptarshi, Dibya da, Subhronel da, Soumyarup da. I sincerely thank Sankha da for his tutorial course and for his valuable advice regarding my postdoc applications. I have also enjoyed the adventurous walk in the institute jungle with Arpan da at night. There are so many moments, so many incidents, so many stories with my friends that it seems impossible to write all those things within a short passage, it is impossible to describe in words too. In short, my HRI life have been eventful in so many ways, and most importantly, I have never felt lonely due to my friends. I am thankful that I have got some amazing friends at HRI.

I am forever grateful to my parents and my amazing sister 'Kung fu Panda' for their support throughout my academic carrier.

Contents

SUMMARY	1
List of Figures	3
List of Tables	7
1 Introduction	9
1.1 Gravity, Space-Time Geometry	9
1.2 Analogue model of spacetime geometry	14
1.2.1 Physical Acoustics	14
1.2.2 General features of the acoustic metric	17
1.2.3 Geometrical Acoustics	20
1.3 Structure of the thesis	24
2 Analogue gravity in the light of Lagrangian Description	27
2.1 Lagrangian Description of Fluid Motion	28
2.2 Linear Perturbations	29
2.3 Coordinate Transformation	31
3 Accretion models, steady state solutions	35
3.1 Accretion Models	37
3.1.1 Spherically Symmetric Accretion	38
3.1.2 Axially Symmetric Accretion	38
3.2 Gravitational field in the accretion models:	39

3.3	Barotropic equation	42
3.4	General Formalism	42
3.4.1	Fluid equations for conical adiabatic flow	43
3.4.2	On the nature of transonic solution	46
4	Linear perturbation in the Bernoulli's constant, emergent spacetime	49
4.1	Acoustic gravity in non-relativistic framework	50
4.1.1	General procedure to obtain the acoustic metric	51
4.1.2	Spherically symmetric radial flow	54
4.1.3	Axially symmetric sub-keplerian disk geometries	55
4.1.4	Vertical equilibrium disk accretion	55
4.1.5	Constant height disk accretion	57
4.2	Acoustic gravity in curved space-time background	58
4.2.1	Spherically symmetric radial flow	59
4.2.2	Axially symmetric disk flow	61
4.3	Astrophysical significance	67
4.3.1	Standing wave analysis	68
4.3.2	Travelling wave analysis	71
4.4	Summary and Concluding Remarks	73
5	Steady State Transonic Solution of self-gravitating spherically symmetric accretion	77
5.1	Governing Equations	78
5.2	Calculations of Critical Point of the flow	79
5.3	Equation of motion of the infalling fluid	81
5.4	The Method of iteration	83
5.5	The limits of the integrals	84
5.6	Physical Importance of Q1 and Q2	86
5.7	Behaviour of the critical parameters	86
5.8	Ambiguity of the velocity gradient	93
5.9	Mach number vs radial distance profile	94

5.10	Validity of Iteration Method	95
5.11	Behaviour in relatively higher values of s	99
5.12	Isothermal Flow	101
5.12.1	About isothermal flow	101
5.12.2	Critical Parameters	103
5.12.3	Equation of Motion	104
5.12.4	The limits of the integrals	104
5.12.5	Changes in Critical parameters	105
5.13	Role of self-gravity	107
5.14	Relation between f, g, h	109
5.15	Summary and Conclusions	110
6	Instabilities in nonrelativistic spherically symmetric self-gravitating accretion	113
6.1	Spherically symmetric self-gravitating accretion model	114
6.2	Linear perturbation in the system	114
6.3	Linear Stability Analysis of stationary solution	117
6.3.1	Standing Wave	118
6.3.2	Radially Travelling Wave	119
7	Lagrangian description for accreting astrophysical systems	123
7.1	Introduction	123
7.2	Astrophysical accretion model	124
7.3	Estimation of the wavelength of the perturbation	125
7.4	Conical Adiabatic Flow	125
7.5	Numerical Estimation of the wavelength	128
7.5.1	Variation with the spin parameter of the pseudo-Newtonian potential	134
8	Further scopes and Discussions	137
	Bibliography	141

SUMMARY

Unruh's work in 1981 [1] opens the field of analogue gravity. If an inviscid barotropic fluid medium in motion, satisfying irrotationality condition, is perturbed (creation of sound wave), the governing equation of the sound wave has similarities with massless scalar field in a curved spacetime; analogies with even the spacetime near black hole horizon can be found. The sound wave in the medium is not a wave in the real curved space-time rather the behaviour of the sound wave in a medium can be compared to (described as) a massless scalar field propagation in curved space-time whereas the metric component of the corresponding spacetime are functions of background fluid density and velocity, i.e. it is like a propagating wave in a curved acoustic spacetime which is embedded in a flat background spacetime for Newtonian description of fluid dynamics. This is an emergent phenomena and the corresponding spacetime metric is named as acoustic metric. Hence, by configuring the background flow, several varieties of space-time geometries can be simulated. The phenomena is called an emergent phenomena because we find the spacetime geometry from the fluid equations, the second order partial differential equation (wave equation) is structurally similar to the massless scalar field equation in curved spacetime. One can also call it simulated spacetime because this is not the spacetime in the real world, this spacetime (the spacetime metric depends on the fluid density, velocity etc), mimicking curved spacetime in the real world, is modelled to describe the behaviour of linear perturbation in the medium. One of the interesting spacetime arising in General Theory of Relativity, is the spacetime near black hole event horizon. Transonic flows give rise to emergent spacetime which is similar to spacetime near black hole horizon, named as 'dumb hole' horizon (because sound is involved in the emergent phenomena) [2]-[6]. Such sonic geometry contains an acoustic horizon from where Hawking like radiation may be produced. We particularly investigate the barotropic condition of the fluid (a necessary condition for such emergent phenomena to happen) in details by using Lagrangian Perturbation Theory (LPT) [7], [8]. Astrophysical accretion can be thought of as natural system where such emergent phenomena can be observed.

Accreting black hole is the only system found in the universe where both type of horizons, gravitational as well as acoustic, can be formed. Hence theoretically if one is interested to

compare the properties of these two types of horizons, accreting black holes may be considered as the best candidate to study the sonic geometry embedded within it. In usual analogue models, the gravitational field does not play any role while formulating the corresponding sonic geometry. For accretion onto astrophysical black holes (for accretion onto any compact massive astrophysical objects in general), the gravity determines the dynamics of the fluid and hence the associated acoustic spacetime itself is influenced by the gravitational field. Therefore, for accretion onto blackhole, the actual spacetime with a event horizon influences the flow of the medium, hence the ‘dumb hole’ horizon (location and the metric corresponding to the acoustic spacetime) depends on the background space time. Considering such analogue system with such two horizons has mainly two advantages, one is that such accretion models, describe accretion phenomena which are ubiquitous in nature and secondly, we will see that these systems are dynamically very interesting (flows become supersonic with multiple critical sonic points). We choose to work with accretion models where the flow of accreting medium is inviscid, irrotational and barotropic. Spherically symmetric accretion [9], sub-keplerian disk accretion [10]-[34] of barotropic fluid medium satisfies such conditions. We specifically choose such accretion models where the conditions referred to the physical acoustics are satisfied to obtain the Lorentzian metric from the wave equation. We extend our analysis to consider the gravitational effect of the mass of the medium by studying spherically symmetric transonic accretion under Newtonian gravity. We consider the growth of the accretor itself to be negligibly small within a reasonable timescale of observation. A novel iterative method is introduced to accomplish that task of finding steady state solution in such a case.

If we look at the phenomena from the reference frame of an observer moving with the background velocity (with the velocity of the steady state solution), Eikonal wave (wave of short wavelength in the geometrical acoustic limit) [36], [5] propagates (within a short distance around the observer) like wave in a uniform static medium. Therefore, in the neighbourhood of that observer, the emergent gravity of the acoustic spacetime is absent. Hence the reference frame of the observer sitting in the comoving frame of the background flow is similar to local inertial frame [37] in General relativity.

List of Figures

1.1	A moving fluid will tip the ‘sound cones’ as it moves. Supersonic flow will tip the sound cones past the vertical. This figure is taken from [5].	24
3.1	The parameter space, the figure is taken from the work [73].	46
5.1	Behaviour of percentage change in x_b where $f = -(Dx/x_b) \times 100$ and $Dx = (x_c - x_b)$	87
5.2	Projection of the surface of Fig. 5.1 for $s=1$ on $(-Dx/x_b) \times 100 - \gamma$ plane.	87
5.3	Projection of the surface of Fig. 5.1 for $s=1$ on $(-Dx/x_b) \times 100 - E$ (in log scale) plane.	87
5.4	Behaviour of percentage change in z_b where $g = (Dz/z_b) \times 100$ and $Dz = (z_c - z_b)$	88
5.5	Projection of the surface of Fig. 5.4 for $s=1$ on $(Dz/z_b) \times 100 - \gamma$ plane.	89
5.6	Behaviour of percentage change in λ_b where $h = (D\lambda/\lambda_b) \times 100$ and $D\lambda = (\lambda_c - \lambda_b)$ according to equation (5.13).	89
5.7	Projection of the surface of Fig. 5.6 for $s=1$ on $(D\lambda/\lambda_b) \times 100 - \gamma$ plane.	89
5.8	Dependence of percentage change in x_b on s and data points are fitted. We choose upper limit of s to be 5.	90
5.9	Dependence of percentage change in z_b on s	91
5.10	Dependence of percentage change in λ_b on s	91
5.11	Dependence of percentage change in λ_b on α	92
5.12	The data points are fitted to the curve $a\alpha^3 + b\alpha^2 + c\alpha + d$	92
5.13	$\frac{q_1}{q}, \frac{q_2}{q}$ are plotted against γ with $s=3$ for comparison.	94
5.14	Mach number vs radial distance profile where mass of the Main-Sequence star is 1 solar mass, γ of the fluid is 1.41 and $s=3$	94

5.15	Close view near transonic surface. δr denotes the shift in radius of transonic surface in km.	95
5.16	Dependence of potential energy ratio due to medium and the star at the critical point x_c for different s and γ	96
5.17	Dependence of gravitational force ratio due to medium and the star at the critical point x_c for different s and γ . αI_{1c} is denoted by $\frac{M_c}{M}$	97
5.18	Dependence of density of fluid at infinity on s . Density of the medium at infinity is more or less same for a particular s for different γ	97
5.19	$\frac{x_i}{x_\infty}$ is plotted against s . $\frac{x_i}{x_\infty}$ does not have any γ and E dependence.	98
5.20	$\frac{x_i}{x_b}$ is plotted against s for different γ	99
5.21	$\frac{\psi_{med}}{\psi_{star}}$ is plotted against f for $\gamma=1.41$. The areas under the discrete lines are shaded to distinguish the behaviour in several ranges of s	101
5.22	Percentage change in radius of transonic surface, $f=\frac{x_c-x_b}{x_b} \times 100$	105
5.23	Percentage change in accretion rate, $h=\frac{\lambda_c-\lambda_b}{\lambda_b} \times 100$ is fitted with a curve.	106
5.24	Variations of $\frac{\psi_{med}}{\psi_{star}} \times 10^3$ and h in different ranges of s . The areas under the discrete lines are shaded to distinguish the behaviour in several ranges of s	107
7.1	Background speed variation (top) and variation in l (bottom). Region in the parameter space: region with single critical point relatively away from the accretor.	129
7.2	Background speed variation (top) and variation in l (bottom). Region in the parameter space: region with single critical point situated relatively away from the accretor.	130
7.3	Background speed variation (top) and variation in l (bottom). Region in the parameter space: region with three critical points, transonic accretion curve passing through the farthest (from the accretor) critical point. Formation of sharp peaks at the turning points in the figure of $l - r$ variation.	131
7.4	Background speed variation (top) and variation in l (bottom). Region in the parameter space: region with three critical points, transonic accretion curve passing through the nearest (from the accretor) critical point. Formation of sharp peaks at the turning points in the figure of $l - r$ variation.	132

7.5	Background speed variation (top) and variation in l (bottom). Region in the parameter space: region with single critical point situated near the accretor. . .	133
7.6	$\frac{1}{ q }$ vs λ , region: accretion curve passing through the critical point situated away from the accretor (top) and $\frac{1}{ q }$ vs λ , region: accretion curve passing through the critical point situated near the accretor (bottom).	134
7.7	$\frac{1}{ q }$ vs λ , region: accretion curve passing through the critical point situated away from the accretor; the curves corresponding to different values of a stop at different λ because that's the end of this kind of region in the parameter space (top) and $\frac{1}{ q }$ vs λ , region: accretion curve passing through the critical point situated near the accretor; the curves corresponding to different values of a start at different λ because that's the beginning of this kind of region (which is again the end of the mentioned region in the top figure) in the parameter space (bottom). .	135

List of Tables

5.1 Variation with s	100
----------------------------------	-----

Chapter 1

Introduction

In this chapter, we discuss about the basics and preliminaries about the subject analogue gravity. This chapter provides the basic building blocks for the relatively advanced notions and applications discussed in the next chapters.

1.1 Gravity, Space-Time Geometry

Newton's theory of gravitation [37] could not explain certain astrophysical phenomena observed experimentally (e.g. precession of the perihelion of Mercury). In 1915, Einstein came up with a new theory, so called General theory of relativity. This theory of gravitation has been successful so far i.e., it is found compatible with up to date experimental evidences. Due to the equality of inertial mass and gravitational mass [37], there arises the Principle of Equivalence. Principle of Equivalence states that at any point in spacetime we can construct a locally inertial coordinate system in which the matter satisfies the laws of special relativity, i.e., in such a coordinate system, in the near vicinity of the point in spacetime, the effect of gravity is absent. For example, a freely falling observer in the Earth's gravitational field feels no gravity, i.e., that freely falling observer has no way of determining the effect of gravity from the relative motion of bodies in the near neighbourhood (because the bodies in the near vicinity of that observer has same acceleration because of the Earth's gravity, due to the equality of inertial mass and gravitational mass). In this new theory, in stead of considering gravity as a force, gravity is considered as space-time geometry [37]-[39]. Space and time are treated in equal footing (three spatial

dimension with an additional special dimension which is time, i.e., 3 + 1D). In the absence of gravity, the spacetime is flat, i.e., the corresponding spacetime metric is Minkowskian, given by

$$ds^2 = \eta_{\mu\nu} dx^\mu dx^\nu \quad (1.1)$$

where, Greek indices run from 0 – 3, while Roman indices run from 1 – 3. Then, introducing (3 + 1)-dimensional space-time coordinates, which we write as $x^\mu \equiv (t; x^i)$ and

$$\eta_{\mu\nu} \equiv \begin{bmatrix} -c^2 & 0 & 0 & 0 \\ 0 & 1 & 0 & 0 \\ 0 & 0 & 1 & 0 \\ 0 & 0 & 0 & 1 \end{bmatrix}, \quad (1.2)$$

where c is the speed of light in vacuum.

Therefore, according to the Principle of Equivalence, thus any spacetime under gravity locally resembles to Minkowski spacetime, thus spacetime is a manifold. Therefore, in such a manifold, the notion of spacetime distance, i.e. the line element or the spacetime metric is given by

$$ds^2 = g_{\mu\nu}(x) dx^\mu dx^\nu \quad (1.3)$$

where $g_{\mu\nu}(x)$ is a symmetric second rank covariant tensor describing the spacetime, x is the spacetime coordinate (t, \mathbf{x}) . Due to symmetric property, in 3 + 1 D, the metric tensor $g_{\mu\nu}$ has ten independent components. According to the Principle of Equivalence, at each point in the spacetime in the laboratory coordinate under gravity, there exists a coordinate transformation (locally inertial coordinate system or freely falling system) such that the metric tensor in the new coordinate system, is reduced to the Minkowski metric and the first derivative of the metric tensor vanishes at that point.

In this spacetime geometry, any particle follows geodesic governed by geodesic equation [37]. Massless particle follows lightlike geodesic ($ds^2 = 0$), massive particle follows timelike geodesic ($ds^2 < 0$).

There exists an alternative version of Principle of Equivalence, known as General Covariance

[37]. It states that physical equations hold in a general gravitational field, if two conditions are satisfied:

1. The equation holds in the absence of gravitation, i.e., it obeys the laws of Special Relativity when in that equation the metric tensor $g_{\mu\nu}$ equals the Minkowski tensor $\eta_{\mu\nu}$ and when the affine connection [37] (a function having first order derivative of $g_{\mu\nu}$) vanishes.
2. The equation is generally covariant, i.e., it preserves its form under general coordinate transformations. General coordinate transformation is defined as a bijective map between two sets of coordinates to describe the spacetime manifold.

Principle of General covariance allows one to treat the quantities appearing in an equation as contravariant tensor, covariant tensor or scalar. Therefore, one can first write down any equation obeying the laws of special relativity in the locally inertial frame of reference and then to obtain the equation under gravity, one has to treat the quantities in that equation like tensors or scalars and make a coordinate transformation to the laboratory coordinate.

For example, equation of a massless scalar field $\phi(t', \mathbf{x}')$, in flat spacetime, is given by

$$\partial'_\mu \partial'^{\mu} \phi(t', \mathbf{x}') = 0. \quad (1.4)$$

where primed notation is used in the locally inertial frame. Now applying Principle of General Covariance, i.e. by treating $\phi(t, \mathbf{x})$ as scalar, ∂'_μ as covariant rank one tensor and ∂'^{μ} as contravariant rank one tensor, we get the desired equation of a massless scalar field (in minimal coupling [38]) under gravity (by coordinate transformation from locally inertial frame to unprimed laboratory frame),

$$D_\mu D^\mu \phi(t, \mathbf{x}) = \frac{1}{\sqrt{-g}} \partial_\mu (\sqrt{-g} g^{\mu\nu} \partial_\nu) \phi(x) = 0, \quad (1.5)$$

where D_μ is the covariant derivative [37].

Therefore, gravity can be viewed as spacetime geometry, but what causes spacetime geometry or gravity? Einstein field equations answer the question. It relates energy and momentum tensor to the metric, given by

$$R_{\mu\nu} - \frac{1}{2} g_{\mu\nu} R = -\frac{8\pi G}{c^4} T_{\mu\nu}, \quad (1.6)$$

where $R_{\mu\nu}$ is Ricci tensor, R is Ricci scalar [37], $T_{\mu\nu}$ is energy momentum tensor and G is universal gravitational constant.

This is a second order nonlinear differential equation in metric tensor.

Solution of Einstein's field equations give rise to interesting spacetime geometry, for example black hole spacetime. This is actually one of the most striking proposals of Albert Einstein's general theory of relativity.

The most general solution of Einstein's equation which represents a stationary (metric components are independent of time), static and isotropic gravitational field (in vacuum) due to a central mass M , is the Schwarzschild solution, given by (in metric form)

$$ds^2 = -c^2 \left(1 - \frac{2GM}{c^2 r}\right) dt^2 + \left(1 - \frac{2GM}{c^2 r}\right)^{-1} dr^2 + r^2 d\Omega^2 \quad (1.7)$$

where r is the spherical polar coordinate, $d\Omega^2 = (d\theta^2 + \sin^2\theta d\phi^2)$, with θ and ϕ being polar angle and azimuth angle. The coordinate (t, r, θ, ϕ) in which the metric is written, is called the Schwarzschild coordinate and the frame of reference which they form is called the Schwarzschild reference frame [39]. The metric is asymptotically flat far from the centre of gravity ($r \rightarrow \infty$).

$r = r_g = \frac{2GM}{c^2}$, is called Schwarzschild radius. g_{tt} changes sign at this radius leading to the singularity in the flow of time, because the physical time interval $d\tau = \left(1 - \frac{2GM}{c^2 r}\right)^{\frac{1}{2}} dt$ or in other words, the worldline of an observer sitting at a fixed point in space, i.e, at constant r , θ and constant ϕ ceases to be timelike at this radius. It is also worth mentioning that at this radius, the free fall acceleration becomes infinity [39]. As light follows lightlike geodesic, therefore, one can show that if a light is emitted from $r = r_g$, it will take an infinite amount of time, t to reach any point at greater radius [39]. At radius less than r_g , motion of any body (massive or massless) becomes unidirectional, i.e, towards the singularity ($r = 0$); thus r_g is identified as event horizon because photon can not escape black hole from radius less than r_g .

Any infinitesimal translation in spacetime coordinate can be given by (in general)

$$x'^{\mu} = x^{\mu} + \epsilon \xi^{\mu}(x). \quad (1.8)$$

The infinitesimal translation vector ξ^μ for which the metric preserves its functional form, i.e. $g'_{\mu\nu}(x') = g_{\mu\nu}(x')$, is called killing vector of that metric. The surface in the spacetime where the norm of the killing vector becomes zero, is defined as the boundary of the ergo region, and the region where the killing vector is spacelike, is defined as the ergo region. As the metric is stationary, i.e., the metric is invariant in form under time translation, giving rise to generator of the symmetry, Killing vector [37], $\xi_{(t)}^\mu = (1, 0, 0, 0)$. The killing vector becomes spacelike (as g_{tt} changes sign at $r = r_g$) at radius less than r_g , therefore $r = r_g$ is the boundary of the ergo region, i.e., ergo sphere [39], or the static limit surface. Therefore, in the case of Schwarzschild black hole, the radius of ergo sphere coincides with the radius of event horizon.

This conclusion, can be drawn in another way. A Schwarzschild black hole in this coordinate is not only stationary, but also it has an additional symmetry, i.e., the time reversal symmetry. For $t \rightarrow -t$, the acoustic metric is invariant, therefore, Schwarzschild black hole represents a static spacetime. According to the theorem by Hawking et al [39], the killing horizon (the radius of ergo sphere) coincides with event horizon for stationary static black hole.

If an acoustic metric does not have the time reversal symmetry (due to cross time with dt), one needs to write down the metric in a new coordinate where it takes the form (where the time and space does not mix with each other):

$$ds^2 = -V^2 dt^2 + h_{ij} dx^i dx^j. \quad (1.9)$$

Now, if the black hole is stationary (V and h_{ij} are independent of t ; one can redefine time of course if V only depends on t to make g_{00} component time independent), the black hole is static [39].

There are also other kind of black holes (e.g. non-static stationary black hole). For brevity and according to the relevance of our thesis, we restrict ourselves to the Schwarzschild black hole.

There are limitations in the General Theory of Relativity too. A black hole forms when a massive star runs out of the fuel needed to balance out gravity, and collapses under its own gravity to a point; thus General relativity predicts that the star collapses to an infinitely small point with infinite density. Such a thing does not really exist in the real world because it contradicts the quantum theories. The appearance of a black hole singularity in general relativity simply indi-

cates that general relativity is inaccurate at very small sizes. One needs quantum field theoretic description to analyse gravity in small length scales, but gravity turns out to be non renormalizable. There is limitation in large length scale (cosmological length scale) too, the problem of accelerating expansion of universe (dark energy in that context) is still not quite understood [37].

1.2 Analogue model of spacetime geometry

William Unruh published the first modern paper on analogue gravity [1]. It is then followed by Matt Visser [2][3][4]. It was nicely showed that the effective propagation of sound waves in a fluid flow is given in terms of geodesics in an acoustic “spacetime geometry”. Since then many works have been done on the topic, now commonly referred to as “Analogue Gravity” [5]. We discuss here briefly about the subject relevant for thesis. We also mention the lines and the paragraphs in this chapter which refers the other chapters in the thesis in *italics* for the convenience of the readers. The contents of this section are mostly followed from the review article on analogue gravity [5].

1.2.1 Physical Acoustics

In non-relativistic fluid dynamics, in the case of inviscid flow, mass conservation equation and the momentum conservation equation for fluid are given by [40] (according to Newton’s laws of dynamics) determine the flow.

The continuity equation of fluid is given by

$$\frac{\partial \rho}{\partial t} + \nabla \cdot (\rho \mathbf{v}) = 0 \quad (1.10)$$

where ρ, \mathbf{v} are fluid density and velocity respectively, and these quantities depend on \mathbf{x} and t in general. Euler momentum equation for inviscid flow in an external field in general is given by

$$\frac{\partial \mathbf{v}}{\partial t} + \mathbf{v} \cdot \nabla \mathbf{v} = -\nabla \psi - \frac{\nabla p}{\rho}, \quad (1.11)$$

where the potential function of the external conservative field is ψ and pressure at any point of the fluid is p .

The flow is taken to be vorticity free, i.e, locally irrotational,

$$\nabla \times \mathbf{v} = 0 \quad (1.12)$$

$$\Rightarrow \mathbf{v} = -\nabla\Psi, \quad (1.13)$$

where Ψ is velocity potential. The flow is assumed to be barotropic, i.e., $p = p(\rho)$. *In the next chapter, we will discuss about barotropic and irrotationality condition in details.*

Sound speed c_s is given by

$$c_s^2 = \frac{dp}{d\rho} \quad (1.14)$$

Now let's assume we have a known solution as background flow, i.e., density is ρ_0 , velocity of moving medium is \mathbf{v}_0 and sound speed is c_{s0} . We now find the propagation of sound over such background flow. Sound is defined as linear perturbation in density and velocity [5], therefore, we have

$$\mathbf{v}(\mathbf{x}, t) = \mathbf{v}_0 + \mathbf{v}'(\mathbf{x}, t)$$

$$\rho(\mathbf{x}, t) = \rho_0 + \rho'(\mathbf{x}, t)$$

In the review [5], they have used a slightly different notation for perturbation. *We have discussed about the perturbation over such velocity and density field in the next chapter in details and also from a different point of view.* ρ_0 and \mathbf{v}_0 are functions of space and time in general. Therefore,

$$\Psi = \Psi_0 + \Psi'. \quad (1.15)$$

After some manipulations, one gets,

$$\partial_\mu (f^{\mu\nu} \partial_\nu) \Psi'(\mathbf{x}, t) = 0 \quad (1.16)$$

where $f^{\mu\nu}$ in Cartesian coordinate is given by

$$f^{\mu\nu} = \frac{\rho_0}{c_{s0}^2} \begin{bmatrix} -1 & \vdots & -v_0^j \\ \dots & \dots & \dots \\ -v_0^j & \vdots & c_{s0}^2 \delta^{ij} - v_0^i v_0^j \end{bmatrix} \quad (1.17)$$

where i, j run over 1, 2, 3 representing three spatial dimensions.

The equation 1.16 represents a wave equation of the linear perturbation of the velocity potential. *In chapter 4, we will be discussing about wave equation of astrophysically more relevant quantities.* Comparing equation 1.16 with equation 1.5

$$f^{\mu\nu} = \sqrt{-g} g^{\mu\nu} \quad (1.18)$$

Immediately one can get

$$\det(f^{\mu\nu}) = (\sqrt{-g})^4 g^{-1} = g = -\frac{\rho_0^4}{c_{s0}^2} \quad (1.19)$$

So $g^{\mu\nu}$ is given by

$$g^{\mu\nu} = \frac{1}{\rho_0 c_{s0}} \begin{bmatrix} -1 & \vdots & -v_0^j \\ \dots & \dots & \dots \\ -v_0^j & \vdots & c_{s0}^2 \delta^{ij} - v_0^i v_0^j \end{bmatrix} \quad (1.20)$$

The acoustic metric is

$$g_{\mu\nu} = \frac{\rho_0}{c_{s0}} \begin{bmatrix} -(c_{s0}^2 - v_0^2) & \vdots & -v_0^j \\ \dots & \dots & \dots \\ -v_0^j & \vdots & \delta_{ij} \end{bmatrix} \quad (1.21)$$

Acoustic metric interval can be expressed as

$$ds^2 = \frac{\rho_0}{c_{s0}} [-(c_{s0}^2 - v_0^2)dt^2 - 2dt\mathbf{v}_0 \cdot d\mathbf{x} + d\mathbf{x}^2] \quad (1.22)$$

where v_0 is the magnitude of the vector, \mathbf{v}_0 .

1.2.2 General features of the acoustic metric

Lorentzian nature: If the background medium is static (non moving), i.e., the acoustic metric resembles the Minkowski metric with two exceptions. One is that there is a conformal factor in front of it and also the sound speed appears in the acoustic metric in stead of speed of light. Here sound speed plays the role of light speed. The signature of this effective metric is indeed $(-, +, +, +)$, as it should be to be regarded as Lorentzian.

If the background medium has zero velocity at infinity, the acoustic metric represents analogue of asymptotically flat spacetime, just like Schwarzschild black hole in Schwarzschild reference frame is asymptotically flat, Kerr black hole in Boyer-Lindquist coordinate is asymptotically flat. *We will be considering the transonic accretion in certain astrophysical models where the accretion flow is assumed to have zero speed (chapter 3 and chapter 5) at very large distance, therefore, the acoustic metric in our coordinate is asymptotically flat.*

An emergent phenomena: We begin with the non-relativistic fluid equations, time and space are absolute according to Newtonian notions [41], but surprisingly, the linear perturbation (sound) in the medium mimics the massless scalar field equation in a curved spacetime. Therefore, the sound ‘feels’ a curved spacetime (the acoustic metric) just like a massless scalar field in a real curved spacetime would have ‘felt’ the curvature of real spacetime. That is why this phenomena is an emergent phenomena and the acoustic spacetime associated with it can also be called emergent spacetime.

Acoustic Horizon: If we assume the flow of the background medium to be steady ($\rho_0 = \rho_0(\mathbf{x})$, $\mathbf{v}_0 = \mathbf{v}_0(\mathbf{x})$ and $c_{s0} = c_{s0}(\mathbf{x})$), the acoustic metric in equation 1.22 becomes stationary. From equation 1.22, one can define a proper time and conclude that the world line of a time like observer sitting at a fixed position (\mathbf{x}) in space becomes space like in the region/s where $v_0 > c_{s0}$ (if there exists such supersonic region/s of flow within the background medium). According to the discussion in section 1.1, time translation symmetry in stationary spacetime gives rise to killing vector, whose norm changes as g_{tt} changes sign. Therefore, the region of flow where $v_0 > c_{s0}$ is identified as the ergo region of the analogue spacetime and the surface where $v_0 = c_{s0}$ can be identified as static limit surface or ergo sphere or killing horizon of the emergent spacetime.

The acoustic metric (equation 1.22) does not have time reversal symmetry, therefore, we make

a coordinate transformation to make it structurally similar to equation 1.9:

$$d\tau = dt + \frac{\mathbf{v}_0 \cdot d\mathbf{x}}{c_{s0}^2 - v_0^2}. \quad (1.23)$$

Now if the second term in the right hand side is integrable, the coordinate transformation from the old time coordinate t to the new time coordinate τ is valid (existence of a bijective map between two new coordinate system). Therefore the integrability condition implies that the second term on the right hand side $\left(= \frac{\mathbf{v}_0 \cdot d\mathbf{x}}{c_{s0}^2 - v_0^2}\right)$ can be written as $\nabla \mathcal{F} \cdot d\mathbf{x}$, where $\mathcal{F} = \mathcal{F}(\mathbf{x})$; we have in this new coordinate system

$$ds^2 = \frac{\rho_0}{c_{s0}} \left[-(c_{s0}^2 - v_0^2) d\tau^2 + \left\{ \delta_{ij} + \frac{v_0^i v_0^j}{c_{s0}^2 - v_0^2} \right\} dx^i dx^j \right]. \quad (1.24)$$

In this new coordinate, (similar to form 1.9), the metric is stationary with time reversal symmetry. Therefore, the acoustic metric is static in this coordinate. Therefore, for an acoustic metric to be static the transformation 1.23 needs to exist. Therefore, for a background flow, producing the emergent spacetime effect, the corresponding spacetime is static if

$$\nabla \times \left(\frac{\mathbf{v}_0}{c_{s0}^2 - v_0^2} \right) = 0 \Rightarrow \mathbf{v}_0 \times \nabla (c_{s0}^2 - v_0^2) = 0 \quad (\because \nabla \times \mathbf{v}_0 = 0) \quad (1.25)$$

As we have discussed already that for static stationary spacetime, the killing horizon is the event horizon. Therefore for a transonic flow (the background flow has both subsonic and supersonic region), if due to symmetry, equation 1.25 is satisfied, the emergent spacetime is static and similar to Schwarzschild spacetime 1.7 and the surface where the speed of the background medium equals the speed of sound, is the analogue of event horizon, i.e., the acoustic horizon. *We consider the accretion models where due to the symmetry of the background medium (spherical symmetry and axial symmetry) and due to the symmetry of the linear perturbation (the linear perturbations also possess the same symmetry as the background flow, for example axially symmetric linear perturbation in axially symmetric background flow), the condition 1.25 is satisfied. Therefore, we limit ourselves in static emergent spacetime.* Thus the assumption of symmetry is important in producing emergent space-time similar to Schwarzschild black hole.

For example, a static spherically symmetric (the background density, velocity, sound speed only depend on the radial distance from the sink) radially ingoing transonic flow, automatically satisfying condition 1.25, gives rise to acoustic horizon similar to horizon of a Schwarzschild black hole. It is worth mentioning that for rotational fluid, in general the local irrotationality condition may not be satisfied. Carefully choosing designing the background flow, one can simulate black hole spacetime and even Kerr spacetime is suggested to be simulated in the literature [135]. As the flow is transonic (say at $r = R$ the ingoing accelerating flow surpasses the thermodynamic sound speed), linear perturbation in the supersonic region of the flow can not propagate upstream across that radius to enter the subsonic region of flow. Sound message can not be sent from the supersonic region of flow (within radius R) to the subsonic region of flow ($r > R$). In this way, analogy with the black hole event horizon can be drawn through the behaviour of a linear perturbation near $r = R$ (for more details, see [1]). In the case of real spacetime, the propagation of light is influenced by the spacetime curvature created by the energy-matter distribution. In the analogue model, the propagation of sound is influenced by the variation of the speed of a moving medium.

The role of background medium: The acoustic metric components depend on the background medium, i.e, on the known solution of the flow over which we examine the linear perturbation. Therefore, by carefully designing the known background solutions, one can realize different interesting spacetime geometries; for example white hole spacetime, spacetime similar to Kerr spacetime in general relativity can be mimicked by different flow geometries [5]. In our thesis, we focus on astrophysical accretion models to produce such emergent effect. *Stationary solutions (known solution or background solution) of such astrophysical accretion models are discussed in chapter 3 and in chapter 5 (for self-gravitating spherically symmetric nonrelativistic accretion).*

General Covariance: In the case of analogue models of gravity, there is no analogous Einstein equation 1.6 to begin with. Therefore, the analogue models of gravity give the half of the picture of general relativity, only the kinematic picture not the dynamic picture. We have the fluid equations: the continuity equation and the momentum equation in the Newtonian framework, where time is universal and space is absolute in sense. Two inertial reference frames

are related via Galilean transformation. *In the next section, we will use Galilean coordinate transformation.* The fluid equations do not transform in a covariant way. The fluid systems, we are talking about, have a privileged coordinate system and each component of the acoustic metric has physical meaning, for example; density, velocity of the background medium, appearing in the acoustic metric. For example fluid density is a scalar field, bulk velocity describes the displacement of a fluid element in background flow per unit amount of Newtonian universal time. Fluid velocity is a vector under certain coordinate transformations (e.g. rotation in space, Galilean transformation etc). Thermodynamic sound speed is a scalar quantity. That is why the components in the acoustic metric do not transform in a covariant way under general coordinate transformation. This is not the case in the general relativistic context where the metric component has no physical meaning rather the metric components merely represents the coordinate system, i.e, treated as rank 2 tensors. Therefore, we do not expect diffeomorphism invariance or general covariance in the context of analogue gravity (for more details, see ‘diffeomorphism invariance’ section in [5]). Therefore, in all analogue models, the background flow is designed to mimic a real spacetime geometry in curved spacetime written in a particular coordinate system. For example, a transonic radially inward spherically symmetric flow, near the critical radius (the radius where $v_0 = c_{s0}$) produces the acoustic analogue of Schwarzschild spacetime in the Schwarzschild reference frame.

1.2.3 Geometrical Acoustics

Sound is treated as ray instead of a wave in the geometrical acoustics. The physical difference between wave and ray is that wave has the tendency to spread over in space (the nature of diffraction) but ray only follows a particular path (a curve in general) in space. This is quite similar to the discussion between wave nature and particle nature in Quantum Mechanics. Rays are defined as lines such that tangent to them at any point in space gives the direction of propagation of it’s phase. We know from the laws of diffraction that ideally if the wavelength of a wave is assumed to be zero then there is no diffraction. In the zero wavelength limit, resolution of an image (in case of light) is infinite. This limit of very short wavelength is the geometrical limit where the ray nature is a very good approximation.

As we have discussed in the section 1.1, that massless particle follows lightlike geodesic ($ds^2 = 0$). Now, we are asking that whether sound, satisfying wave equation 1.16, follow the acoustic analogue of lightlike geodesic ($ds^2 = 0$ where ds^2 is the acoustic metric) or not. For $ds^2 = 0$ between two neighbouring points in the spacetime, sound (linear perturbation) has to propagate in a certain direction, here the geometrical acoustics (short wavelength-high frequency limit) becomes useful. Although the limitation is that the wavelength of the sound is always much greater than the mean free path of the constituent particles. Ultrashort wavelengths modify the dispersion relation [136]-[140]. Therefore, we use basic equation for determining the direction of rays, by writing

$$\Psi' = ae^{i\phi}, \quad (1.26)$$

where the amplitude a is slowly varying function of spacetime coordinate, and the phase ϕ is called eikonal. This approximation is called Eikonal approximation [42]. The intensity (energy flux) of a steady ray never diminishes with distance (because it does not get diffracted) as it travels in space, that is why a is assumed to be a slowly varying function of spacetime coordinate. The wave vector, having the direction perpendicular to the constant ϕ surface at fixed time t , is given by

$$\mathbf{k} = \frac{\partial \phi(\mathbf{x}, t)}{\partial \mathbf{x}}. \quad (1.27)$$

Angular frequency ω is defined as

$$\omega = -\frac{\partial \phi}{\partial t}. \quad (1.28)$$

We can write the above expressions in tensor notation as

$$k_\mu = \nabla_\mu \phi, \quad (1.29)$$

where $k_0 = \frac{\partial \phi}{\partial t} = -\omega$ and $k_i \equiv \mathbf{k} = \nabla \phi(\mathbf{x}, t)$. Therefore, over a short distance from a point in space at an instant of time, the wavefront (the surface over which the phase is constant) of a ray is a plane. The normal to that constant phase surface at that point represents the direction of the ray at that instant of time. Hence, the eikonal wave, having high frequency (or short wavelength), is insensitive to the variation $f^{\mu\nu}$ within short distance in short time around a point

in spacetime. Using the above expression of linear perturbation in velocity potential in the wave equation 1.16, we find by equating the real and imaginary part:

$$k_\mu k^\mu = 0 \quad (1.30)$$

$$\partial_\mu k^\mu = 0. \quad (1.31)$$

where $k^\mu = h^{\mu\nu} k_\nu$, $h_{\mu\nu}$ are components of the acoustic metric without the conformal factor in front of them, because equation 1.30 and equation 1.31 does not depend on the overall conformal factor due to the insensitivity of the eikonal wave on the variation of density and overall conformal factor in front of the physical acoustic metric. Therefore, we write down $h_{\mu\nu}$ and $h^{\mu\nu}$ as

$$h_{\mu\nu} = \begin{bmatrix} -(c_{s0}^2 - v_0^2) & \vdots & -v_0^j \\ \dots & \dots & \dots \\ -v_0^j & \vdots & \delta_{ij} \end{bmatrix}, \quad (1.32)$$

$$h^{\mu\nu} = \frac{1}{c_{s0}^2} \begin{bmatrix} -1 & \vdots & -v_0^j \\ \dots & \dots & \dots \\ -v_0^j & \vdots & c_{s0}^2 \delta^{ij} - v_0^i v_0^j \end{bmatrix}. \quad (1.33)$$

With the above expressions in mind, equation 1.30 refers to the dispersion relation of sound wave in high frequency-short wavelength limit (Eikonal approximation). Therefore, we find after some manipulation:

$$\omega = \pm c_{s0} k + \mathbf{v}_0 \cdot \mathbf{k} \quad (1.34)$$

where $k = |\mathbf{k}|$. We work with the ‘+’ sign in the above equation because in a static medium, $\omega = c_{s0} k$. The above equation is the dispersion relation of the wave in eikonal limit. ω is linear in k due to the Lorentzian nature of the wave equation 1.16. *We will see violation of the Lorentzian invariance in the chapter 7 where the dispersion relation is modified because the gravity of the medium is taken into account.* The first term in the right hand side is due to the Doppler effect (because of moving background medium). This term vanishes if the speed of the background medium tends to zero, where the emergent spacetime is analogous to Minkowskii spacetime.

Now using equation of rays [42],

$$\dot{x}_i = \frac{\partial \omega}{\partial k_i} \quad (1.35)$$

\dot{x}_i , the i th component of the group velocity of the wave, does not depend on wavelength of the sound, i.e., the medium is dispersive in nature. From the above equation,

$$\frac{d\mathbf{x}}{dt} = c_{s0}\hat{n} + \mathbf{v}_0, \quad (1.36)$$

where \hat{n} is the unit vector along \mathbf{k} . Therefore, we have

$$-(c_{s0}^2 - v_0^2)dt^2 - 2dt\mathbf{v}_0 \cdot d\mathbf{x} + d\mathbf{x}^2 = 0 \quad (1.37)$$

$$\Rightarrow ds^2 = 0. \quad (1.38)$$

Hence in the geometrical acoustics limit, sound follows null geodesic. The line element from equation 1.32, given by

$$ds^2|_{\text{geometric}} = -(c_{s0}^2 - v_0^2)dt^2 - 2\mathbf{v}_0 dt \cdot d\mathbf{x} + d\mathbf{x}^2. \quad (1.39)$$

This is the emergent metric in geometric acoustics regime. The conformal factor does not appear in the metric because null geodesic is insensitive to the conformal factor.

The equation 1.36 can also be derived by directly using Galilean transformation (for more details see [5]). Therefore, in the geometric acoustics limit, one does not even need to consider the wave equation 1.16, i.e, one can start with velocity addition rule by Galilean transformation. Along the downstream the speed of sound in the laboratory reference frame gets added by the speed of the medium and along the upstream, the speed of sound gets subtracted by the speed of the moving medium, illustrated in the figure below;

In the next chapter and in the chapter 7, we are going to make use of the geometrical acoustics.

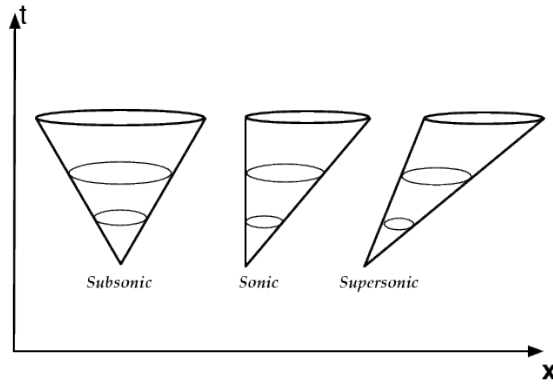


Figure 1.1: A moving fluid will tip the ‘sound cones’ as it moves. Supersonic flow will tip the sound cones past the vertical. This figure is taken from [5].

1.3 Structure of the thesis

We will focus on the nature of perturbation from a different point of view, i.e. the Lagrangian view of perturbation in a fluid and we will make use of such notion to discuss the compatibility between the irrotationality condition and the barotropic condition in a fluid (*chapter 2*). We examine the phenomena from the reference frame of an observer moving with the background flow *in chapter 2*. We discuss again about this issue in astrophysical accretion models for conical flow *in chapter 7*. As we have already discussed that the emergent spacetime metric components depend on the quantities in the background flow, in the case of stationary geometry, the background medium has to be time independent. Hence, the stationary emergent spacetime is designed by the steady state solutions of the continuity equation and the Euler equation. We consider some natural systems; some astrophysical accretion models, and we discuss about steady state accretion solutions in *chapter 3* and in *chapter 6* (the gravity of the moving medium is considered). In *chapter 4*, we discuss about the role of the Bernoulli’s constant in emergent gravity. We generalize the concept that not only the steady state solutions are governed by the integrals of motion (the Bernoulli’s constant and mass accretion rate) but also in the linearised perturbation regime, the linear perturbation does play a crucial role in determining the stability of the steady state solutions. Therefore, the stability analysis not only determines the stability of emergent black hole but also it cross checks the very assumption about the stability of the steady state solutions. In *chapter 6*, we have discussed about the frequency dependence of the

stability due to the inclusion of the gravity of the medium. As we have seen in the geometric acoustics regime that the medium is nondispersive due to the Lorentz invariance of the emergent spacetime, we discuss about the breaking of the Lorentz invariance in *chapter 6* due to inclusion of gravity, i.e, the medium becomes dispersive in nature due to the inclusion of gravity of the medium. Therefore, the whole thesis thoroughly focuses on some details and key issues to find some interestingly beautiful aspects of the subject analogue gravity by considering some astrophysical accretion models as candidate systems available in nature. We work with small perturbations (in linearised order) in adiabatic flows. We assume the perturbations to have the same symmetry as the steady state solution corresponding to the accretion model. The emergent phenomena can also be obtained through the linear perturbation of mass accretion rate [35], i.e., analogue gravity also emerges when accretion rate is perturbed. We've shown that linear perturbation of the Bernoulli's constant which is the integral solution of the corresponding Euler equation, also produces similar acoustic geometry. The analysis of such linear perturbation has astrophysical significance to determine the stability of the steady state solutions. We conclude that not only the integrals of motion of a accretion problem govern the steady state solutions but also govern the time dependent solutions (in linear order) of the fluid quantities. Our main motivation in the thesis is not to simulate artificial/analogue black hole spacetime in laboratory, rather we focus on the behaviour of the linear perturbations over the steady flow of such accretion models. We can not observe an effect connected to surface-gravity/Hawking radiation. Although in the article [75], [146]-[148], the authors have discussed about surface-gravity and existence of Hawking like temperature in sub-Keplarian axisymmetric accretion flow but there is no way to experimentally observe such effect directly. We check the stability of the steady state flow and the validity of the method of linearising density and velocity over the steady state solutions.

Chapter 2

Analogue gravity in the light of Lagrangian Description

We make use of the Lagrangian description of fluid motion to highlight certain features in the context of spacetime geometry as emergent phenomena in fluid systems. We find by using Lagrangian Perturbation Theory (LPT), that not all kind of perturbations on a steady state flow can produce analogue spacetime effect. We make use of Lagrangian description of motion to examine the propagation of Eikonal wave from the reference frame of the observer moving with the background flow. We restrict ourselves to nonrelativistic flows.

In that context of emergent gravity, linear perturbation is introduced on the density field and the velocity field in the flow; the whole approach is done by treating density and velocity as fields which is the essence of Eulerian description of fluid motion. Here we explore the Lagrangian description of motion to describe the phenomena from a different point of view and we use LPT [7], [8] to find certain restrictions on the perturbation itself to mimic massless KG field equation in a curved spacetime. *Just like as before, when we refer other chapters, we use 'italic' font.* The contents of this chapter are mostly from our work on Lagrangian perturbation theory in the field of analogue gravity [118].

2.1 Lagrangian Description of Fluid Motion

In the Lagrangian description of fluid motion [40], instead of using fluid density and velocity as fields, one follows the motion of a fluid element [40]. Inviscid fluid equations in Lagrangian description are given by [40]

$$\frac{d\rho}{dt} + \rho \nabla \cdot \mathbf{v} = 0 \quad (2.1)$$

$$\frac{d\mathbf{v}}{dt} = -\frac{\nabla p}{\rho} - \nabla \psi(\mathbf{x}) \quad (2.2)$$

where ρ , \mathbf{v} , p , ψ are fluid density, velocity, fluid pressure and scalar potential corresponding to external body force respectively. $\frac{d}{dt}$ is Lagrangian time derivative ¹. Lagrangian time derivative is defined as change in some quantity (e.g. density, velocity etc) in unit time while the change is measured in the reference frame of a particle in flow, unlike Eulerian derivative where the rate of change of any quantity is measured from a fixed location. The first equation describes the conservation of mass in a fluid element in motion and the second one describes the equation of motion by Newton's law of motion.

The position coordinate of fluid element is given by $\mathbf{x}(\mathbf{R}, t)$ where $\mathbf{x}(\mathbf{R}, 0) = \mathbf{R}$. The velocity of the element is

$$\dot{\mathbf{x}}(\mathbf{R}, t) = \mathbf{v} \quad (2.3)$$

'Dot' means $\frac{d}{dt}$. Using equation 2.2 and another initial condition on velocity, one can uniquely find the position of a fluid element in the flow as a function of time.

Let us consider a steady flow, i.e. $\frac{\partial(\cdot)}{\partial t} = 0$. In the steady state flow, we denote the pressure field, density field and velocity field by p_0, ρ_0 respectively. The velocity vector of a fluid element, $\mathbf{V}(\mathbf{R}, t)$, satisfies the following equation:

$$\frac{d\mathbf{V}}{dt} = -\frac{\nabla p_0}{\rho_0} - \nabla \psi(\mathbf{x}). \quad (2.4)$$

Position of the fluid element is $\mathbf{X}(t)$ and $\dot{\mathbf{X}}(t) = \mathbf{V}$.

¹Lagrangian time derivative is also denoted by $\frac{D}{Dt}$ in some text books and the literature.

2.2 Linear Perturbations

We introduce linear perturbations in the fluid quantities as follows,

$$p(\mathbf{x}, t) = p_0(\mathbf{x}) + p'(\mathbf{x}, t)$$

$$\rho(\mathbf{x}, t) = \rho_0(\mathbf{x}) + \rho'(\mathbf{x}, t)$$

$$\mathbf{v}(\mathbf{x}, t) = \mathbf{v}_0(\mathbf{x}) + \mathbf{v}'(\mathbf{x}, t)$$

The Eulerian perturbations are denoted by p' , ρ' and \mathbf{v}' in linearised order.

The Lagrangian perturbations in LPT are related to the Eulerian perturbations via another vector field, called Lagrangian displacement, $\delta(\mathbf{x}, t)$. δ represents the displacement of fluid elements in space from their position of equilibrium, $\mathbf{X}(t)$ s. Therefore, Lagrangian perturbation represents the net change in pressure and density of a fluid element under sound propagation. The Lagrangian perturbations in the first order of smallness are given by [7][40]

$$\begin{aligned}\Delta p &= p' + \delta \cdot \nabla p_0 \\ \Delta \rho &= \rho' + \delta \cdot \nabla \rho_0 \\ \Delta \mathbf{v} &= \frac{d\delta}{dt} = \frac{\partial \delta}{\partial t} (= \mathbf{v}'(\mathbf{x}, t)) + \delta \cdot \nabla \mathbf{v}_0\end{aligned}$$

where Δp and $\Delta \rho$ are related by

$$\frac{\Delta p}{p_0} = \gamma \frac{\Delta \rho}{\rho_0} \text{ or } \frac{\Delta p}{\Delta \rho} = c_{s0}^2 \quad (2.5)$$

where c_{s0} is the thermodynamic sound speed in the medium, γ is the specific heat ratios, $\gamma = 1$ if the perturbation is isothermal in nature. For air, sound propagates adiabatically [40], i.e., no heat transfer occurs between adjacent volume elements.

We write inviscid irrotational fluid equations in Eulerian description as

$$\frac{\partial \rho}{\partial t} + \nabla \cdot (\rho \mathbf{v}) = 0 \quad (2.6)$$

$$\frac{\partial \mathbf{v}}{\partial t} + \mathbf{v} \cdot \nabla \mathbf{v} = -\frac{\nabla p}{\rho} - \nabla \psi(\mathbf{x}) \quad (2.7)$$

$$\nabla \times \mathbf{v} = 0 \quad (2.8)$$

Defining velocity potential as $\mathbf{v} = -\nabla \Psi$, we find the Euler equation for the perturbed quantity as

$$-\nabla \frac{\partial \Psi'}{\partial t} + \nabla(\mathbf{v}_0 \cdot \mathbf{v}') = -\frac{\nabla p'}{\rho_0} + \frac{\rho'}{\rho_0^2} \nabla p_0 \quad (2.9)$$

Now from equation 2.5 and from the expression of Lagrangian perturbations,

$$p' = c_{s0}^2 \rho' + \left(c_{s0}^2 - \frac{dp_0}{d\rho_0} \right) \delta \cdot \nabla \rho_0 \quad (2.10)$$

Now if the background medium has different kind of stratification than the nature of perturbation, the term in the right hand side of equation 2.9, would involve an extra quantity δ and the term in the right hand side can not be written as gradient of a quantity, i.e, enthalpy in the perturbed medium can not be defined and as a result the motion would not be irrotational in that case, evident from equation 2.9. For example, let us consider a medium of isothermal stratification and the propagating disturbance to be adiabatic in nature, therefore the sound speed is $c_{s0} = \sqrt{\frac{\gamma p_0}{\rho_0}}$ and $\frac{dp_0}{d\rho_0} = \frac{p_0}{\rho_0} = \frac{1}{\gamma} c_{s0}^2$, the second term in the right hand side, in equation 2.10 does not vanish. Similarly, for isothermal sound propagating in a medium of adiabatic stratification, the same thing happens.

If the back ground medium has same kind of stratification as the nature of disturbance, from equation 2.10,

$$p' = c_{s0}^2 \rho' \quad (2.11)$$

From equation 2.9,

$$\partial_t \Psi' = \mathbf{v}_0 \cdot \mathbf{v}' - \frac{p'}{\rho_0} \quad (2.12)$$

Now after some manipulations one can find the field equation for $\Psi'(\mathbf{x}, t)$; given by

$$\partial_\mu (f^{\mu\nu}(\mathbf{x}) \partial_\nu) \Psi'(\mathbf{x}, t) = 0 \quad (2.13)$$

where

$$f^{\mu\nu}(\mathbf{x}) \equiv \frac{\rho_0}{c_{s0}^2} \begin{bmatrix} -1 & \vdots & -v'^j \\ \dots & \dots & \dots \\ -v'^j & \vdots & c_{s0}^2 \delta^{ij} - v'^i v'^j \end{bmatrix} \quad (2.14)$$

Now comparing with massless scalar field equation in a curved spacetime in general, one can find the analogue acoustic metric by using $f^{\mu\nu} = \sqrt{-g}g^{\mu\nu}$. Then one can write down the acoustic metric as

$$ds^2 = g_{\mu\nu} dx^\mu dx^\nu = \frac{\rho_0}{c_{s0}} \left(-(c_{s0}^2 - v_0^2) dt^2 - 2\mathbf{v}_0 dt \cdot d\mathbf{x} + d\mathbf{x}^2 \right) \quad (2.15)$$

Therefore, the emergent spacetime feature through the perturbations in a steady flow can be realized if and only if the perturbation's nature matches with the stratification of the background medium². Hence the emergent phenomena is restricted to isothermal perturbation in a isothermal background medium or adiabatic perturbation in a adiabatic background medium. Therefore, the flow has to remain barotropic in nature even in the presence of perturbation for the acoustic analogue of spacetime geometry to emerge. Additionally, if the flow is barotropic in nature in the presence of sound, then only the flow will be irrotational.

2.3 Coordinate Transformation

Let's follow the equilibrium position of an element, in the other words, the location of a fluid element in the absence of any disturbance. The equilibrium position vector is denoted by $\mathbf{X}(t)$ in general. Let the equilibrium position of a particular fluid element be denoted $\mathbf{X}(\mathbf{R}, t)$ where $\mathbf{X}(\mathbf{R}, 0) = \mathbf{R}$. This notation indeed uniquely specify a particular fluid which was at \mathbf{R} at $t = 0$; and at a given time two fluid elements can not be in the same position. The velocity is $\mathbf{V}(\mathbf{R}, t) = \dot{\mathbf{X}}(\mathbf{R}, t)$. So far, we have described the motion in a coordinate system (\mathbf{x}, t) which is rest in absolute space [41] or moving with uniform velocity with respect to the absolute space or which is stationary with the source or sink (if exists) of the system; so that Newton's law is valid in the reference frame. Now we try to describe things from the equilibrium position of a particular

²There is another possibility, if the medium is uniform, in that case the emergent spacetime metric is flat; here we are considering the medium to be stratified in general.

fluid element which is accelerating in general due to external body force and pressure imbalance in the system. Coordinate of any point in the system with respect to the new coordinate system is (\mathbf{x}', t') . (\mathbf{x}', t') is related to (\mathbf{x}, t) via Galilean transformation [43], given by

$$\mathbf{x}' = \mathbf{x} - \mathbf{X}(\mathbf{R}, t) = \mathbf{x} - \int^t \mathbf{V}(\mathbf{R}, t) dt - \mathbf{R} \quad (2.16)$$

$$t' = t \quad (2.17)$$

$$\frac{d\mathbf{x}'}{dt'} = \frac{d\mathbf{x}}{dt} - \mathbf{V}(\mathbf{R}, t) \quad (2.18)$$

Therefore, using chain rule of partial derivatives, one can find

$$\frac{\partial}{\partial t} = \frac{\partial}{\partial t'} - \mathbf{V}(\mathbf{R}, t') \cdot \nabla' \quad (2.19)$$

$$\nabla = \nabla' \quad (2.20)$$

As a result, fluid equations, relating the density field and the velocity field, in this new coordinate system³ can be written in Eulerian description as

$$\frac{\partial \rho}{\partial t'} - \mathbf{V}(\mathbf{R}, t') \cdot \nabla' \rho + \nabla' \cdot (\rho \mathbf{v}) = \mathbf{0} \quad (2.21)$$

$$\frac{\partial \mathbf{v}}{\partial t'} + (\mathbf{v} - \mathbf{V}(\mathbf{R}, t')) \cdot \nabla' \mathbf{v} = -\frac{\nabla' p}{\rho} - \nabla' \Psi(\mathbf{x}') \quad (2.22)$$

In our case, the flow is irrotational, therefore

$$\nabla' \times \mathbf{v} = \mathbf{0} \quad (2.23)$$

For the steady flow, $\frac{\partial(\cdot)}{\partial t} = 0$, therefore we have

$$\frac{\partial \rho_0}{\partial t'} - \mathbf{V}(\mathbf{R}, t') \cdot \nabla' \rho_0 = 0 \quad (2.24)$$

$$\Rightarrow \nabla' \cdot (\rho_0 \mathbf{v}_0) = \mathbf{0} \quad (2.25)$$

³The transformation is passive here, it does not change the field rather it changes the coordinate to describe those fields.

$$\frac{\partial \mathbf{v}_0}{\partial t'} - \mathbf{V}(\mathbf{R}, t') \cdot \nabla' \mathbf{v}_0 = 0 \quad (2.26)$$

$$\Rightarrow \mathbf{v}_0 \cdot \nabla' \mathbf{v}_0 = -\frac{\nabla' p_0}{\rho_0} - \nabla' \Psi(\mathbf{x}') \quad (2.27)$$

Therefore, for steady flow the fluid equations (equation 2.25 and equation 2.26) in (\mathbf{x}', t') and (\mathbf{x}, t) are same in form.

Linear Eulerian perturbations over the steady flow are introduced in the fluid system in the (\mathbf{x}, t) coordinate system, the equation for Eulerian perturbation fields in the (\mathbf{x}', t') coordinate system, are given by

$$\frac{\partial \rho'}{\partial t'} - \mathbf{V}(\mathbf{R}, t') \cdot \nabla' \rho' + \nabla' \cdot (\rho' \mathbf{v}_0 + \rho_0 \mathbf{v}') = 0 \quad (2.28)$$

$$\frac{\partial \mathbf{v}'}{\partial t'} + (\mathbf{v}_0 - \mathbf{V}) \cdot \nabla' \mathbf{v}' + \mathbf{v}' \cdot \nabla' \mathbf{v}_0 = -\frac{\nabla' p'}{\rho_0} + \frac{\rho'}{\rho_0^2} \nabla' p_0 \quad (2.29)$$

One can easily see that again by doing coordinate transformation to (\mathbf{x}, t) , one recovers the original equations of the perturbations.

If the nature of perturbation and the stratification of the background medium are of same kind, one can find the emergent spacetime metric in this new coordinate, as follows

$$ds^2 = g_{\mu\nu}(\mathbf{x}', t') dx'^{\mu} dx'^{\nu} = \frac{\rho_0}{c_{s0}} \left(-(c_{s0}^2 - (\mathbf{v}_0 - \mathbf{V})^2) dt'^2 - 2(\mathbf{v}_0 - \mathbf{V}) dt' \cdot d\mathbf{x}' + d\mathbf{x}'^2 \right) \quad (2.30)$$

The metric is no more time independent because (\mathbf{x}', t') frame is moving with respect to (\mathbf{x}, t) frame. The same metric can be directly derived from equation 2.15 and using the above coordinate transformation. Sound wave of very short wavelength, i.e, in the eikonal limit (*discussed in the previous chapter*), follows null geodesic insensitive to the conformal factor, described by the acoustic metric in the geometric limit, given by

$$ds^2|_{\text{geometric}} = \tilde{g}_{\mu\nu}(\mathbf{x}', t') dx'^{\mu} dx'^{\nu} = \left(-(c_{s0}^2 - (\mathbf{v}_0 - \mathbf{V})^2) dt'^2 - 2(\mathbf{v}_0 - \mathbf{V}) dt' \cdot d\mathbf{x}' + d\mathbf{x}'^2 \right) \quad (2.31)$$

with the null geodesic condition, given by

$$ds^2|_{\text{geometric}} = 0. \quad (2.32)$$

As the wavelength of the sound wave is very small, an observer moving with the fluid element can examine the wave within a very short radius around him such that $v_0 \approx \mathbf{V}$. Therefore, the acoustic metric perceived by them in the near vicinity around them will be

$$ds^2|_{\text{geometric}} = -c_{s0}^2 dt'^2 + d\mathbf{x}'^2. \quad (2.33)$$

As the frequency of such wave is very high, within a short period of time, the observer moving with the element, will perceive c_{s0} to be independent of time. Therefore, in the eikonal limit, an observer moving with a fluid element (more precisely moving with the background velocity of the medium), perceives sound in the neighbourhood of him/her as sound moving in a uniform medium. Within, small distance from that observer, the wavefront of the sound wave is not only plane but also does not change orientation, i.e., within short distance of the observer, the sound propagates in a particular direction. This is exactly similar to the principal of equivalence (*discussed in the previous section*) that a falling observer feels no gravity. Therefore, under the above coordinate transformation, in the near vicinity of the fluid element, the emergent spacetime metric corresponds to acoustic analogue of Minkowski spacetime. Now as the fluid element moves in (x, t) spacetime, the above coordinate transformation describes the coordinate transformation to the local inertial frames [37] at $X(R, t)$ at different time. Similarly, in the very near vicinities of different fluid elements in motion, the emergent spacetime is flat. *In chapter 7, we have discussed about the wavelength of such eikonal wave in astrophysical accretion models, and in the next chapter, we will be discussing about accretion models to produce emergent gravity effect.*

Chapter 3

Accretion models, steady state solutions

Except for the supersonic stellar wind fed accretion [44]-[46], accretion flows onto astrophysical black holes are necessarily supersonic [10]. In a binary system, accretion from the wind of a star to the compact accretor (neutron star) can be categorised as wind fed accretion. For low angular momentum accretion with practically constant specific angular momentum, more than one sonic points may form in such flow and a stationary shock may join two such transonic solutions passing through two such sonic points [10]-[34]. The formation of such shocks can be explained through time dependent numerical simulation works [47]-[51]. Such post shock flow can manifest its properties through the characteristic black hole spectra and can help to understand the observational signature of the astrophysical black holes in the universe ([52], [53] and references therein). Such shocked multi-transonic flows are essentially barotropic, inviscid, irrotational transonic fluid flow under the influence of the strong gravitational field in presence of gravitational (black hole) event horizon.

It is, however, to be noted that the characteristic black hole spectra for transonic accretion are usually computed for steady state flow, considering that such steady state is stationary. Time variability and various kind of fluctuations are, however, not very uncommon in large scale astrophysical flows. It is thus imperative to ensure that the steady state integral transonic accretion solutions are stable under perturbation.

In recent years, much attention have been paid to study the analogue gravity phenomena [5], [6], [135] in classical (non quantum), where for a supersonic irrotational inviscid flow governed by a barotropic equation of state, the propagation of the linear acoustic perturbation (sound

wave) within that fluid can be described by acoustic metric and a sonic spacetime can be formed embedded within such stationary background fluid flow ([1]-[6]). Such sonic geometry contains an acoustic horizon from where Hawking like radiation may be produced.

Study of such sonic geometries embedded within the transonic accretion flow can thus be very important to investigate certain novel features of such phenomena. Accreting black holes is the only system found in the universe where both type of horizons, gravitational as well as acoustic, can be formed, and the same fluid can pass through both type of horizons as well. Hence theoretically if one would like to compare the properties of these two types of horizons, accreting black holes may be considered as the best candidate to study the sonic geometry embedded within it. It is also needless to say that the fluid approximation of the accreting medium is a very good approximation [9]. Also, in usual analogue models, the gravitational field does not play any role while formulating the corresponding sonic geometry. For accretion onto astrophysical black holes (for accretion onto any compact massive astrophysical objects in general), the gravity determines the dynamics of the fluid and hence the associated acoustic spacetime itself is influenced by the gravitational field.

For purely classical analogue systems, the detailed analysis of the quantum Hawking like effects may not always be possible to study, however, the study of the acoustic surface gravity can have deep significance in such systems. The acoustic surface gravity itself is a rather crucial entity to understand the flow structure as well as the associated sonic metric, and can thus be studied independently without looking into the existence of any analogue radiation (of phonons) like thermal phenomena characterized by their very feeble temperature too impractical to detect through any present day experimental set up. In recent years, the role of the analogue surface gravity in studying the non negligible effects associated with the emergence of the stimulated Hawking effects has been highlighted by examining such effects through the modified dispersion relations. Such study have been performed from the purely analytical point of view as well as within the experimental set up [54]-[59]. The deviation of the Hawking like effects within a dispersive media [141], i.e., within the fluid under consideration, from the universal behaviour of the original Hawking effect, depends sensitively on the gradient of the background bulk stationary velocity, as it has recently been suggested. It is, however, important to note that such

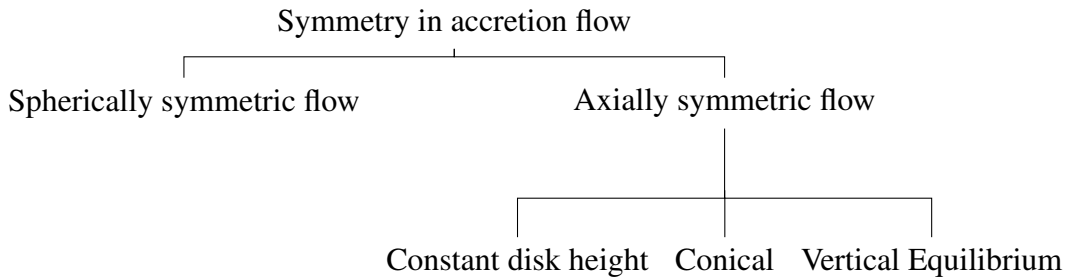
theory of the non universal feature of the Hawking radiation has been postulated essentially for the isothermal flow and hence the space gradient for the sound velocity has not been taken into account. Also, the exact numerical values corresponding to the velocity gradient has not been possible to found yet and has been approximated by making certain assumptions.

For stationary integral accretion solutions as discussed in aforementioned paragraphs, the values of the space gradient of *both* the dynamical flow velocity as well as the speed of propagation of the acoustic perturbation have been computed very accurately using numerical schemes [74], [75], [77], [78], [119], [123], [124]. It is thus obvious that the accreting black hole systems, although may not provide any direct signature of the Hawking like temperature (analogue temperature arising out from the phonon radiation) can still be considered as a very important as well as a unique theoretical construct to study the analogue gravity effects. These accretion models are useful to study analogue gravity because the analytical scheme and numerical techniques to find the density, velocity of the background medium (the quantities to find the acoustic metric) are readily available; these systems are very interesting due to coexistence of the black hole horizon and the ‘dumbhole horizon’.

All accreting matter, just like most of the material in the Universe, is in a gaseous form. The constituent particles, interact directly only by collisions (electromagnetic interaction). If the gas is approximately uniform over lengthscales exceeding a few mean free paths, the effect of all these collisions is to randomize the particle velocities about some mean velocity, the velocity of the gas, v . Viewed in a reference frame moving with a bulk velocity, the particles have a Maxwell-Boltzmann distribution of velocities, and can be described by a temperature T . Now one can consider inviscid flow by using Euler equation to describe such inviscid flow. If the constituent particles do not scatter (for very dilute medium, or dust), the information of some disturbance (mechanical), can not propagate because any particle do not ‘see’ the others.

3.1 Accretion Models

We consider spherically symmetric and axially symmetric flow of fluid onto star or black hole. The accretion flow can be divided into the following classes depending on the symmetry of the flow.



3.1.1 Spherically Symmetric Accretion

Fluid elements (for details about fluid element, see [40]) having zero angular momentum falls freely due to the accretor's gravitational pull. Thus the flow is inviscid and spherically symmetric. *In the next chapter, we are going to analyze the time dependent problem in perturbative way, and we will see how emergent gravity emerge in such flow through perturbation.*

3.1.2 Axially Symmetric Accretion

The inviscid flow assumption requires that the accretion flow is characterized by reasonably low angular momentum. By low angular momentum flow, we mean sub-Keplerian flow. In Keplerian flow, gravitational pull balances with outward body force. Motion of Saturn's ring is an example of Keplerian flow. If the flow is sub-Keplerian, gravity wins against outward body force (pressure gradient and specific angular momentum), and fluid falls onto the accretor [34]. Therefore, low angular momentum axisymmetric blackhole accretion [66], [67] is a good candidate where analogue gravity emerges too [35]. Such weakly rotating sub-Keplerian flows are ubiquitous in nature; such as detached binary systems fed by accretion from OB stellar winds ([60], [61]), semi-detached low-mass non-magnetic binaries ([62]), and super-massive black holes fed by accretion from slowly rotating central stellar clusters ([63] and [64]). In standard Keplerian accretion disc, turbulence sometimes produce such low angular momentum flows too (see, e.g., [65], and references therein).

We don't need to consider viscosity in such weakly rotating sub-Keplerian flows due to low angular momentum of the infalling fluid. There are mainly three disk models for sub-Keplerian disk by categorising them with respect to disk height or thickness H .

1. Constant Height Disk Model: H is taken to be constant in the simplest possible model, i.e., in uniform thickness disk model.

2. Conical Model: In conical model [66] the disk thickness H is proportional to cylindrical radial distance from the accretor.

3. Vertical equilibrium model: In the most physical disk model, i.e., in the vertical equilibrium model [67], [68], the disk height $H(r)$ is a function of cylindrical radial distance r from the accretor such that there is no flow along z direction considering the equatorial plane of the disk to be on the X - Y plane. Disk height is a function of r such that the disk is in hydrostatic equilibrium along z - axis, i.e., there is no flow in the z - direction.

In this type of models, due to symmetry, the problem becomes effectively 1+1 dimensional. In all the cases, there is no flow in the z - direction.

3.2 Gravitational field in the accretion models:

In the nonrelativistic case, the star/accretor, the source of gravity, correspond to the Newtonian gravitational potential, given by,

$$\Phi_0(r) = -\frac{GM_{BH}}{r} \quad (3.1)$$

where r is the radial distance from the accretor, and M_{BH} is the mass of the accretor. By scaling radial distance by $\frac{2GM_{BH}}{c^2}$ and potential (energy) by c^2 , we rewrite, Newtonian potential in the dimensional form as

$$\Phi_0(r) = -\frac{1}{2r} \quad (3.2)$$

Since relativistic effects play an important role in the regions close to the accreting black hole, Newtonian gravity can not be a good description, Newtonian potential is modified. One can avoid relatively more complicated pure general relativistic calculations by introducing such modified potentials, and thus most of the crucial properties of the dynamics of the flow can be retained with high accuracy. Hence, those potentials are named as ‘pseudo-Kerr’ or ‘pseudo-Schwarzschild’ potentials, depending on whether they are used to mimic the spacetime around a rapidly rotating or nonrotating/slowly rotating (Kerr parameter $a \sim 0$) black hole, respectively. Here we introduce such potentials. *The discussions about these potentials are mostly taken from*

the literature [28].

Potential 1:

$$\Phi_1(r) = -\frac{1}{2(r-1)} \quad (3.3)$$

The Keplerian distribution of angular momentum, reproduced by this potential 3.3 [69], is exactly same as that obtained in pure Schwarzschild geometry.

Potential 2: In the literature [70], some of the dominant relativistic effects of the accreting black hole (slowly rotating or nonrotating), are approximated by introducing a modified Newtonian potential which is very useful to study the normal modes of the acoustic oscillations within a thin accretion disk around a compact object (slowly rotating black hole or weakly magnetized neutron star). The potential is given by,

$$\Phi_2(r) = -\frac{1}{2r} \left[1 - \frac{3}{2r} + 12 \left(\frac{1}{2r} \right)^2 \right]. \quad (3.4)$$

Potential 3: Artemova et al. [71] proposed a potential which produces exactly the same value of the free-fall acceleration of a test particle at a given value of r as is obtained for a test particle at rest with respect to the Schwarzschild reference frame and is given by

$$\Phi_3(r) = -1 + \left(1 - \frac{1}{r} \right)^{\frac{1}{2}}. \quad (3.5)$$

Potential 4: Artemova et al. [71] proposed another potential which produces the value of the free-fall acceleration which equals to the covariant component of free-fall acceleration of a test particle in three dimensional space at a given value of r rest with respect to the Schwarzschild reference frame, given by

$$\Phi_4(r) = \frac{1}{2} \ln \left(1 - \frac{1}{r} \right). \quad (3.6)$$

Potential 5 (inclusion of Black hole spin):

$$\Phi_5(r) = \frac{1}{2r_1(1-\beta)} \left[\frac{r^{\beta-1}}{(r-r_1)^{\beta-1}} - 1 \right], \quad (3.7)$$

where

$$r_1 = \frac{1}{2} \left(1 + (1 - a^2)^{\frac{1}{2}} \right) \quad (3.8)$$

$$Z_1 = 1 + (1 - a^2)^{\frac{1}{3}} \left[(1 + a)^{\frac{1}{3}} + (1 - a)^{\frac{1}{3}} \right] \quad (3.9)$$

$$Z_2 = (3a^2 + Z_1^2)^{\frac{1}{2}} \quad (3.10)$$

$$r_{in} = \frac{3 + Z_2 - [(3 - Z_1)(3 + Z_1 + 2Z_2)]^{\frac{1}{2}}}{2} \quad (3.11)$$

$$\beta = \frac{r_{in}}{r_1} - 1, \quad (3.12)$$

and dimensionless black hole spin is a with $0 \leq a \leq 1$. The above potential [72], [73], the simplest form (in functional form) among all the proposed pseudo-Kerr black hole potentials, nicely reproduces the dynamics of accretion astrophysics in the Kerr metric within a reasonable Newtonian framework, especially while simulating the multitransonic accretion flow around rotating black holes. One can see that as the black hole spin $a = 0$ in the above form of potential, it takes the form of 3.3.

Therefore, when one works with these potentials in the non-general relativistic cases, the external field (*In the last two chapters*), $\psi(r) = \Phi_\alpha(r)$, where α runs from 0 to 5. It is also worth mentioning that the potentials: 3.3 to 3.6, asymptotically reaches the Newtonian potential 3.2 at large r . In the absence of the black hole spin, i.e., considering the potential 1 to potential 4, potential 1 is the best approximation of general relativistic spacetime (it is the closest to the effective potential experienced by a moving test particle/fluid in Schwarzschild space-time [74]), potential 2 is the worst approximation, and potential 4 and potential 3 are the second and the third best approximations for the dynamics of the slowly rotating accreting fluid (for more details, see [74]).

However, in the next chapter, we also consider full general relativistic case for spherically symmetric spacetime, only to show that the formalism and the methodology of our work (in the next chapter) is also valid in the pure general relativistic case.

3.3 Barotropic equation

In the introduction section, we have discussed that the barotropic equation of the fluid plays an important role in the subject, analogue gravity. In the second chapter, we have discussed the compatibility between the barotropic condition and irrotationality. Therefore, in the astrophysical flows, the infalling accreting medium has to obey the barotropic equation, given by

$$p = F(\rho). \quad (3.13)$$

In the case of ideal gas, there are two physically possible scenarios (because we are working with compressible classical fluids satisfying ideal gas law along with barotropic equation. One can in principle imagine more situations other than adiabatic and isothermal processes. In that case, we are not very sure about the physicality in those thermodynamic permissible processes.): the flow isothermal or adiabatic. $p \propto \rho$ for isothermal relation and $p \propto \rho^\gamma$ ($1 \leq \gamma \leq \frac{5}{3}$) (the range is chosen because for $\gamma > \frac{5}{3}$, the radius of the sonic point for the simplest model of accretion, i.e., the Bondi flow, becomes less than equals to zero, see [9]; and $\gamma = 1$ corresponds to isothermal flow, $\gamma > 1$ corresponds to adiabatic flow). For adiabatic relation between pressure and density [40]. γ is the ratio of specific heat at constant temperature and specific heat at constant volume.

3.4 General Formalism

As we have discussed in the *Introduction (Chapter-1)* that the background steady state solutions produce the stationary spacetime metric. If the steady state solution is transonic (by transonic flow, we mean such flow of medium that the bulk speed of the medium surpasses the sound speed (the thermodynamic speed)), the interesting features of General relativity emerge, i.e., the emergence of a black hole spacetime. Therefore, we seek transonic solutions of the fluid equations in the aforementioned accretion models. Considering three mentioned accretion models, four different gravitational potentials (pseudo-Newtonian) and two barotropic equations, therefore, there are twenty four possibilities. We discuss here steady state solutions for adiabatic flow in conical disk model under potential 1 and potential 5 (the pseudo Kerr potential). As we have

already mentioned that potential 1 gives the best approximation to General relativistic approach and potential 5 reduces to potential 1 when the black hole spin a is fixed to zero in the potential 5. Therefore, assuming the flow to be transonic, our first aim will be to find the point (the radius/surface in three dimensional space in general) where the speed of the medium surpasses the sound speed.

3.4.1 Fluid equations for conical adiabatic flow

Some calculations of this section are taken from our work [118]. We scale speed by the light speed ($= c$), radial distance by Schwarzschild radius ($r_g = \frac{2GM_{BH}}{c^2}$), density by $\frac{M_{BH}}{r_g^3}$, pressure by $\frac{M_{BH}c^2}{r_g^3}$ and angular momentum by cr_g . Therefore, we work with dimensionless variables. In a conical flow, accreting fluid falls under gravity, having velocity components along radial and azimuthal direction, with axial symmetry. The rotating fluid falls into the star/accretor under the gravitational pull of the accretor through a channel having a solid Θ . The gravity of the medium is not taken into account, i.e, we are using test fluid approximation in this chapter. *In chapter 5, we consider the gravity of the medium itself.* The continuity equation can be written as

$$\frac{\partial \rho(r,t)}{\partial t} + \frac{1}{rH(r)} \frac{\partial}{\partial r} (rH(r)\rho(r,t)v(r,t)) = 0 \quad (3.14)$$

where $\rho(r)$ and $v(r)$ are the fluid density and radial velocity having spherical symmetry. $H(r)$, the height of the disk, is proportional to r . Therefore, for a steady flow, we have the expression of the conserved quantity along the flow, i.e, the mass accretion rate ($\because H \propto r$)

$$\dot{M} = \Theta \rho v r^2, \quad (3.15)$$

derived from the steady state continuity equation (without using the explicit form of $H(r)$), given by

$$\frac{d(\rho v r H)}{dr} = 0. \quad (3.16)$$

Euler momentum equation is given by

$$\frac{\partial v}{\partial t} + v \frac{\partial v}{\partial r} = -\psi'(r) - \frac{1}{\rho} \frac{\partial p}{\partial r} + \frac{\lambda^2}{r^3} \quad (3.17)$$

where $\psi'(r)$ is the external field term and in this case it is gravitational force per unit mass of fluid exerted by the accretor. λ is the specific angular momentum of the fluid having small value such that viscosity is negligible [35]. Therefore for a steady flow, we have, another conserved quantity, i.e, the Bernoulli's constant, given by

$$\zeta = \frac{1}{2}v^2 + \int \frac{dp}{\rho} + \psi(r) + \frac{\lambda^2}{2r^2}, \quad (3.18)$$

derived from the equation of motion, given by

$$v \frac{dv}{dr} = -\frac{1}{\rho} \frac{dp}{dr} - \psi'(r) + \frac{\lambda^2}{r^3}. \quad (3.19)$$

We consider adiabatic relation between pressure and density as

$$p = K\rho^\gamma. \quad (3.20)$$

K is a constant, a function of specific entropy [42]. Therefore, using the barotropic equation and the above steady state equations, we have

$$\frac{dc_s}{dr} = c_s(1 - \gamma) \left(\frac{1}{2v} \frac{dv}{dr} + \frac{1}{r} \right), \quad (3.21)$$

$$\frac{dv}{dr} = \frac{\frac{2c_s^2}{r} + \frac{\lambda^2}{r^3} - \psi'(r)}{v - \frac{c_s^2}{v}}. \quad (3.22)$$

We seek transonic solution with finite $\frac{dv}{dr}$. Therefore, there exists a finite radius at which $v_0 = c_{s0}$. From, the expression of $\frac{dv}{dr}$, for the physical existence of such a finite radius ($=r_c$), the numerator of the equation 3.21 has to be zero because already the denominator is zero at that radius. Sound speed at the critical radius

$$c_{sc} = \sqrt{\frac{r_c \psi'(r_c)}{2} - \frac{\lambda^2}{2r_c^2}} \quad (3.23)$$

Therefore, we have from the expression of ζ 3.18 and from the aforementioned condition,

$$\zeta - \frac{\lambda^2}{2r_c^2} - \psi(r_c) - \frac{\gamma+1}{4(\gamma-1)} \left[r_c \psi'(r_c) - \frac{\lambda^2}{r_c^2} \right] = 0. \quad (3.24)$$

Therefore, for a given value of ζ , γ , λ under a gravitational potential, we can find the critical radius (the ‘dumb hole’ horizon or the sonic horizon) [35] [73]. In general

$$r_c = r_c(\zeta, \gamma, \lambda). \quad (3.25)$$

From the expression 3.23, for a physical transonic solution to exist,

$$\psi'(r_c) > \frac{\lambda^2}{r_c^3}. \quad (3.26)$$

To find the steady state solution for the transonic accretion, we first find $\frac{dv}{dr}$ at the critical radius, r_c . Using L’Hospital’s rule for finding value of a function at a x value where it has $\frac{0}{0}$ form, we get

$$\left. \frac{dv}{dr} \right|_{r=r_c} = q, \quad (3.27)$$

with q satisfying a quadratic equation, as follows

$$q^2 + Bq + C = 0. \quad (3.28)$$

The coefficients are given by

$$B = \frac{4c_{sc}(\gamma-1)}{(\gamma+1)r_c}, \quad (3.29)$$

$$C = \frac{1}{\gamma+1} \left[\frac{2c_{sc}^2}{r_c^2} + \frac{3\lambda^2}{r_c^4} + \psi''(r_c) + \frac{4c_{sc}^2(\gamma-1)}{r_c^2} \right]. \quad (3.30)$$

Using equation 3.22, one can find the value of $\frac{dc_s}{dr}$ at the critical point. Therefore, using these values at the critical point as initial conditions, one can find the steady state solution in general in the conical model (for more details with the other models, see [73][75]).

Now we take the gravitational potential, $\psi = \Phi_1$ and Φ_5 , i.e., we consider two cases. For the

potential Φ_1 , we find critical point, from the equation (the equation 3.25),

$$8\zeta(\gamma-1)r_c^2(r_c-1)^2 - (\gamma+1)r_c^3 + 2\lambda^2(\gamma+1)(r_c-1)^2 + 4(\gamma-1)r_c^2(r_c-1) - 4\lambda^2(\gamma-1)(r_c-1)^2 = 0. \quad (3.31)$$

For the potential Φ_5 , we get

$$4\zeta(\gamma-1)[2\zeta r_1(1-\beta)+1]r_c^{3-\beta}(r_c-r_1)^\beta - r_c^2[(\gamma+1)r_1(1-\beta)+4(\gamma-1)(r_c-r_1)] + 2\lambda^2 r_1(1-\beta)(3-\gamma)r_c^{1-\beta}(r_c-r_1)^\beta = 0. \quad (3.32)$$

With $a = 0$ equation 3.32 reduces to equation 3.31. Thus, we can find the steady state transonic solution under the considered gravitational potentials. *In chapter 7, we use the steady state solution of the the flow under these two gravitational potentials to estimate the wavelength of the eikonal wave.*

3.4.2 On the nature of transonic solution

The nature of solution varies depending on the parameter values. In general, the parameters for the adiabatic flow are ζ , λ , a and γ . The equation 3.31 and 3.32 can have multiple critical point solutions depending on the parameter values. In the above figure, region marked by O and I

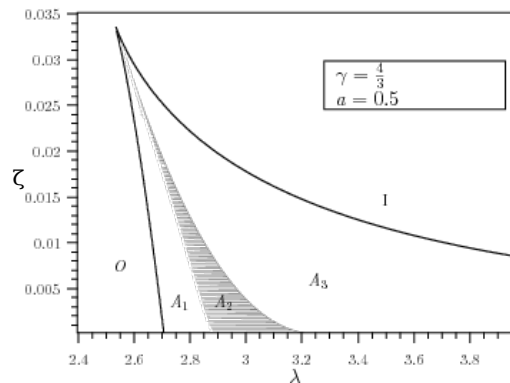


Figure 3.1: The parameter space, the figure is taken from the work [73].

provide monotransonic solutions exclusively passing through the outer type (located far away

from the black hole) and the inner type (located close to the black hole) sonic points, respectively. Region A1, A2 and A3 represents the multi-critical solutions (three critical points). The shaded region A2 allows shock formation. However, in our work we do not consider discontinuity in flow, i.e., we do not consider shock. Therefore, in our case, the accretion solution passes through one critical point. We consider all the regions, and yet we limit ourselves only to the continuous flow (continuous flow only passes through one critical point) so that in the acoustic space-time geometry there is no discontinuity in the metric components.

Chapter 4

Linear perturbation in the Bernoulli's constant, emergent spacetime

The contents of this chapter are mostly taken from our work on the emergent spacetime through the linear perturbation of the Bernoulli's constant [119]. Mass accretion rate is a quantity having a reasonable physical significance in accretion phenomena. Linear perturbation of mass accretion rate in sub-Keplerian disk accretion in non relativistic framework also behaves like a massless scalar field in curved space-time [73], i.e., analogue gravity also emerges when accretion rate is perturbed. Several works have been done in general relativistic framework as well. Linear perturbation of velocity potential in curved space-time background shows analogue gravity effect [76]. Similarly, linear perturbation of mass accretion rate in accretion of perfect fluid in curved space-time background also shows same effect [76]-[78].

In this chapter, we've shown that linear perturbation of another quantity, the Bernoulli's constant which is the integral solution of the corresponding Euler equation, also produces similar acoustic geometry. The whole work is being done in the non-relativistic framework and relativistic framework as well. Accretion phenomena of adiabatic flow are chosen to illustrate the fact. Radial accretion having spherical symmetry as well as disk accretion having axial symmetry are considered. The linear perturbation technique also has astrophysical significance. We get a wave equation of the linear perturbation of the Bernoulli's constant which is similar to the massless scalar field Klein-Gordon equation in curved space-time geometry. The nature of the solution of

this wave equation tells us whether the existing steady state solutions like steady state solution for Bondi accretion, are stable or not under such perturbation in the medium. We have done stability analysis for that and we have concluded that not only the integrals of motion play a crucial role to determine the dynamics of the accretion flow in steady state but also their linear perturbations govern the behaviour of all the dynamical and thermodynamic quantities in the time dependent problem within the perturbative framework. The correspondence between a classical (non-quantum) analogue model and the accretion processes onto astrophysical black holes has been established through the process of linear stability analysis of stationary integral transonic accretion solutions corresponding to the steady state flow only. That means, only such accreting black hole systems have been considered which are in steady state. The body of literature in accretion astrophysics, however, is huge and diverse. There are several steady state flow models which may not be multitransonic, and there are several excellent works which deal with non steady hydrodynamic accretion (which may not contain multiple sonic points or shocks) which may include various kind of time variabilities and instabilities, using complete time-dependent numerical simulation ([49], [50], [79]-[108]). We, however, did not concentrate on such approach. In the present chapter, our main motivation is to explore how the analogue gravity phenomena can be addressed through the linear stability analysis of steady-state solutions of hydrodynamic accretion.

4.1 Acoustic gravity in non-relativistic framework

In non-relativistic frame work, fluid velocity is much less than light speed. The momentum conservation equations and mass conservation equation for fluid is taken[40] according to Newton's laws of dynamics. The continuity equation of fluid is given by

$$\frac{\partial \rho}{\partial t} + \nabla \cdot (\rho \mathbf{v}) = 0 \quad (4.1)$$

where ρ, \mathbf{v} are fluid density and velocity respectively. Euler momentum equation for inviscid flow in an external field in general is given by

$$\frac{\partial \mathbf{v}}{\partial t} + \mathbf{v} \cdot \nabla \mathbf{v} = -\nabla \psi - \frac{\nabla p}{\rho} \quad (4.2)$$

where the potential function of the external conservative field is ψ and pressure at any point of the fluid is p .

The flow is taken to be irrotational.

$$\nabla \times \mathbf{v} = 0 \quad (4.3)$$

Using irrotationality condition one can write Euler equation as

$$\frac{\partial \mathbf{v}}{\partial t} + \nabla \left(\frac{1}{2} \mathbf{v}^2 + \int \frac{dp}{\rho} + \psi \right) = 0. \quad (4.4)$$

The Bernoulli's constant, ζ is given by

$$\zeta = \frac{1}{2} \mathbf{v}^2 + \int \frac{dp}{\rho} + \psi \quad (4.5)$$

For steady irrotational flow it's a constant along the streamline. Adiabatic sound speed is given by

$$c_s^2 = \frac{dp}{d\rho} = \frac{\gamma p}{\rho} \quad (4.6)$$

where γ is the specific ratio of the ideal gas. We mention the sound speed because we work with barotropic flow, even though γ does not appear in the next sections. We assume there is a stationary solution in general for the above equations, and we introduce linear perturbations in the fluid discussed in the next section.

4.1.1 General procedure to obtain the acoustic metric

Linear perturbation of fluid velocity and fluid pressure is introduced as

$$\mathbf{v}(\mathbf{x}, t) = \mathbf{v}_0(\mathbf{x}) + \mathbf{v}'(\mathbf{x}, t)$$

$$\rho(\mathbf{x}, t) = \rho_0(\mathbf{x}) + \rho'(\mathbf{x}, t)$$

where $\rho_0(\mathbf{x})$, $\mathbf{v}_0(\mathbf{x})$ are the stationary solution of fluid density and velocity field and $\mathbf{v}'(\mathbf{x}, t)$, $\rho'(\mathbf{x}, t)$ are the introduced linear perturbation terms in the velocity and the density of the fluid.

As a result, the linear perturbation term in the Bernoulli's constant is given by

$$\zeta' = \mathbf{v}_0 \cdot \mathbf{v}' + \frac{c_{s0}^2}{\rho_0} \rho' \quad (4.7)$$

c_{s0} is the stationary unperturbed sound speed. Continuity equation in terms of linear perturbation is given by

$$\frac{\partial \rho'}{\partial t} + \nabla \cdot (\rho' \mathbf{v}_0 + \rho_0 \mathbf{v}') = 0 \quad (4.8)$$

Momentum equation in terms of linear perturbation is given by

$$\frac{\partial \mathbf{v}'}{\partial t} + \nabla(\zeta') = 0 \quad (4.9)$$

We have used equation (4.7) to find the above equation. Using equation (4.7) and equation (4.9) and taking another partial time derivative in equation (4.8) we get

$$\partial_\mu (f^{\mu\nu}(\mathbf{x}) \partial_\nu) \zeta'(\mathbf{x}, t) = 0 \quad (4.10)$$

where $f^{\mu\nu}(\mathbf{x})$ in Cartesian coordinate is given by

$$f^{\mu\nu}(\mathbf{x}) = \frac{\rho_0}{c_{s0}^2} \begin{bmatrix} -1 & \vdots & -v_0^j \\ \dots & \dots & \dots \\ -v_0^j & \vdots & c_{s0}^2 \delta^{ij} - v_0^i v_0^j \end{bmatrix} \quad (4.11)$$

where i, j run over 1, 2, 3 representing three spatial dimensions. This $f^{\mu\nu}$ is exactly the same as $f^{\mu\nu}$ obtained when velocity potential is perturbed [2]. We mean that the $f^{\mu\nu}$ in the wave equation obtained through the linear perturbation of velocity potential is same as what we obtained through the linear perturbation of Bernoulli's constant.

Massless scalar field equation in a spacetime background is given by

$$\square\varphi = \frac{1}{\sqrt{-g}}(\partial_\mu \sqrt{-g}g^{\mu\nu}\partial_\nu)\varphi = 0 \quad (4.12)$$

where φ is the scalar field, $g^{\mu\nu}$ is the background metric and g is the determinant of the metric.

Comparing equation (4.12) and equation (4.10)

$$f^{\mu\nu} = \sqrt{-g}g^{\mu\nu} \quad (4.13)$$

Immediately one can get

$$\det(f^{\mu\nu}) = (\sqrt{-g})^4 g^{-1} = g = -\frac{\rho_0^4}{c_{s0}^2} \quad (4.14)$$

So $g^{\mu\nu}$ is given by

$$g^{\mu\nu}(\mathbf{x}) = \frac{1}{\rho_0 c_{s0}} \begin{bmatrix} -1 & \vdots & -v_0^j \\ \dots & \dots & \dots \\ -v_0^j & \vdots & c_{s0}^2 \delta^{ij} - v_0^i v_0^j \end{bmatrix} \quad (4.15)$$

The acoustic metric is

$$g_{\mu\nu}(\mathbf{x}) = \frac{\rho_0}{c_{s0}} \begin{bmatrix} -(c_{s0}^2 - v_0^2) & \vdots & -v_0^j \\ \dots & \dots & \dots \\ -v_0^j & \vdots & \delta_{ij} \end{bmatrix} \quad (4.16)$$

Acoustic metric interval can be expressed as

$$ds^2 = \frac{\rho_0}{c_{s0}} [-(c_{s0}^2 - v_0^2)dt^2 - 2dt\mathbf{v}_0 \cdot d\mathbf{x} + d\mathbf{x}^2] \quad (4.17)$$

The same kind of analysis can be done for isothermal flow as well and the metric will be same except that the definition of sound speed will be different there, in the acoustic metric, sound speed will be appearing as a constant rather than a function of position vector. The metric appearing in equation (4.16) has 3+1 dimension. It reduces to 1+1 dimension when symmetries in the flow is considered. The next section deals with some astrophysical accretion phenomenon having different kind of symmetries.

4.1.2 Spherically symmetric radial flow

Bondi accretion[9] is spherically symmetric and radial. The Bernoulli's constant is given by

$$\zeta = \frac{1}{2}v^2 + \int \frac{dp}{\rho} - \frac{GM}{r}, \quad (4.18)$$

where M is the mass of the star and G is gravitational constant. Introducing linear perturbation in adiabatic flow

$$v(r,t) = v_0(r) + v(r,t)'$$

$$\rho(r,t) = \rho_0(r) + \rho(r,t)'$$

Perturbation in the Bernoulli's constant is given by

$$\zeta' = v_0 v' + \frac{c_{s0}^2}{\rho_0} \rho' \quad (4.19)$$

Now in the same way discussed earlier we find that the linear perturbation of the Bernoulli's constant obeys massless scalar field equation in acoustic analogue of spacetime background.

$$\partial_\mu (f^{\mu\nu}(r) \partial_\nu) \zeta'(r,t) = 0 \quad (4.20)$$

where

$$f^{\mu\nu}(r) = \frac{\rho_0 r^2}{c_{s0}^2} \begin{bmatrix} -1 & -v_0 \\ -v_0 & c_{s0}^2 - v_0^2 \end{bmatrix} \quad (4.21)$$

$f_{\mu\nu}$ is taken as effective metric[35]. Hence 2×2 effective acoustic metric is given by

$$g_{\mu\nu}^{eff}(r) = \frac{1}{\rho_0 r^2} \begin{bmatrix} -(c_{s0}^2 - v_0^2) & -v_0 \\ -v_0 & 1 \end{bmatrix} \quad (4.22)$$

The right hand side of the equation above equation 4.20 is zero, therefore the dimensionality of $f^{\mu\nu}$ is not an issue. There would be no r^2 in $f^{\mu\nu}$. Since we are working in 1+1 D, we construct $g_{\mu\nu}^{eff}(r)$, from $f^{\mu\nu}$ as described above. Observation of the acoustic metric shows that acoustic horizon is produced.

Similarly, the same analysis can be done for isothermal flow as well.

4.1.3 Axially symmetric sub-keplerian disk geometries

4.1.4 Vertical equilibrium disk accretion

Continuity equation in cylindrical polar coordinate in disk accretion having axial symmetry and having no net flow in z direction is given by

$$\frac{\partial \bar{\rho}(r, z)}{\partial t} + \frac{1}{r} \frac{\partial}{\partial r} (\bar{\rho}(r, z) \bar{v}(r, z) r) = 0 \quad (4.23)$$

where $\bar{\rho}(r, z)$ and $\bar{v}(r, z)$ are the fluid density and radial velocity at a cylindrical radial distance r and at height z from the equatorial plane of the disk. Now averaging in z direction over disk height H

$$\frac{\partial \rho(r)}{\partial t} + \frac{1}{rH(r)} \frac{\partial}{\partial r} (\rho(r) v(r) r H(r)) = 0 \quad (4.24)$$

where $\rho(r)$ and $\rho(r)v(r)$ are the averaged fluid density and momentum respectively. The problem is now reduced in 1+1 dimension. Euler momentum equation is given by

$$\frac{\partial v}{\partial t} + v \frac{\partial v}{\partial r} = -\psi'(r) - \frac{1}{\rho} \frac{\partial p}{\partial r} + \frac{\lambda^2}{r^3} \quad (4.25)$$

where $\psi'(r)$ is the external field term and in this case it is gravitational force per unit mass of fluid exerted by the accretor. λ is the specific angular momentum of the fluid having small value.

The Bernoulli's constant is given by

$$\zeta = \frac{1}{2} v^2 + \int \frac{dp}{\rho} + \psi(r) + \frac{\lambda^2}{2r^2} \quad (4.26)$$

Considering thin disk in vertical equilibrium and adiabatic flow, balancing pressure gradient force term and gravitational force term along z direction, vertical equilibrium condition is given[35]

$$H(r) = c_s(r) \sqrt{\frac{r}{\gamma \Psi'}} \quad (4.27)$$

As a consequence, continuity equation is given by

$$\partial_t(\rho^{\frac{\gamma+1}{2}}) + \frac{\sqrt{\Psi'}}{r^{\frac{3}{2}}} \partial_r \left(\frac{\rho^{\frac{\gamma+1}{2}} v r^{\frac{3}{2}}}{\sqrt{\Psi'}} \right) = 0 \quad (4.28)$$

γ is specific heat ratio. Introducing linear perturbation in the adiabatic flow, perturbation of the Bernoulli's constant is given by

$$\zeta'(r, t) = v_0 v' + \frac{c_{s0}^2 \sigma}{\rho_0^{\frac{(\gamma+1)}{2}}} \delta(\rho^{\frac{(\gamma+1)}{2}}) \quad (4.29)$$

where $\sigma = \frac{2}{\gamma+1}$ and $\delta(\rho^{\frac{(\gamma+1)}{2}})$ is linear perturbation in $\rho^{\frac{(\gamma+1)}{2}}$.

Linear perturbation of the Bernoulli's constant obeys massless scalar wave equation

$$\partial_\mu (f^{\mu\nu}(r) \partial_\nu) \zeta'(r, t) = 0 \quad (4.30)$$

where

$$f^{\mu\nu}(r) = \frac{\rho_0^{\frac{(\gamma+1)}{2}} r^{\frac{3}{2}}}{c_{s0}^2 \sigma \sqrt{\Psi'}} \begin{bmatrix} -1 & -v_0 \\ -v_0 & \sigma c_{s0}^2 - v_0^2 \end{bmatrix} \quad (4.31)$$

$f_{\mu\nu}$ is taken as effective metric. Hence 2×2 effective acoustic metric is given by

$$g_{\mu\nu}^{eff}(r) = \frac{\sqrt{\Psi'}}{\rho_0^{\frac{(\gamma+1)}{2}} r^{\frac{3}{2}}} \begin{bmatrix} -(\sigma c_{s0}^2 - v_0^2) & -v_0 \\ -v_0 & 1 \end{bmatrix} \quad (4.32)$$

For isothermal flow one similarly gets acoustic metric like equation (4.32) where γ is 1 and sound speed is a constant number.

4.1.5 Constant height disk accretion

In case of constant thickness model, H is a constant. The linear perturbation of the Bernoulli's constant is given by

$$\zeta'(r, t) = v_0 v' + \frac{c_{s0}^2}{\rho_0} \rho' \quad (4.33)$$

The linear perturbation of continuity equation is given by

$$\partial_t(\rho') + \frac{1}{rH} \partial_r(rH(\rho' v_0 + \rho_0 v')) = 0 \quad (4.34)$$

where H is a non zero constant number. The linear perturbation of momentum equation is given by

$$\partial_t(v') + \partial_r(\zeta') = 0 \quad (4.35)$$

Now proceeding in the same way discussed earlier one gets equation of massless scalar field in curved space time background

$$\partial_\mu f^{\mu\nu}(r) \partial_\nu \zeta' = 0 \quad (4.36)$$

where after taking inverse of $f^{\mu\nu}(r)$, $f_{\mu\nu}(r)$ can be taken as 2×2 effective metric as

$$f_{\mu\nu} = g_{\mu\nu}^{eff}(r) = \frac{1}{\rho_0 r H} \begin{bmatrix} -(c_{s0}^2 - v_0^2) & -v_0 \\ -v_0 & 1 \end{bmatrix} \quad (4.37)$$

For conical disk model $H \propto r$. Just like the constant height disk model, linear perturbation in fluid does not have any influence on disk height. Hence the procedure of getting massless Klein Gordon equation is exactly same and the effective acoustic metric is exactly same as obtained in constant height disk model. The above expression is structurally same for the conical model. The only difference is that is that for conical model, H is proportional to r . This is because, in the conical model, disk height is not perturbed.

4.2 Acoustic gravity in curved space-time background

In the present chapter, we consider the following metric for static space-time

$$ds^2 = -g_{tt}dt^2 + g_{rr}dr^2 + g_{\theta\theta}d\theta^2 + g_{\phi\phi}d\phi^2 \quad (4.38)$$

where the metric elements are functions of r and can also be functions of θ and ϕ . We assume a perfect fluid with the energy-momentum tensor given by

$$T^{\mu\nu} = (\varepsilon + p)v^\mu v^\nu + pg^{\mu\nu} \quad (4.39)$$

with the velocity four-vector normalized as $v^\mu v_\mu = -1$ and ε is the internal energy per unit volume of the fluid. The fluid is assumed to be ideal and so obeys equation of state for ideal gas. Also it is assumed to be under adiabatic condition i.e it obeys barotropic equation of state, i.e., $p = k\rho^\gamma$. The specific enthalpy of the fluid is given by

$$h = \frac{\varepsilon + p}{\rho} \quad (4.40)$$

The speed of sound for adiabatic flow is given by

$$c_s^2 = \frac{\partial p}{\partial \varepsilon} \quad (4.41)$$

which can be also written as[76]

$$c_s^2 = \frac{\rho}{h} \frac{\partial h}{\partial \rho} \quad (4.42)$$

In our calculation of acoustic geometry we make use of two basic equations. First one is the continuity equation given by

$$\nabla_\mu(\rho v^\mu) = 0 \quad (4.43)$$

and the second one is the irrotationality condition as the fluid is assumed to be irrotational. The condition is given by

$$\partial_\mu(hv_\nu) - \partial_\nu(hv_\mu) = 0 \quad (4.44)$$

4.2.1 Spherically symmetric radial flow

In the first case in curved space-time background we derive the acoustic geometry for spherically symmetric flow. This implies that $v_\theta = v_\phi = 0$ and all the derivatives with respect to θ and ϕ vanish. Using $\mu = t$ and $\nu = r$ in the irrotationality condition equation given by equation (4.44) gives

$$\partial_t(hv_r) - \partial_r(hv_t) = 0 \quad (4.45)$$

In stationary case where ∂_t term vanishes the above equation implies $\partial_r(hv_t) = 0$. So for stationary flow $\zeta = hv_t$ is a constant of the flow. This is called the specific energy for adiabatic flow or it can be thought of as the Bernoulli's constant equivalent in GR. Due to spherical symmetry, the continuity equation given by equation (4.43) becomes

$$\frac{1}{\sqrt{-g}}\partial_t(\sqrt{-g}\rho v^t) + \frac{1}{\sqrt{-g}}\partial_r(\sqrt{-g}\rho v) = 0 \quad (4.46)$$

where $v = v^r$ is the radial velocity. Using the normalization condition of the four-velocity given $v^\mu v_\mu = -1$, v^t can be expressed as

$$v^t = \sqrt{\frac{1 + g_{rr}v^2}{g_{tt}}} \quad (4.47)$$

Now we linearly perturb the radial velocity, density and the Bernoulli's constant about their stationary values.

$$v(r,t) = v_0(r) + v'(r,t) \quad (4.48)$$

$$\rho(r,t) = \rho_0(r) + \rho'(r,t) \quad (4.49)$$

and

$$\zeta(r,t) = \zeta_0 + \zeta'(r,t) \quad (4.50)$$

Using these quantities we do linear perturbation of the continuity equation and the irrotationality condition equation given by equation (4.46) and equation (4.45) respectively.

Linear perturbation of the irrotationality condition equation gives the following equation

$$\partial_r \zeta' = g_{rr} h_0 \partial_t v' + \frac{g_{rr} h_0 v_0 c_{s0}^2}{\rho_0} \partial_t \rho' \quad (4.51)$$

where h_0 is the stationary or background value of the enthalpy h and $c_{s0}^2 = \frac{\rho_0}{h_0} \frac{\partial h}{\partial \rho}$ again perturbing $\zeta = h v_t = -g_{tt} h v^t$ gives the equation

$$\zeta' = -g_{tt} h_0 \alpha v' - \frac{g_{tt} v_0^t h_0 c_{s0}^2}{\rho_0} \rho' \quad (4.52)$$

where $\alpha = \frac{g_{rr} v_0}{g_{tt} v_0^t}$ and we have used the normalization condition of four-velocity to obtain $(v^t)' = \alpha v'$. Taking time derivative of the above equation gives

$$\partial_t \zeta' = -g_{tt} h_0 \alpha \partial_t v' - \frac{g_{tt} v_0^t h_0 c_{s0}^2}{\rho_0} \partial_t \rho' \quad (4.53)$$

Using equation (4.51) and equation (4.53) we are able to write $\partial_t v'$ and $\partial_t \rho'$ in terms of ζ' only.

Thus we have

$$\partial_t v' = \frac{-1}{\Delta} \left[\frac{g_{rr} h_0 v_0 c_{s0}^2}{\rho_0} \partial_t \zeta' + \frac{g_{tt} v_0^t h_0 c_{s0}^2}{\rho_0} \partial_r \zeta' \right] \quad (4.54)$$

$$\partial_t \rho' = \frac{1}{\Delta} [g_{rr} h_0 \partial_t \zeta' + g_{tt} h_0 \alpha \partial_r \zeta'] \quad (4.55)$$

where $\Delta = -\frac{g_{rr} h_0^2 c_{s0}^2}{\rho_0 v_0^t}$

Linear perturbation of the continuity equation gives

$$\rho_0 \alpha \partial_t v' + v_0^t \partial_t \rho + \frac{1}{\sqrt{-g}} \partial_r (\sqrt{-g} \rho_0 v' + \sqrt{-g} v_0 \rho') = 0 \quad (4.56)$$

taking the time derivative of the above equation gives

$$\partial_t (\sqrt{-g} \rho_0 \alpha \partial_t v') + \partial_t (\sqrt{-g} v_0^t \partial_t \rho) + \partial_r (\sqrt{-g} \rho_0 \partial_t v') + \partial_r (\sqrt{-g} v_0 \partial_t \rho') = 0 \quad (4.57)$$

Substituting $\partial_t v'$ and $\partial_t \rho'$ in the above equation using equation (4.54) and equation (4.55) gives

$$\begin{aligned} & \partial_t \left[\frac{\sqrt{-g} g_{rr} h_0}{\Delta v_0^t} \left\{ \frac{g_{tt} (v_0^t)^2 (1 - c_{s0}^2) + c_{s0}^2}{g_{tt}} \right\} \partial_t \zeta' \right] + \partial_t \left[\frac{\sqrt{-g} h_0 g_{rr} v_0}{\Delta} \{1 - c_{s0}^2\} \partial_r \zeta' \right] \\ & + \partial_r \left[\frac{\sqrt{-g} h_0 g_{rr} v_0}{\Delta} \{1 - c_{s0}^2\} \partial_t \zeta' \right] + \partial_r \left[\frac{\sqrt{-g} g_{rr} h_0}{\Delta v_0^t} \left\{ \frac{v_0^2 g_{rr} (1 - c_{s0}^2) - c_{s0}^2}{g_{rr}} \right\} \partial_r \zeta' \right] = 0 \end{aligned} \quad (4.58)$$

The above equation is of the form $\partial_\mu (f^{\mu\nu} \partial_\nu \zeta') = 0$ with $f^{\mu\nu}$ given by after multiplying by -1

$$f^{\mu\nu} = \frac{\sqrt{-g} \rho_0}{h_0} \begin{bmatrix} -g^{tt} + (v_0^t)^2 (1 - \frac{1}{c_{s0}^2}) & v_0 v_0^t (1 - \frac{1}{c_{s0}^2}) \\ v_0 v_0^t (1 - \frac{1}{c_{s0}^2}) & g^{rr} + v_0^2 (1 - \frac{1}{c_{s0}^2}) \end{bmatrix} \quad (4.59)$$

4.2.2 Axially symmetric disk flow

Three low angular momentum disk models (as discussed in previous sections) are considered for adiabatic flow. The normalization condition is given by

$$v_\mu v^\mu = -1 \quad (4.60)$$

The spherically symmetric diagonal metric of equation (4.38) is considered. We consider the dynamics only on the equatorial plane ($\theta = \frac{\pi}{2}$) plane of the disk. The accretion flow is irrotational, i.e., it obeys equation (4.44). The infalling fluid has a small azimuthal component of velocity, v^ϕ . From equation (4.60)

$$(v^t)^2 = \frac{1 + g_{rr}(r)v^2 + g_{\phi\phi}(r)(v^\phi)^2}{g_{tt}(r)} \quad (4.61)$$

Similarly, equation (4.45) gives the Bernoulli's constant. Using equation (4.44) and axial symmetry of the flow

$$\partial_t (h v_\phi) = 0$$

$$\partial_r (h v_\phi) = 0$$

$$\Rightarrow hv_\phi = \text{constant} = \ell \quad (4.62)$$

hv_ϕ is called specific angular momentum and it is a constant number for non-stationary flow as well due to irrotationality and azimuthal symmetry. We assume that there is a stationary solution of the accretion $(v_0(r), \rho_0(r), v_0^\phi(r), \zeta_0)$ and linear perturbation is introduced.

$$v(r, t) = v_0(r) + v'(r, t) \quad (4.63)$$

$$\rho(r, t) = \rho_0(r) + \rho'(r, t) \quad (4.64)$$

$$v^\phi(r, t) = v_0^\phi(r) + v'_\phi(r, t) \quad (4.65)$$

and

$$\zeta(r, t) = \zeta_0 + \zeta'(r, t) \quad (4.66)$$

The symbols carries usual meaning as before. The addition of linear perturbations do not make the accretion flow to violate irrotationality, azimuthal symmetry (obvious from the above expressions). The accretion flow is still inviscid and adiabatic. From equation (4.62), linear perturbation term, ℓ' is given by

$$\ell' = 0 \quad (4.67)$$

Using equation (4.42) and equation (4.67) we get

$$v'_\phi = -\frac{v_0^\phi c_{s0}^2}{\rho_0} \rho' \quad (4.68)$$

Using equation (4.61) and equation (4.68) we get

$$(v')' = \alpha_1(r)v' + \alpha_2(r)\rho' \quad (4.69)$$

where

$$\alpha_1(r) = \frac{g_{rr}v_0}{g_{tt}v_0^t}$$

$$\alpha_2(r) = -\frac{g_{\phi\phi}(v_0^\phi)^2 c_{s0}^2}{g_{tt}v_0^t \rho_0}$$

Irrotationality condition gives

$$\partial_r \zeta' = f_1(r) \partial_t \rho' - f_2(r) \partial_t v' \quad (4.70)$$

where

$$f_1(r) = \frac{g_{rr}v_0 h_0 c_{s0}^2}{\rho_0}$$

$$f_2(r) = -g_{rr} h_0$$

Using equation (4.69) and expression of $\zeta (= -h g_{tt} v^t)$

$$\partial_t \zeta' = -f_3(r) \partial_t \rho' + f_4(r) \partial_t v' \quad (4.71)$$

where

$$f_3(r) = \frac{g_{tt}v_0^t h_0 c_{s0}^2}{\rho_0} + g_{tt} h_0 \alpha_2$$

$$f_4(r) = -g_{tt} h_0 \alpha_1$$

From equation (4.70) and (4.71) we get

$$\partial_t \rho' = g_4(r) \partial_r \zeta' + g_2(r) \partial_t \zeta' \quad (4.72)$$

$$\partial_t v' = g_3(r) \partial_r \zeta' + g_1(r) \partial_t \zeta' \quad (4.73)$$

where

$$g_i = \frac{f_i}{\Delta} \text{ where } i \in \mathbb{N} \text{ and } i = 1 \text{ to } 4 \text{ where } \mathbb{N} \text{ is the set of natural numbers.}$$

$$\text{and } \Delta = f_1 f_4 - f_2 f_3 = \frac{g_{rr} h_0^2 c_{s0}^2}{\rho_0 v_0^t}$$

Until and unless we don't have the expression of disk height, we can not use the continuity equation. In the next section several sub-keplerian (discussed before) disk models are considered.

Vertical equilibrium disk model

The expression of $H(r)$ ¹ satisfying vertical equilibrium condition is given by [78], [109]

$$H(r)^2 v_\phi^2 F(r) = \frac{p}{\rho}$$

The linear perturbation of H is H' and stationry solution of H is $H_0(r)$. Using barotropic equation and equation (4.68)

$$\frac{\partial_t H'}{H_0} = \frac{\beta}{\rho_0} \partial_t \rho' \quad (4.74)$$

where $\beta = c_{s0}^2 + \frac{\gamma-1}{2}$.

Continuity equation is given by

$$\frac{1}{\sqrt{-g}} \partial_t (\sqrt{-g} \rho v^t H) + \frac{1}{\sqrt{-g}} \partial_r (\sqrt{-g} \rho v^r H) = 0 \quad (4.75)$$

Introducing linear perturbation in the fluid and using equation (4.69) and (4.74), one gets after partially differentiating equation (4.75),

$$(\partial_t F_1 \partial_t) \rho' + (\partial_t F_2 \partial_t) v' + (\partial_r F_3 \partial_t) \rho' + (\partial_r F_4 \partial_t) v' = 0 \quad (4.76)$$

¹ $H(r)$ is not the flow thickness of the disk, this is a dimensionless quantity which appears in continuity equation after averaging in θ direction.

where each F_i ($i \in \mathbb{N}, i = 1$ to 4) is function of r , the expressions are given below

$$F_1(r) = \sqrt{-g}(H_0 v_0^t (1 + \beta) + \alpha_2 \rho_0 H_0)$$

$$F_2(r) = \sqrt{-g} \rho_0 H_0 \alpha_1$$

$$F_3(r) = \sqrt{-g} H_0 v_0 (1 + \beta)$$

$$F_4(r) = \sqrt{-g} \rho_0 H_0$$

Using equation (4.72), (4.73) and (4.76) we get

$$\partial_\mu (f^{\mu\nu}(r) \partial_\nu) \zeta' = 0 \quad (4.77)$$

where μ, ν indices run over t and r . 2×2 matrix, $f^{\mu\nu}$ is given by

$$f^{\mu\nu} = \frac{\sqrt{-g} H \rho_0}{h_0} \begin{bmatrix} -g^{tt} + (v_0^t)^2 \left(1 - \frac{1+\beta}{c_{s0}^2}\right) & v_0 v_0^t \left(1 - \frac{1+\beta}{c_{s0}^2}\right) \\ v_0 v_0^t \left(1 - \frac{1+\beta}{c_{s0}^2}\right) & g^{rr} + v_0^2 \left(1 - \frac{1+\beta}{c_{s0}^2}\right) \end{bmatrix} \quad (4.78)$$

Constant height disk model

For constant height disk model $H \propto \frac{1}{r}$. H does not change when linear perturbations are introduced in the fluid velocity and density. Now using continuity equation (4.75) and introducing linear perturbations, one gets after partially differentiating with t

$$(\partial_t F_1 \partial_t) \rho' + (\partial_t F_2 \partial_t) v' + (\partial_r F_3 \partial_t) \rho' + (\partial_r F_4 \partial_t) v' = 0 \quad (4.79)$$

where each F_i ($i \in \mathbb{N}, i = 1$ to 4) is function of r , the expressions are given below

$$F_1(r) = \sqrt{-g}(H v_0^t + \alpha_2 \rho_0 H)$$

$$F_2(r) = \sqrt{-g} \rho_0 H \alpha_1$$

$$F_3(r) = \sqrt{-g} H v_0$$

$$F_4(r) = \sqrt{-g} \rho_0 H$$

We get in similar fashion,

$$\partial_\mu(f^{\mu\nu}(r)\partial_\nu)\zeta' = 0 \quad (4.80)$$

where μ, ν indices run over t and r . 2×2 matrix, $f^{\mu\nu}$ is given by

$$f^{\mu\nu} = \frac{\sqrt{-g}H\rho_0}{h_0} \begin{bmatrix} -g^{tt} + (v_0^t)^2(1 - \frac{1}{c_{s0}^2}) & v_0v_0^t(1 - \frac{1}{c_{s0}^2}) \\ v_0v_0^t(1 - \frac{1}{c_{s0}^2}) & g^{rr} + v_0^2(1 - \frac{1}{c_{s0}^2}) \end{bmatrix} \quad (4.81)$$

Conical disk model

For conical disk model, H is a constant number. H does not change when linear perturbations are introduced in the fluid velocity and density because H does not depend on those quantities. Now using continuity equation (4.75) and introducing linear perturbations, one gets after partially differentiating with t

$$(\partial_t F_1 \partial_t)\rho' + (\partial_t F_2 \partial_t)v' + (\partial_r F_3 \partial_t)\rho' + (\partial_r F_4 \partial_t)v' = 0 \quad (4.82)$$

where each F_i ($i \in \mathbb{N}, i = 1$ to 4) is function of r , the expressions are given below

$$F_1(r) = \sqrt{-g}(Hv_0^t + \alpha_2\rho_0H)$$

$$F_2(r) = \sqrt{-g}\rho_0H\alpha_1$$

$$F_3(r) = \sqrt{-g}Hv_0$$

$$F_4(r) = \sqrt{-g}\rho_0H$$

Using equation (4.72), (4.73) and (4.82) we get

$$\partial_\mu(f^{\mu\nu}(r)\partial_\nu)\zeta' = 0 \quad (4.83)$$

where μ, ν indices run over t and r . 2×2 matrix, $f^{\mu\nu}$ is given by

$$f^{\mu\nu} = \frac{\sqrt{-g}H\rho_0}{h_0} \begin{bmatrix} -g^{tt} + (v_0^t)^2(1 - \frac{1}{c_{s0}^2}) & v_0 v_0^t(1 - \frac{1}{c_{s0}^2}) \\ v_0 v_0^t(1 - \frac{1}{c_{s0}^2}) & g^{rr} + v_0^2(1 - \frac{1}{c_{s0}^2}) \end{bmatrix} \quad (4.84)$$

One trivial observation is that for constant height disk model and conical disk model as the disk height is not disturbed due to linear perturbations in the fluid, hence putting β to be zero in the matrix (80) one can obtain $f^{\mu\nu}$ for these models.

4.3 Astrophysical significance

The linear perturbation of the Bernoulli's constant satisfies a wave equation in the case of accretion onto a black hole or a massive body. The generic equation is

$$\partial_\mu (f^{\mu\nu}(X) \partial_\nu) \zeta' = 0 \quad (4.85)$$

where $\zeta' = \zeta'(X, t)$ and X is spherical polar radial coordinate for spherically symmetric accretion or cylindrical polar radial coordinate for axisymmetric accretion. The above equation is true for both general relativistic framework as well as for Newtonian-gravity framework. The original fluid equations, i.e., continuity equation, Euler equation, are time dependent partial differential equations. Here our approach is perturbative, i.e., there is an existing steady state solution for astrophysical accretion problem and over that we are introducing linear perturbation of the fluid quantities. Now the solution of ζ' of the equations could tell us whether the steady state solutions are stable under small perturbations or not. As the linear perturbation of density, velocity are all related to ζ' , hence if we could find certain conditions under which ζ' grows in time then the other related quantities would grow in time, the perturbation could not be small at all time, the steady solution of the quantities would not be stable in that case and in that case a full numerical approach where partial time derivatives in the fluid equations are taken care of would give a more accurate result in stead of steady state solution.

To find ζ' , we use the same approach done by Jacobus A. Petterson et al [110]. We take the

form of the wave to be as

$$\zeta'(X, t) = P_\omega(X)e^{i\omega t} \quad (4.86)$$

Hence from equation (4.87), we find

$$\omega^2 P_\omega(X) f^{tt} + i\omega [\partial_X (P_\omega(X) f^{Xt}) + f^{tX} \partial_X P_\omega(X)] - [\partial_X (f^{XX} \partial_X P_\omega(X))] = 0. \quad (4.87)$$

We implement two different methodologies in the next sections to check the stability of the steady state solutions.

4.3.1 Standing wave analysis

Standing wave means that there will be nodes and antinodes. There will exist a standing wave across X direction if and only if there are at least two different X s in space, called nodes, where the amplitude of the $\zeta'(X, t)$ is zero for all time where unlike θ, ϕ ; X is a noncompact dimension. Therefore, there exist at least two radii X_1, X_2 ; $X_1 \neq X_2$ such that $P_\omega(X_1) = P_\omega(X_2) = 0$. Hence ζ' is zero at these two points for all time. Standing wave is produced when two waves moving in opposite direction superpose with each other in space. When a wave moving along a particular direction face an obstacle another wave moving along the opposite direction is produced due to the reflection from that obstacle and in time superposition of these two waves produce standing wave confined between two points or radii in space. The outer radius, say X_2 may be a very large radius, for example the boundary of the accreting cloud surrounding the star. In case of accretion on to a black hole, there is no solid surface to produce a standing wave by reflection, i.e., in the supersonic region of flow, nowhere ζ' is zero, i.e., there is no inner radius to confine the wave between two radii which is required to produce a standing wave. In the case of accretion on to a compact object like neutron star, on the surface of the star, the accreting fluid collides, hence the fluid quantities undergo a discontinuity, as a result of this, a shock wall is formed according to Rankine-Hugoniot relations around the star where the pre shock supersonic inflow becomes post shock subsonic flow. As in our analysis we are not considering any discontinuity in the fluid equations. We restrict this analysis for subsonic flows. We consider standing waves because the wave equation 4.85, being a second order linear differential equation, permits the possibility of

a superposition (linear combinations) of two waves (one going downstream of the background flow and the other going upstream of the flow), thus forming a standing wave.

After multiplying the equation (4.87) and then integrating it between X_1 and X_2 and imposing the condition of vanishing amplitude of ζ' at the two radii, we get

$$\omega^2 = -\frac{C}{A} \quad (4.88)$$

where

$$A = \int_{X_1}^{X_2} (P_\omega)^2 f^{tt} dX$$

$$C = \int_{X_1}^{X_2} (\partial_X P_\omega)^2 f^{XX} dX$$

ω^2 from the equation 4.88 can be both positive and negative because of the sign in f^{tt} and f^{XX} . For example, in the non-relativistic spherically symmetric accretion f^{XX} is proportional to $(c_{s0}^2 - v_0^2)$ and $f^{tt} = \frac{1}{\rho_0 r^2}$ from equation 4.21. Therefore, from the above expression, ω^2 is positive in the subsonic flow region (when both X_1 and X_2 in the subsonic region) and negative in the supersonic region of flow (when both X_1 and X_2 in the supersonic region). For linear perturbation of mass accretion rate, ω^2 happens to be positive in the subsonic region of flow in both relativistic and nonrelativistic flows [110][77][78]. Since $f^{\mu\nu}$ for linear perturbation of the Bernoulli's constant and $f^{\mu\nu}$ for the linear perturbation of mass accretion rate only differ by a conformal factor, hence the sign of the conformal factor cancels out in the numerator and denominator. Hence the conclusion is same for both the perturbations. Hence ζ' is of oscillatory kind, it does not blow up with time. ζ' , being not blown up, validates the applicability of the linear stability analysis through standing waves in the subsonic region.

We introduced linear perturbation in the fluid medium by introducing linear perturbation in density and velocity of the medium. We see that linear perturbation, ζ' is the linear combination of linear perturbation of density and linear perturbation of radial fluid velocity, it has the

following generic structure for all the cases.

$$\zeta'(X, t) = f_{\zeta\rho}(X)\rho'(X, t) + f_{\zeta v}(X)v'(X, t) \quad (4.89)$$

where $f_{\zeta\rho}(X)$ and $f_{\zeta v}(X)$ are the functions of the radial coordinate X .

Linear perturbation of mas accretion rate, λ' also has the similar structure.

$$\lambda'(X, t) = f_{\lambda\rho}(X)\rho'(X, t) + f_{\lambda v}(X)v'(X, t) \quad (4.90)$$

In other words the above two equations can be expressed as a matrix equation

$$\begin{pmatrix} \zeta' \\ \lambda' \end{pmatrix} = \begin{pmatrix} f_{\zeta\rho} & f_{\zeta v} \\ f_{\lambda\rho} & f_{\lambda v} \end{pmatrix} \begin{pmatrix} \rho' \\ v' \end{pmatrix} = \hat{f} \begin{pmatrix} \rho' \\ v' \end{pmatrix} \quad (4.91)$$

The expressions of f' and ζ' for all the cases show that $\det(\hat{f})$ is nonzero in general for subsonic flows, i.e., \hat{f} is a non-singular matrix. One easy way to see this is that $f_{\zeta\rho}(X)$ contains c_{s0}^2 but $f_{\zeta v}(X)$, $f_{\lambda\rho}(X)$, $f_{\lambda v}(X)$ do not contain c_{s0}^2 . For subsonic flow, the right hand side of the equation (4.89) and the right hand side of the equation (4.90) do not differ just by a conformal factor and this implies non-singularity of the matrix \hat{f} . Hence both ρ' and v' can be expressed as a linear combination of ζ' and λ' . Now considering the physical situation, X_1, X_2 are same for both ζ' and λ' . Hence at these two radii, not only ζ' and λ' vanish but also ρ' and v' vanish. In the next section we have introduced some thermodynamic quantities like entropy, temperature. Since ρ' is zero at these two radii and the linear perturbations of the thermodynamic quantities like enthalpy, entropy are proportional to ρ' , the linear perturbation of all thermodynamic quantities are zero at these two radii. Similarly the linear perturbation of dynamical quantities like kinetic energy per unit mass are zero at these two radii because linear perturbation of the dynamical quantities are proportional to v' ¹.

As the standing wave analysis, valid for subsonic flows, show that both ζ' and λ' do not blow in time, the linear perturbation of all the dynamical quantities and the thermodynamic quantities do not blow in time too. Therefore, the steady state solution for subsonic flows are stable under

¹there is an exception, in the case of axially symmetric disk accretion we have seen that $v'_\phi \propto \rho'$

standing wave perturbations (perturbations which are formed due to the superposition of two travelling sound wave (one going upstream and the other going down stream of the flow). We discuss about travelling wave in the next section.)

The steady state solutions are governed by the integrals of motions, i.e., Bernoulli's constant, mass accretion rate and specific angular momentum (for axisymmetric disk accretion). For the disk accretion models which we have considered, the linear perturbation of specific angular momentum happens to be zero due to symmetry (see equation 4.62). The non-trivial linear perturbations are the perturbation of the accretion rate and the perturbation of the Bernoulli's constant. For time dependent case in the linear perturbation method, the time dependent solutions are also governed by the linear perturbation of these two integrals of motion.

4.3.2 Travelling wave analysis

We study high frequency travelling wave. We assume the wavelength of the wave to be smaller than the relevant smallest length scale of the problem. We assume the travelling wave to be of the following form.

$$P_\omega(X) = \exp \left[\sum_{n=-1}^{n=\infty} \frac{K_n(X)}{\omega^n} \right] \quad (4.92)$$

This form is assumed because when we assume ω to be high, $\frac{1}{\omega}$ tends to zero. After multiplying the equation (4.87) by $\frac{1}{\omega^2}$, we see that the coefficient of the second derivative of $P_\omega(X)$ is proportional to $\frac{1}{\omega^2}$. This equation is now structurally somewhat similar to the Schrödinger equation where to solve by WKB method, we expand the phase of the wave function in a perturbation series using \hbar (the Planck's constant) as parameter. Here $\frac{1}{\omega}$ takes the role of \hbar . Using equation (4.86) in (4.87) and equating the coefficients of ω and ω^2 , we get

$$K_{-1}(X) = i \int^X \frac{f^{Xt} \pm \sqrt{(f^{Xt})^2 - f^{tt} f^{XX}}}{f^{XX}} dX \quad (4.93)$$

$$K_0(X) = -\frac{1}{2} \ln \left(\sqrt{(f^{Xt})^2 - f^{tt} f^{XX}} \right) \quad (4.94)$$

From the expression, it is obvious that $K_{-1}(X)$ is a purely imaginary quantity ($((f^{Xt})^2 - f^{tt} f^{XX}) > 0$ because the wave equation 4.85 is hyperbolic and one can also check it by putting

explicitly the values of $f^{\mu\nu}$ s in the expression). For consistency in the solution, the following relation must hold.

$$\omega K_{-1}(X) \gg K_0(X) \gg \dots \quad (4.95)$$

Nonrelativistic framework

In Newtonian-gravity framework, for all the geometries (spherically symmetric accretion and disk geometries) discussed earlier, $K_{-1}(X)$ and $K_0(X)$ have the following general structure.

$$K_{-1}(X) = i \int^X \frac{1}{v_0(X') \pm \sqrt{\sigma} c_{s0}(X')} dX' \quad (4.96)$$

and

$$K_0(X) = \text{constant} + \frac{1}{2} \ln(v_0(X) c_{s0}(X)) \quad (4.97)$$

where $\sigma = \frac{2}{\gamma+1}$ for vertical equilibrium disk accretion and $\sigma = 1$ for spherically symmetric accretion and other disk geometries. The expressions are very similar to the case of linear perturbation of mas accretion rate. At large radii, equation (4.95) is true due to the virtue of high frequency approximation. The expressions of $K_{-1}(X)$ demonstrates that near the critical point, for the wave travelling upstream of motion, $\frac{\partial K_{-1}(X)}{\partial X}$ is very large near acoustic event horizon (or dumbhole horizon). The condition (4.95) is well satisfied there. The conclusions are same for both the cases, i.e., the case of linear perturbation of mas accretion rate and the case of linear perturbation of the Bernoulli's constant.

General relativistic framework

The expression of K_0 and K_{-1} is given by

$$K_0(X) = \text{constant} + \frac{1}{2} \ln \left(\frac{v_0 c_{s0} \sqrt{g_{tt} g_{XX}}}{v_0^t} \Omega(X) \right) \quad (4.98)$$

and

$$K_{-1}(X) = i \int^X dX \frac{\left(v_0 v_0^t \left(1 - \frac{\sigma}{c_{s0}^2} \right) \pm \frac{1}{\sqrt{g_{tt} g_{XX} c_{s0}}} \Omega(X) \right)}{g^{XX} + v_0^2 \left(1 - \frac{\sigma}{c_{s0}^2} \right)} \quad (4.99)$$

where

$$\sigma = 1 + \beta \quad \text{for vertical equilibrium disk model}$$

$$\sigma = 1 \quad \text{for spherically symmetric radial accretion and other disk models}$$

$$\Omega(X) = 1 \quad \text{for spherically symmetric radial flow}$$

$$\Omega(X) = \sqrt{\sigma + g_{\phi\phi}(v_0^\phi)^2(\sigma - c_{s0}^2)} \quad \text{for disk accretion}$$

$\frac{\partial K_{-1}(X)}{\partial X}$ is very large near the critical point (The critical point is effectively same as the sonic point, we use the word ‘effectively’ because in the vertical equilibrium model sound speed gets modified.) as the denominator approaches zero there. Hence condition (97) is well satisfied near sonic horizon. For very large X , $K_0(X)$, $K_{-1}(X)$ are close to non-relativistic values, the criteria (97), is true at large X due to the virtue of high ω .

4.4 Summary and Concluding Remarks

In this section, we are going to give some more insights about the problem. Linear perturbation of several quantities obey massless scalar field equation in acoustic space time background. Unruh[1] first shown that linear perturbation of velocity potential obeys massless scalar field equation in curved space time background. In these papers[78], it is explicitly shown that linear perturbation of mass accretion rate also gives acoustic metric. In this chapter, we’ve shown that the Bernoulli’s constant also produces analogue gravity.

For non-general relativistic background flow of adiabatic fluid, the Bernoulli’s constant can be expressed as an additive term of various energy contribution to the total energy of the system. If one is interested to learn how the various sources of energy of the system, i.e., gravitational, mechanical, thermal and rotational, gets perturbed individually, the perturbation scheme of the Bernoulli’s constant will be of great help to understand such physics and related issues. For instance, one can directly connect the Bernoulli’s constant to some dynamical and thermodynamic

energy quantities. One can define specific total energy[40] as

$$E = \left(\frac{1}{2}v^2 + \xi + V_{ext}\right)$$

where ξ is specific internal energy. After a little manipulation, using equation (4.10), i.e., for non relativistic case, one can find a set of equations relating some dynamical energy quantities and thermodynamic quantities for adiabatic flow that

$$\begin{aligned} \partial_\mu(f^{\mu\nu}(\mathbf{x})\partial_\nu)E'(\mathbf{x},t) + \frac{\gamma-1}{\gamma}\partial_\mu(f^{\mu\nu}(\mathbf{x})\partial_\nu)h' &= 0 \\ \partial_\mu(f^{\mu\nu}(\mathbf{x})\partial_\nu)E'(\mathbf{x},t) + (\gamma-1)\partial_\mu(f^{\mu\nu}(\mathbf{x})\partial_\nu)\xi'(\mathbf{x},t) &= 0 \\ \partial_\mu(f^{\mu\nu}(\mathbf{x})\partial_\nu)E'(\mathbf{x},t) + (\gamma-1)(\partial_\mu(f^{\mu\nu}(\mathbf{x})\partial_\nu)F' + s_0\partial_\mu(f^{\mu\nu}(\mathbf{x})\partial_\nu)T' &= 0 \\ \partial_\mu(f^{\mu\nu}(\mathbf{x})\partial_\nu)E'(\mathbf{x},t) + \frac{\gamma-1}{\gamma}\partial_\mu(f^{\mu\nu}(\mathbf{x})\partial_\nu)G'(\mathbf{x},t) + \frac{\gamma-1}{\gamma}s_0\partial_\mu(f^{\mu\nu}(\mathbf{x})\partial_\nu)T' &= 0 \end{aligned}$$

where E' , h' , G' , F' and ξ' are linear perturbation in E , specific enthalpy, specific Gibbs free energy, specific Helmholtz's free energy and specific internal energy. s_0 is constant entropy value for adiabatic case, i.e., $s_0 = \ln\left(\frac{\rho_0}{\rho}\right)$. For isothermal case we find that

$$\begin{aligned} \partial_\mu(f^{\mu\nu}(\mathbf{x})\partial_\nu)E'(\mathbf{x},t) + \partial_\mu(f^{\mu\nu}(\mathbf{x})\partial_\nu)G'(\mathbf{x},t) &= 0 \\ \partial_\mu(f^{\mu\nu}(\mathbf{x})\partial_\nu)E'(\mathbf{x},t) - \partial_\mu(f^{\mu\nu}(\mathbf{x})\partial_\nu)F'(\mathbf{x},t) &= 0 \end{aligned}$$

For General Relativistic case and for adiabatic flow, $\therefore h = g - Ts$ and $\zeta = hv_t$, defining $\alpha' = (gv_t)'$ and $\beta' = (Tv_t)'$

$$\partial_\mu(f^{\mu\nu}(\mathbf{r})\partial_\nu)\alpha'(\mathbf{r},t) + s_0\partial_\mu(f^{\mu\nu}(\mathbf{r})\partial_\nu)\beta'(\mathbf{r},t) = 0$$

Clearly not all energy quantities satisfy the differential equation satisfied by linear perturbation of the Bernoulli's constant but if one can perturb only the thermodynamic quantities without perturbing the dynamical quantities, then one can find again acoustic geometry and do analogue gravity on that. We introduce here another important finding of related interest. Linear perturbation of any algebraic function of ζ obeys massless scalar field equation in acoustic space time

if the function and it's first derivative with respect to ζ exist at the background value, i.e., at ζ_0 . The wave equation satisfied by linear perturbation of the function is exactly the same as the wave equation obeyed by linear perturbation of ζ . Same argument holds for the linear perturbation of mass accretion rate as well. To prove this, let's consider an algebraic function of ζ , $F(\zeta)$. We have

$$\partial_\mu f^{\mu\nu}(\mathbf{x})\partial_\nu \zeta' = 0 \quad (4.100)$$

where ζ is perturbed linearly as

$$\zeta(\mathbf{x}, t) = \zeta_0(\mathbf{x}) + \zeta'(\mathbf{x}, t)$$

$$\begin{aligned} \Rightarrow F(\zeta(\mathbf{x}, t)) &= F(\zeta_0(\mathbf{x}) + \zeta'(\mathbf{x}, t)) \\ &= F(\zeta_0 + \zeta'(\mathbf{x}, t)) \\ &= F(\zeta_0) + \left(\frac{dF}{d\zeta}\right)_{\zeta_0} \zeta'(\mathbf{x}, t) \\ &= F_0 + F' \end{aligned}$$

$\zeta_0, \left(\frac{dF}{d\zeta}\right)_{\zeta_0}$ are constant numbers because $F(\zeta)$ and it's first derivative exist at ζ_0 and ζ_0 is a constant of motion. Linear perturbation of $F(\zeta)$ is a constant multiple of ζ' . Hence linear perturbation of $F(\zeta)$ obeys exactly same massless scalar field equation as obeyed by ζ' .

This is another advantage of constants of motion, ζ and f , over the velocity potential ψ , is that one can construct infinitely many quantities with any of constants of motion, ζ or f , whose linear perturbation obeys massless scalar field equation in curved space time.

Similar argument holds for the case of mass accretion rate in 1+1 dimension as well. In this fashion one can construct two disjoint sets of algebraic functions from two independent constants of motion ζ and f respectively. At this point, we thus argue that the linear perturbation of any quantity of fluid motion if obeys a massless scalar field equation, that equation will be same as wave equation satisfied by either of ζ' or f' .

One can also proceed with velocity potential in the analysis instead of the Bernoulli's constant. Here we have started by analysing the linear perturbation of the Bernoulli's constant

instead of velocity potential. This is an independent approach to the same problem of analogue gravity. There is so far no work, of course to the best of our knowledge, analysing linear perturbation of velocity potential in the case of vertical equilibrium disk model for both relativistic and non relativistic case; we find that for vertical equilibrium disk model (not shown for brevity)

$$\partial_{\mu} f^{\mu\nu}(\mathbf{x}) \partial_{\nu} \psi' = 0 \quad (4.101)$$

where ψ' is linear perturbation of velocity potential, ψ . One can use the relation $\partial_t \psi' = \zeta'$ to find

$$\partial_{\mu} f^{\mu\nu}(\mathbf{x}) \partial_{\nu} \zeta' = 0. \quad (4.102)$$

This is clearly an alternative approach.

Chapter 5

Steady State Transonic Solution of self-gravitating spherically symmetric accretion

Most of the contents of this chapter are taken from our work 'Bondi flow revisited' [120]. Spherically symmetric Bondi flow [9] studies the dynamics of the infalling test fluids. In the present chapter, a novel iterative method is introduced to study the effect of the inclusion of the mass of the accreting material. The growth of the accretor is not considered as a consequence of the accretion and hence the direct effect of the inclusion of the self gravity is not studied. For usual astrophysical accretion, the aforementioned approximation, that the accretion rate as well as the time scale to study the problem is not so large that the mass of the accretor will change – is a valid approximation.

Steady state accretion of one temperature fluid onto a non spinning stationary (the observer is in the co-moving frame) accretor is considered. A more appropriate effective gravitational potential in comparison to what had been assumed by Chia [111] is considered. In that work by Chia [111], the considered potential which includes the gravity of the medium, does not satisfy Poisson's equation for gravity.

We find that the inclusion of fluid mass alters the location of the critical point of the flow as well as the values of the accretion variables measured at the critical point. It is found that the

Mach number vs radial distance profile, the usual topology of the phase portrait of the Bondi flow, takes a different form for such massive accretion. The flow profile is characterized using a realistic set of astrophysically relevant parameters.

5.1 Governing Equations

As steady flow is considered, the Bernoulli's equation [40] is

$$\frac{v^2}{2} + \int \frac{dp}{\rho} + \psi(r) = \text{constant} \quad (5.1)$$

where fluid velocity is v , pressure is p and $\psi(r)$ is the gravitational potential due to the accretor and the infalling fluid itself. $\psi(r)$ satisfying Poisson's equation is as below,

$$\psi(r) = -\frac{GM}{r} - \frac{4\pi G}{r} \int_{R_*}^r \rho(r)r^2 dr - 4\pi G \int_r^\infty \rho(r)r dr \quad (5.2)$$

where R_* is the radius of the accretor.¹ The barotropic equation is

$$p = K\rho^\gamma \quad (5.3)$$

where K is a constant. The sound speed follows the relation,

$$c_s^2 = \left(\frac{\partial p}{\partial \rho} \right)_s = \frac{\gamma p}{\rho} \quad (5.4)$$

where s = entropy. The energy of fluid element per unit mass is E ². Fluid velocity at infinity is zero, so according to Bernoulli's equation,

$$\frac{v^2}{2} + \frac{c_s^2}{(\gamma-1)} + \psi(r) = E = \frac{c_{s\infty}^2}{(\gamma-1)} \quad (5.5)$$

Physically, infinity is taken to be a large distance such that the potential energy terms are vanishing there. This issue discussed in details later in section 5.6. Some dimensionless variables

¹We do not scale the the variables similar to the chapter 3, we will use different scaling for simplicity.

²This is the Bernoulli's constant, ζ having the dimension of energy.

are defined as

$$x = \frac{r}{\frac{GM}{c_{s\infty}^2}}, y = \frac{v}{c_{s\infty}}, z = \frac{\rho}{\rho_\infty}$$

where $c_{s\infty}$ is the sound speed at infinity and ρ_∞ is the density of fluid at infinity. From equation (5.5), introducing the dimension less variables, we get

$$\frac{y^2}{2} + \frac{z^{(\gamma-1)}}{(\gamma-1)} - \frac{1}{x} - \alpha \left(\frac{I_1}{x} + I_2 \right) = 0 \quad (5.6)$$

where $\alpha = 4\pi\rho_\infty G^3 M^2 c_{s\infty}^{-6}$, $I_1 = \int_{x^*}^x z x^2 dx$ and $I_2 = \int_x^\infty z x dx$ with $x^* = \frac{R_*}{\left(\frac{GM}{c_{s\infty}^2}\right)}$

The mass accretion rate is obtained by integrating the continuity equation (using spherical symmetry) 4.1,

$$\dot{M} = 4\pi r^2 \rho v = 4\pi (GM)^2 c_{s\infty}^{-3} \rho_\infty x^2 y z$$

Another dimensionless variable is defined as $\lambda = x^2 y z$ and from the above equation mass accretion rate is proportional to λ . Now, equation (5.6) can be rewritten as follows,

$$\frac{\lambda^2}{2z^2} + \frac{(z^{\gamma-1} - 1)}{(\gamma-1)} x^4 - (1 + \alpha I_1) x^3 - \alpha x^4 I_2 = 0 \quad (5.7)$$

In the next section, we find the differences in critical points of the flow dynamics due to the inclusion of the gravity of the medium.

5.2 Calculations of Critical Point of the flow

Now, our aim is to maximize the accretion rate. We find x , y , z for which λ is maximized. From equation (5.7) setting $\frac{\partial \lambda}{\partial x} \Big|_{(x=x_c, y=y_c, z=z_c)} = 0$ and $\frac{\partial \lambda}{\partial z} \Big|_{(x=x_c, y=y_c, z=z_c)} = 0$, we get respectively

$$\frac{4(z_c^{(\gamma-1)} - 1)x_c}{(\gamma-1)} - 3(1 + \alpha I_{1c}) - 4\alpha x_c I_{2c} = 0 \quad (5.8)$$

and

$$\lambda_c^2 = z_c^{\gamma+1} x_c^4 \quad (5.9)$$

Using equation (5.9), from equation (5.7), we get

$$\frac{z_c^{(\gamma-1)} x_c}{2} + \frac{(z_c^{(\gamma-1)} - 1) x_c}{(\gamma - 1)} - 1 - \alpha(I_{1c} + x_c I_{2c}) = 0 \quad (5.10)$$

As a consequence we have the following:

The critical values x_c , y_c and z_c correspond to the Mach one, i.e; the transonic curve corresponds to maximum accretion rate. It is worth mentioning that the Mach number is defined as the ratio of the speed of the medium and the thermodynamic sound speed.

From definition,

$$\lambda_c = x_c^2 y_c z_c$$

Using equation (5.9) and from the expression of Mach number, m

$$m = \frac{v}{c_s} = y_c z_c^{-\frac{(\gamma-1)}{2}} = 1$$

We get from equation (5.8) and (5.10), ,

$$\frac{x_c}{x_b} = \frac{1 + \alpha I_{1c}}{1 + \alpha(\gamma - 1) I_{2c}} \quad (5.11)$$

$$\left(\frac{z_c}{z_b}\right)^{(\gamma-1)} = (1 + \alpha(\gamma - 1) I_{2c}) \quad (5.12)$$

Using equation (5.9), we get

$$\frac{\lambda_c}{\lambda_b} = (1 + \alpha I_{1c})^2 (1 + \alpha(\gamma - 1) I_{2c})^{\frac{(5-3\gamma)}{2(\gamma-1)}} \quad (5.13)$$

where x_b , z_b , λ_b are the critical values in the case of spherical Bondi accretion where fluid mass is not considered. These values are as follows:

$$\begin{aligned}x_b &= \frac{(5-3\gamma)}{4} \\z_b^{(\gamma-1)} &= \frac{1}{2x_b} \\ \lambda_b^2 &= z_b^{(\gamma+1)} x_b^4\end{aligned}$$

5.3 Equation of motion of the infalling fluid

We have to know the equation of motion of the infalling fluid to find the behaviour of the Mach number vs radial distance profile for self gravitating steady state Bondi accretion. According to Euler's momentum conservation equation,

$$\rho \frac{D\mathbf{v}}{Dt} = -\nabla p - \rho \nabla \psi$$

$\frac{D}{Dt}$, the Lagrangian derivative, the acceleration of a fluid element in flow, can also be denoted by $\frac{d}{dt}$ as described in Chapter-2.

ψ is the external potential energy; in our case, ψ is the gravitational potential energy term. Considering steady flow, we have

$$v \frac{dv}{dr} = -\frac{1}{\rho} \frac{dp}{dr} - \frac{GM}{r^2} - \frac{4\pi G}{r^2} \int_{R_*}^r \rho r^2 dr \quad (5.14)$$

Considering spherically symmetric steady flow, we get accretion rate from the continuity equation, although we have already assumed spherical symmetry in the beginning

$$\dot{M} = 4\pi r^2 \rho v = \text{constant} \quad (5.15)$$

Considering steady flow, using equation (5.3), (5.4), (5.14), we have

$$\frac{dv}{dr} = \frac{\left(\frac{2c_s^2}{r} - \frac{GM}{r^2} - \frac{4\pi G}{r^2} \int_{R_*}^r \rho r^2 dr\right)}{\left(v - \frac{c_s^2}{v}\right)} \quad (5.16)$$

Now, using equation (5.15), (5.3), (5.4), we have

$$\frac{dc_s}{dr} = \frac{c_s(1-\gamma)}{2} \left(\frac{2}{r} + \frac{1}{v} \frac{dv}{dr}\right) \quad (5.17)$$

If we can solve these equations we can get the Mach number vs radial distance profile except sonic point because equation (16) takes 0/0 form at the transonic point. We seek for transonic solution which has finite velocity gradient at the critical/sonic point.

Applying L'Hospital's rule there we get a quadratic equation as

$$Aq^2 + Bq + C = 0$$

where,

$$\begin{aligned} A &= (1 + \gamma) \\ B &= \frac{4c_{sc}(\gamma - 1)}{r_c} \\ C &= \frac{2c_{sc}^2(2\gamma - 1)}{r_c^2} - \frac{2GM}{r_c^3} + 4\pi G\rho_c - \frac{8\pi G}{r_c^3} I_{1c} \\ q &= \left. \frac{dv}{dr} \right|_{\text{critical point}} \end{aligned}$$

c_{sc} is the sound speed at critical point. r_c is the radial distance of critical point from the centre of the accretor. So,

$$q = \frac{-B \pm \sqrt{B^2 - 4AC}}{2A}. \quad (5.18)$$

The problem is still unsolvable because we need to know the density profile of the infalling fluid in the first place to find the values of the dimensionless variables at critical point (which will serve as the initial conditions to solve differential equations (5.16) and (5.17)) and we have no idea about the density profile. In the next section, we develop a methodology to solve the problem.

5.4 The Method of iteration

In equation (5.11), (5.12), (5.13) and (5.16) ρ appears to be a variable about which we have no information. We assume that even if we include mass of the medium it does not change the critical values x_c , y_c , z_c and λ_c abruptly, i.e; we are dealing with a problem where inclusion of fluid mass effect the system weakly. This issue is discussed in details in section 5.11. We find the values of the dimensionless quantities from equations (5.11), (5.12) and (5.13) by method of iteration. We use the value of z as the usual z of spherically symmetric Bondi flow to find the integrals I_{1c} and I_{2c} and thus the changes in critical parameters is found . x_c appears in the definite integrals I_{1c} and I_{2c} as upper limit and lower limit respectively and we replace x_c by $x_b(= (5 - 3\gamma)/4)$ in the 1st iteration. We can compute the critical parameters from equation (5.11), (5.12) and (5.13). We are considering weak gravitational field due to fluid mass, so we are satisfied with only the 1st iteration. The values of I_{1c} and I_{2c} in the 1st iteration are as below.

$$I_{1c} = \int_{x^*}^{x_b} z_{\text{Bondi}}(x)x^2 dx \quad (5.19)$$

$$I_{2c} = \int_{x_b}^{\infty} z_{\text{Bondi}}(x)x dx \quad (5.20)$$

where $z_{\text{Bondi}}(x)$ is z of the usual Bondi accretion (where the gravity of the medium is not taken into account.). As there is no proper analytic form for $z_{\text{Bondi}}(x)$, we find the integrals using the numerical values of $z_{\text{Bondi}}(x)$ at different x .

5.5 The limits of the integrals

x_b is the upper limit and lower limit of the integrals, I_{1c} and I_{2c} respectively. x^* is the lower limit of the integral I_{1c} . We can put x^* and mass in the equation using values of mass and radius of some known stars. Alternatively, we can find the radius of a star when the mass of a star is given from any empirical relation. We use the following empirical relations [112] between mass and radius of a Main Sequence star.

$$\frac{R_{\star}}{R_{\odot}} = 1.06 \left(\frac{M}{M_{\odot}} \right)^{0.945} \quad M < 1.66M_{\odot} \quad (5.21)$$

and

$$\frac{R_{\star}}{R_{\odot}} = 1.33 \left(\frac{M}{M_{\odot}} \right)^{0.555} \quad M > 1.66M_{\odot} \quad (5.22)$$

where R_{\star} , R_{\odot} are the radius of the star and of the Sun and M , M_{\odot} are the mass of the star and of the Sun respectively. Thus the lower limit of the integral I_{1c} is fixed. One can use mass and radius of any kind of stars not necessarily that the accretor has to be a Main Sequence star until if the relativistic effects are not significant. ∞ appears in the upper limit of the integral I_{2c} . By ∞ we mean some large distance from the accretor where gravity is weak. Let's call this large distance to be r_{∞} and corresponding value of the dimensionless parameter to be x_{∞} . The mass, the energy and γ of the fluid are given. At infinity as the velocity of the fluid is zero, we have

$$\frac{c_{s\infty}^2}{(\gamma-1)} - \frac{GM}{r_{\infty}} - \frac{4\pi G}{r_{\infty}} \int_{R_{\star}}^{r_{\infty}} \rho r^2 dr = E \quad (5.23)$$

We compare the magnitude of the 1st term in potential energy with the specific energy. We set r_{∞} to some value such that the term $\frac{GM}{r_{\infty}}$ is negligibly small compared to energy of the infalling fluid.

Quantitatively, we set a very small quantity $Q1$ according to our desired precision as below.

$$Q1 = \frac{\left(\frac{GM}{r_{\infty}} \right)}{E} \quad (5.24)$$

Now we can easily find r_∞ . We use the density profile of Bondi accretion to evaluate the 2nd term of the potential energy (whereas the first term of the potential energy at r_∞ is $-\frac{GM}{r_\infty}$) in equation(5.23) (The Method of Iteration which is described in section 5.5). We need the density of the fluid at infinity. We choose the density of fluid at infinity to be small such that the term $\frac{4\pi G}{r_\infty} \int_{R_*}^{r_\infty} \rho r^2 dr$ is negligible compared to the energy E of the fluid.

Quantitatively, we set a very small quantity Q2 according to our desired precision as below.

$$\begin{aligned}
 Q2 &= \frac{\frac{4\pi G}{r_\infty} \int_{R_*}^{r_\infty} \rho r^2 dr}{E} \\
 &= \frac{\left[\frac{4\pi G \rho_\infty (GM)^3 I_{1\infty}}{r_\infty c_{s\infty}^6} \right]}{E} \\
 \rho_\infty &= \frac{Q2 E r_\infty (E(Y-1))^3}{4\pi G (GM)^3 I_{1\infty}} \tag{5.25}
 \end{aligned}$$

where we have used the method of iteration to find $I_{1\infty}$. As the 2nd and 3rd term of the equation (5.23) are taken to be negligibly small compared to the energy (E) of the infalling fluid,

$$E \cong \frac{c_{s\infty}^2}{(\gamma-1)} \tag{5.26}$$

Using method of iteration and putting the value of r_∞ from equation (5.24),

$$I_{1c} = \int_{x^*}^{x_b} z_{Bondi}(x) x^2 dx \tag{5.27}$$

$$I_{2c} = \int_{x_b}^{x_\infty} z_{Bondi}(x) x dx \tag{5.28}$$

Equation (5.28) is different from equation (5.20), here we have the physical upper limit which is x_∞ . Now we can numerically calculate the values I_{1c} and I_{2c} and put them in equation (5.11), (5.12) and (5.13) to find the changes in the critical parameters due to inclusion of fluid mass.

5.6 Physical Importance of Q1 and Q2

We can write the energy of infalling fluid at infinity as

$$E = \frac{c_{s\infty}^2}{(\gamma-1)} + EQ$$

where $Q(= Q1 + Q2)$ gives total precision of the problem. Hence in a summary, for a given E, M, γ and Q, we set at first Q1 to find appropriate r_∞ of the problem and setting Q2 accordingly gives us density of the infalling matter at infinity. If we closely look at the expressions of Q1 and Q2, we see that the ratio

$$s = \frac{Q2}{Q1} = \frac{\text{Mass of the entire medium}}{\text{Mass of the accretor}} \quad (5.29)$$

where mass of the medium is calculated mass by using density profile of Bondi accretion. We can intuitively say that greater the value of ratio Q2/Q1 greater the effect of inclusion of fluid mass, i.e; greater the departure from the usual Bondi accretion.

5.7 Behaviour of the critical parameters

We can now find the critical parameters. We have the mass M of the accretor, E or the temperature of the fluid at infinity, γ of the fluid as inputs and also we have fixed Q to be 0.02. Choosing s gives us r_∞ and density of fluid at infinity. Our parameter space is γ (4/3 to 5/3), E (0 to 1 in units of c^2). Temperature varies nearly from 10°K to few hundred degree kelvin (H1 region) for neutral hydrogen-interstellar medium [113]. This gives a rough idea about the input of specific energy of the infalling fluid. The specific energy varies in that temperature range nearly of the order of 10^{-12} to 10^{-10} in units of c^2 . We have plotted percentage change in the critical values due to inclusion of fluid mass with the γ -E parameter space. Temperature of the fluid at infinity is taken to vary nearly in the range of 10°K to few hundred degree kelvin. We find the shift in transonic surface due to inclusion of fluid mass for different s.

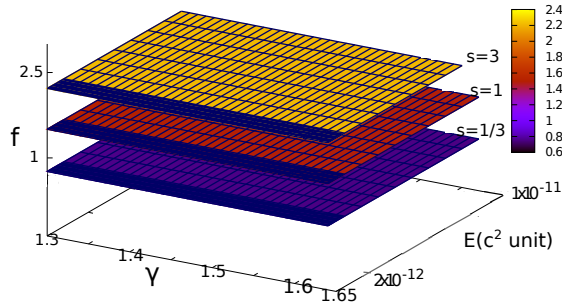


Figure 5.1: Behaviour of percentage change in x_b where $f = -(Dx/x_b) \times 100$ and $Dx = (x_c - x_b)$

The planes corresponding to different s seem parallel to γ - E plane because the variations in x_b for different s are incomparable. The whole picture becomes clear when we plot the behaviour for a single s .

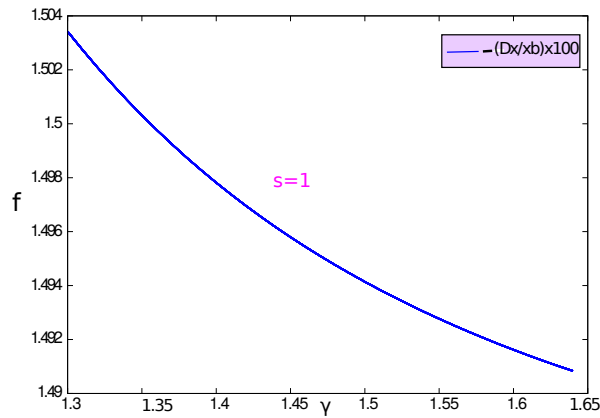


Figure 5.2: Projection of the surface of Fig. 5.1 for $s=1$ on $(-Dx/x_b) \times 100$ - γ plane.

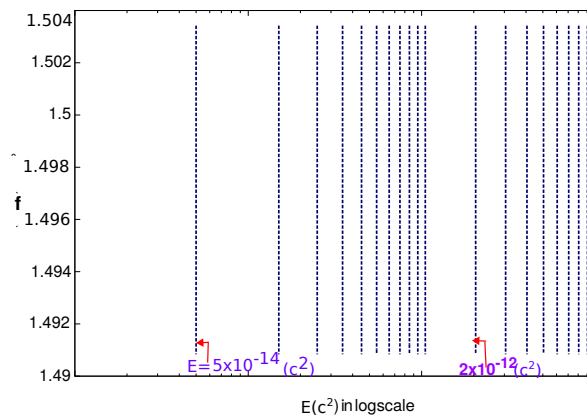


Figure 5.3: Projection of the surface of Fig. 5.1 for $s=1$ on $(-Dx/x_b) \times 100$ - E (in log scale) plane.

Fig. 5.2 and Fig. 5.3 implies that when s and E are given and also total precision Q is given, the shift in transonic surface does not depend on E and that's why only a single curve appear in Fig. 5.2, otherwise there would be several different curves for different E s. We can generate the surface for $s=1$ just by translation of the curve in Fig. 5.2 along E axis. The shift in critical point x_b is same for all E for a particular γ and Q . In the Fig. 5.3 the vertical lines signify the same thing, i.e; the points on a single vertical line gives the percentage change in x_b for different γ s. A single vertical line corresponds to a single energy. Actually fixing Q and s of the problem give Q_1 and Q_1 in return gives r_∞ for a given E . The dependence of changes in critical parameters on E is somehow wiped out when ρ_∞ is calculated after setting Q_2 of the problem. Inclusion of fluid mass decreases the radius of the transonic surface. More the total mass of the medium, greater the shift in x_b is (from figure (5.1)). Relatively small γ s give significant changes. We find the changes in other critical parameters.

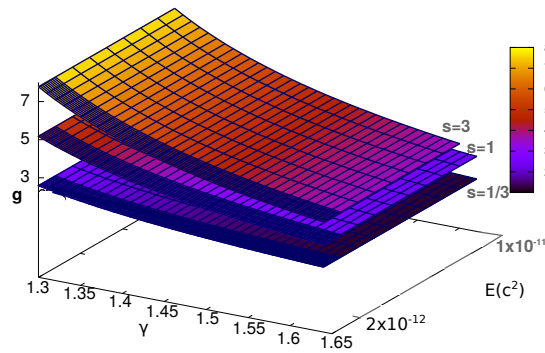


Figure 5.4: Behaviour of percentage change in z_b where $g = (Dz/z_b) \times 100$ and $Dz = (z_c - z_b)$

In the above figures, the colour is dark blue near energy 2×10^{-12} because we have worked with small energy steps near this region of energy, this can be seen in the projection plane too (Figure 5.3). For brevity, we have not plotted $E-(Dz/z_b) \times 100$. Similarly, percentage change in z_b does not depend on E and z_b increases significantly for γ close to $4/3$. Fig. 5.4 implies that if we increase s we increase the change in z_b which is intuitively obvious.

Another important point is that if we compare the percentage changes in z_b with x_b we see that inclusion fluid mass effect z_b more than x_b . The surfaces seem to converge towards $\gamma=1.65$. Similarly, percentage change in λ_b does not depend on E and it significantly increases for γ close to $4/3$. Observation of Fig. 5.6 shows that λ_b increases with s . Increasing s increases the

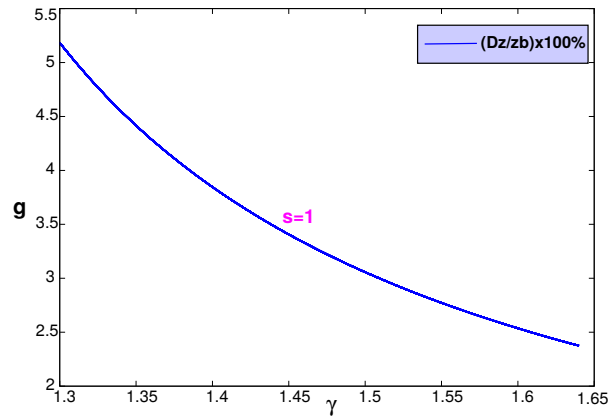


Figure 5.5: Projection of the surface of Fig. 5.4 for $s=1$ on $(Dz/z_b) \times 100 - \gamma$ plane.

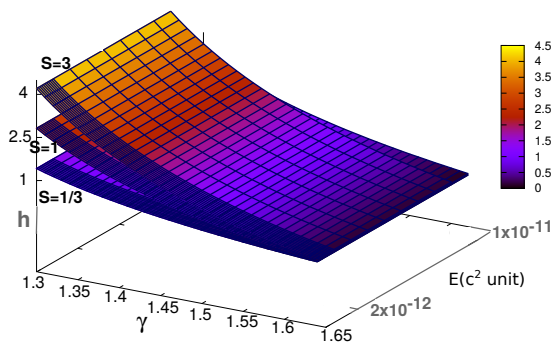


Figure 5.6: Behaviour of percentage change in λ_b where $h = (D\lambda/\lambda_b) \times 100$ and $D\lambda = (\lambda_c - \lambda_b)$ according to equation (5.13).

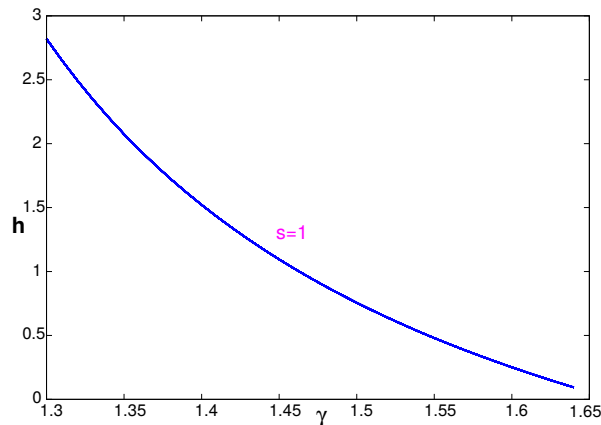


Figure 5.7: Projection of the surface of Fig. 5.6 for $s=1$ on $(D\lambda/\lambda_b) \times 100 - \gamma$ plane.

shift in the critical parameters. Another important observation is that the percentage change in x_b with respect to γ is not only smaller than the other critical parameters but also the variation in percentage change of x_b with γ is negligible compared to that for the other critical parameters.

One can safely say that percentage change in x_b doesn't depend on γ at all and actually it's a function of only one variable, s . Inclusion of fluid mass changes z_b much more significantly than the other critical parameters.

We find how do the critical parameters depend on the mass ratio of the fluid medium and the star. As percentage change in x_b is only a function of s , we fit the data points to find the nature

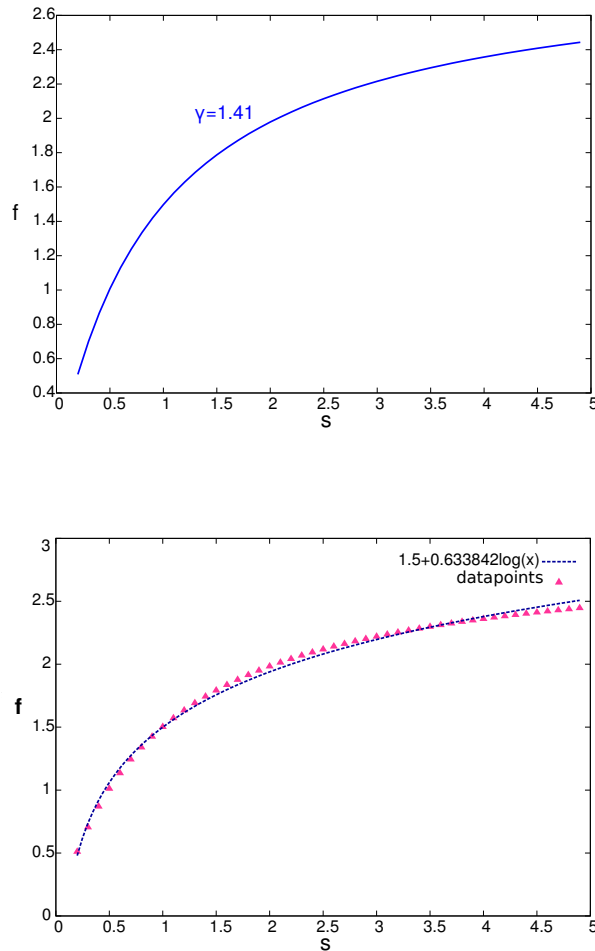
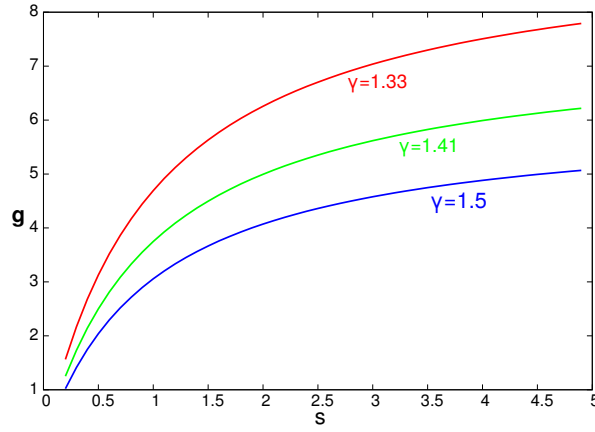
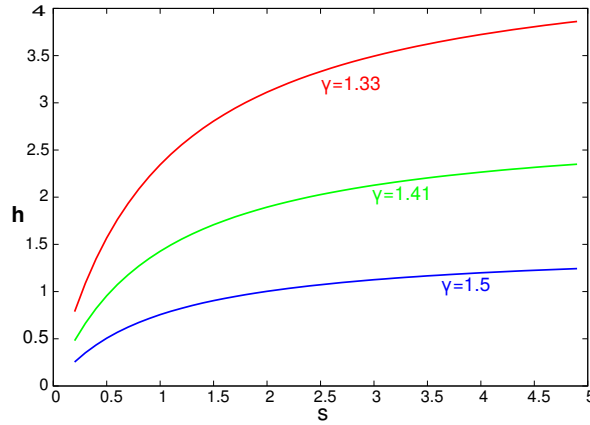


Figure 5.8: Dependence of percentage change in x_b on s and data points are fitted. We choose upper limit of s to be 5.

of dependence on s . We obtain an empirical relation as

$$f = \left(-\frac{Dx}{x_b} \times 100\right) = a + b \ln(s) \tag{5.30}$$

In our case, the positive constants are as $a = 1.5$ and $b = 0.633842$. Fig. 5.2 also shows that a has to be 1.5.

Figure 5.9: Dependence of percentage change in z_b on s .Figure 5.10: Dependence of percentage change in λ_b on s .

The changes in critical parameters increase with s . Fig. 5.9 and Fig. 5.10. also shows that why do the surfaces for z_b and λ_b converge towards $\gamma = 1.65$. We see that the separations between the curves of Fig. 5.9 and 5.10 for $\gamma = 1.33$ and 1.41 is greater than the separation between the curves for $\gamma = 1.41$ and 1.5.

Equation (5.30) implies that the test fluid approximation is good for $s \leq \exp(-a/b)$. This is the range of s where Bondi's assumptions and his results are applicable. In our case, that region corresponds to $s \leq 0.094$ and it's important to mention that a and b depends on Q . Similarly one can fit the same for λ_b and z_b as well and one will find some best fitting curves as $(f_{\lambda,z}(\gamma) + g_{\lambda,z}(\gamma)\ln(s))$ respectively. We can conclude from Fig. 5.7 and 5.5 that $f_{\lambda,z}(\gamma)$ are monotonically decreasing functions of γ . As the curves for other s have same nature as $s=1$, $g_{\lambda,z}(\gamma)$ can not be monotonically increasing function and as the surfaces are not parallel to each other which is obvious from Fig. 5.6 and 5.4, $g_{\lambda,z}(\gamma)$ has to be also monotonically decreasing function of γ . Now we find α [111] dependence (see section 5.1) of the percentage change in critical

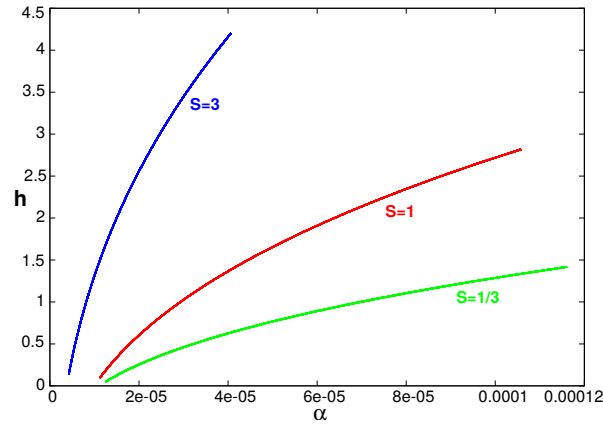


Figure 5.11: Dependence of percentage change in λ_b on α .

parameters. For brevity, we have not plotted the same for x_b and z_b because they are more or less of the same nature. Increasing α increases percentage change in the critical parameters. As percentage change in x_b is a slowly varying function of γ , it is also a slowly varying function of α . We have fitted the above plot as below,

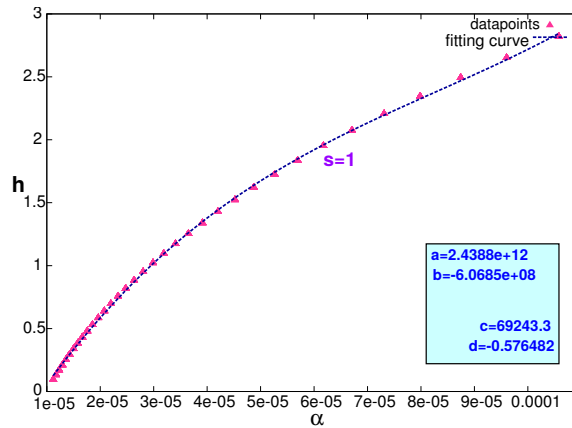


Figure 5.12: The data points are fitted to the curve $a\alpha^3+b\alpha^2+c\alpha+d$

We have found empirically a cubic polynomial,

$$h = \left(\frac{D\lambda}{\lambda_b}\right) \times 100 = a\alpha^3 + b\alpha^2 + c\alpha + d \quad (5.31)$$

The coefficients a, b, c, d depend on s, E and Q. Similarly percentage change in z_b and x_b have

cubic dependence on α and in the same way, we can fit them into cubic polynomials (not shown for brevity).

5.8 Ambiguity of the velocity gradient

Now we calculate du/dr at transonic surface from equation (5.18). We have got the critical parameters, we use them to find q . Important point is that we use the new value of x_c (found by 1st iteration) in I_{1c} appearing in the term C of the quadratic equation of q . Now according to equation (5.18), we obtain two values of q . As inclusion of fluid mass does not change the nature of flow abruptly, we choose the value of q which is closer to the value of critical (du/dr) in Bondi accretion. We plot the behaviour of the derivatives and compare those values with the spherical Bondi flow. We are calling the solutions of q as below,

$$q_1 = \frac{-B + \sqrt{B^2 - 4AC}}{2A}$$

$$q_2 = \frac{-B - \sqrt{B^2 - 4AC}}{2A}$$

we are calling

$$q = \left. \frac{dv}{dr} \right|_{\text{Bondi}}$$

where $\left. \frac{dv}{dr} \right|_{\text{Bondi}}$ is the value of $\frac{dv}{dr}$ at transonic surface in Bondi accretion.

From the above figure, we see that q_2 is much closer to q than q_1 . As we are considering that the inclusion of fluid mass does not alter the critical values abruptly (therefore, the sign of q will be negative which is the considered sign in the case of Bondi flow), we choose q_2 over q_1 .

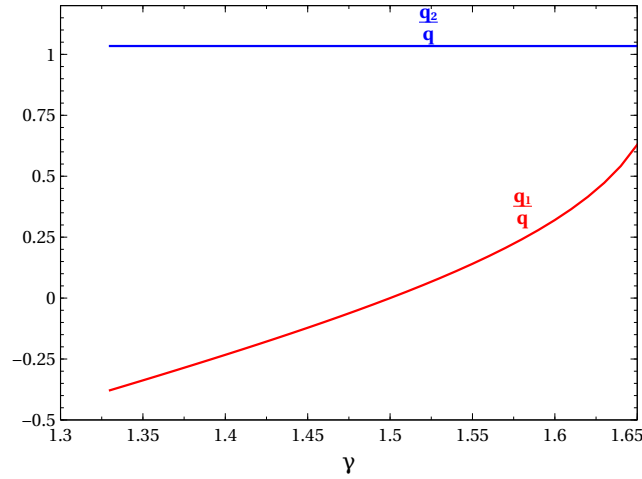


Figure 5.13: $\frac{q_1}{q}$, $\frac{q_2}{q}$ are plotted against γ with $s=3$ for comparison.

5.9 Mach number vs radial distance profile

Now we have found the initial conditions to find variation of Mach number with radial distance from the centre of the accretor. We have to numerically solve equation (5.16) and (5.17) simultaneously. We have now x_c, y_c, z_c and q_2 as initial conditions and we use the numerical values of density for spherically symmetric Bondi flow. Now Mach number(= u/c_s) profile can be found.

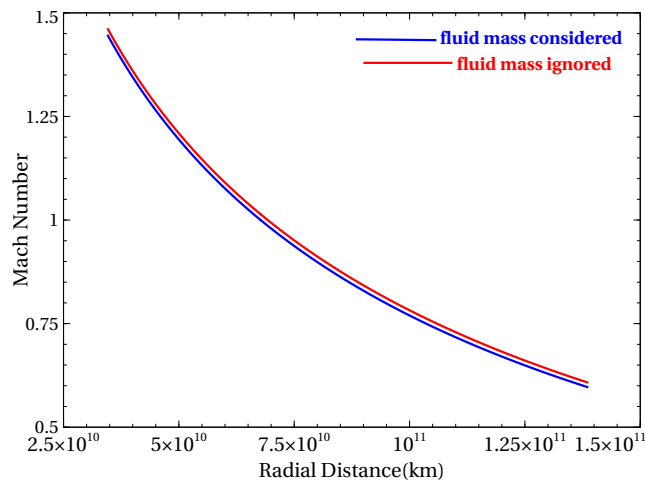


Figure 5.14: Mach number vs radial distance profile where mass of the Main-Sequence star is 1 solar mass, γ of the fluid is 1.41 and $s=3$

Inclusion of fluid mass make the infalling fluid to cross the sound speed nearer to the accretor (figure (5.15)).

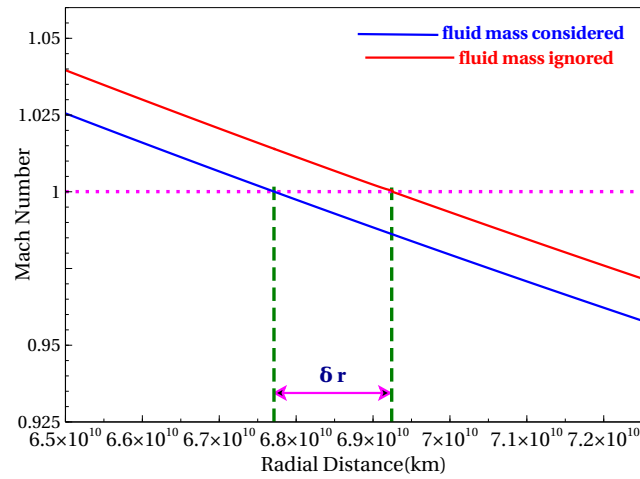


Figure 5.15: Close view near transonic surface. δr denotes the shift in radius of transonic surface in km.

5.10 Validity of Iteration Method

The density profile of the infalling fluid described by Bondi accretion is used in two places. At first it is used to find the critical parameters by evaluating I_{1c} and I_{2c} and by putting those values in the equations (5.27) and (5.28). It is used second time to find the Mach Number vs radial distance profile in the equation (5.16). This method of iteration is valid when the contributions from the additional terms which are considered to find the effect of inclusion of fluid mass are small compared to the other relevant terms[114]. Critical parameters satisfy the Bernoulli's equation(equation(5.10)). Observing equation (5.8) and (5.10) one can say that method of iteration is valid when

$$\alpha(I_{1c} + x_c I_{2c}) \ll 1 \quad (5.32)$$

The left hand side of the above inequality denotes the ratio of potential energies due to medium and the star at the critical point. Consequently, the method of iteration to find the critical parameters is valid when the ratio of potential energies at the critical point due to medium and due to the star($= \frac{\psi_{med}}{\psi_{star}}$) is small.

Momentum equation of fluid is used to find Mach Number vs radial distance profile in equation (5.16) and (5.17). The method of iteration will be valid to get the phase portrait until and unless the gravitational force term due to the medium is small compared to the force term due

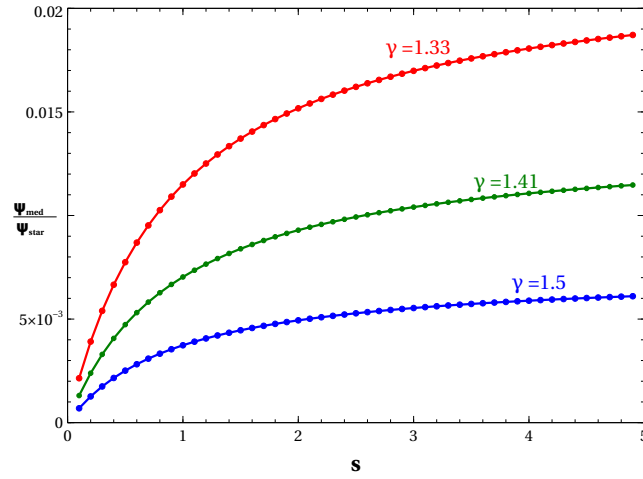


Figure 5.16: Dependence of potential energy ratio due to medium and the star at the critical point x_c for different s and γ

to the star. Using Gauss’s law, the ratio of inverse-square gravitational forces at a distance due to the medium and due to the star is simply the ratio of fluid-mass and the stellar mass where the fluid is considered to be inside of the sphere having centre at the origin (in this case due to spherical symmetry, this is the centre of mass of the star which is also the centre of mass of the composite system consisting of the star and the medium) and passing through the point in question. This mass ratio has to be less than unity. This condition should hold at least at the initial point, i.e; at the critical point x_c .

$$\alpha I_{1c} \ll 1 \tag{5.33}$$

From the above expressions, if the inequality (5.32) is satisfied the equation (5.33) is automatically is satisfied.

Surprisingly, for a fixed γ and Q , the mass ratio $\frac{M_c}{M}$ first increases with $s(\leq 1)$ and then after having a maxima, the mass ratio falls (see figure (5.17)). Actually, increasing s increases r_∞ and hence increases the extent of the medium and also effects density ρ_∞ (where ρ_∞ is fixed from Q_2 in section (5.6))which is shown in Fig. 5.18.

For a fixed Q of the problem, from equation(5.24) and (5.29),

$$r_\infty = \frac{GM(1+s)}{QE}$$

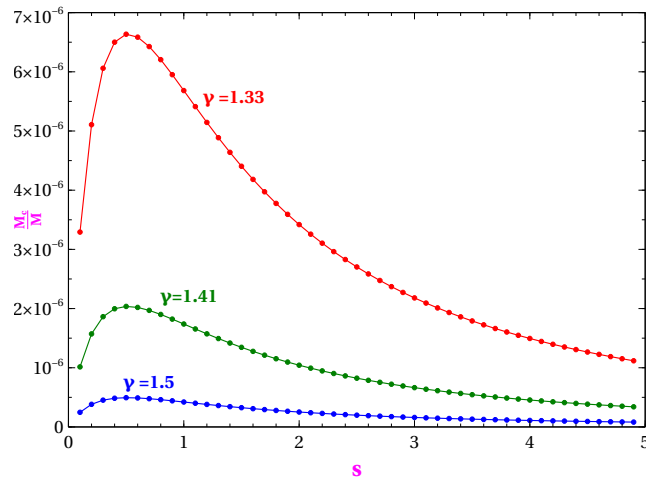


Figure 5.17: Dependence of gravitational force ratio due to medium and the star at the critical point x_c for different s and γ . αI_{1c} is denoted by $\frac{M_c}{M}$.

Transonic radius, r_{Bondi} for Bondi accretion is given by,

$$r_{\text{Bondi}} = \frac{GM(5-3\gamma)}{4E(\gamma-1)}$$

So, the ratio of transonic radius and r_∞ is

$$\frac{r_{\text{Bondi}}}{r_\infty} = \frac{x_b}{x_\infty} = \frac{Q(5-3\gamma)}{4(\gamma-1)(1+s)} \quad (5.34)$$

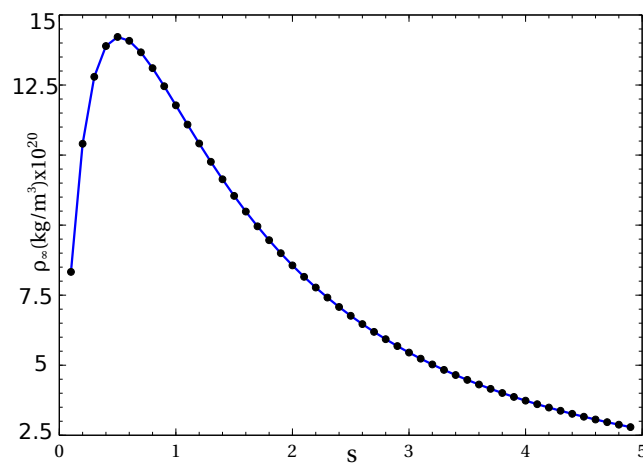


Figure 5.18: Dependence of density of fluid at infinity on s . Density of the medium at infinity is more or less same for a particular s for different γ .

That is how compared to the length scale of the problem, the radius of the medium increases with s .

Increase in r_∞ with s do simultaneously two things having opposite effects. Increase in r_∞ increases the extent of the medium which has the tendency to decrease $\frac{M_c}{M}$ and at the same time it gives more scope to the density of the fluid to increase to high value for small r in the neighbourhood of the star thus increasing $\frac{M_c}{M}$. One can also conclude this by drawing density profile of fluid in Bondi accretion for different s . This explains the Fig. 5.17. For $x < x_c$, gravitational force due to medium is much smaller than that due to the star which is obvious from inequality (33). With increasing distance from the star, the gravitational force due to the medium begins to become significant. It becomes equal to the gravitational force due to the star at $x = x_i$ (see figure (5.19)).

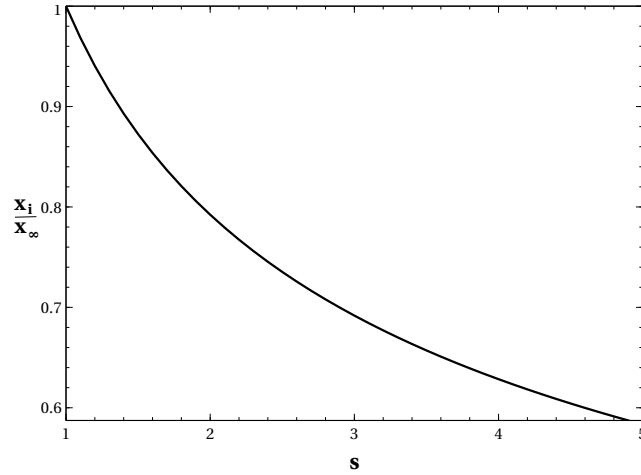


Figure 5.19: $\frac{x_i}{x_\infty}$ is plotted against s . $\frac{x_i}{x_\infty}$ does not have any γ and E dependence.

Using Gauss's law, the total mass of the medium extending from the surface of the star to x_i is equal to the mass of the star. For $s=1$, $\frac{x_i}{x_\infty}=1$, $s < 1$, $\frac{x_i}{x_\infty}$ is undefined and $s > 1$, $\frac{x_i}{x_\infty} < 1$ for obvious reasons. For $s \geq 1$ or $s \lesssim 1$, at $x \lesssim x_i$, the method of iteration starts to become invalid. For $x \geq x_i$, this method is invalid. In other words, x_i is roughly the upper limit up to which the Mach number plotted against radial distance from the stellar surface is more or less correct. Fig. 5.20 implies that with the increase in s , one gets less information about the phase portrait of the whole medium. If the Mach number is plotted against radial distance from the accretor with a upper limit of dimensionless radial distance, $x_u \ll x_i$ then it is correct.

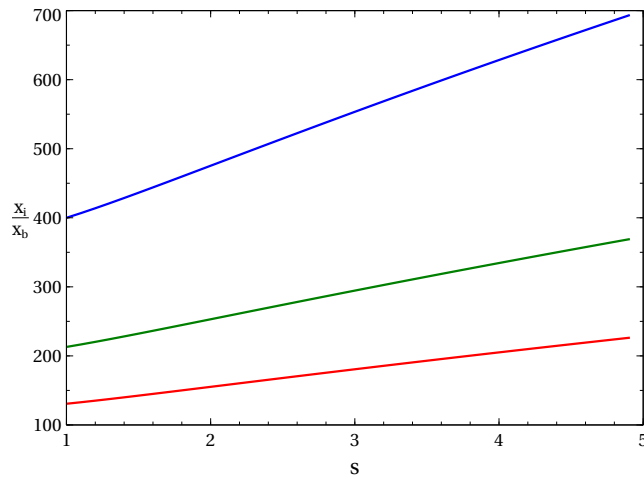


Figure 5.20: $\frac{x_i}{x_b}$ is plotted against s for different γ

Fig. 5.20 shows linear dependence of $\frac{x_i}{x_b}$ on s. In Fig. 5.14, $x_u = 2x_b$, $s=3$ and $\gamma = 1.41$. It is needless to say that the parameters in the figure (5.14) does not violate $x_i \gg x_b$ because in figure (5.20), we see that at $s = 3$, $\frac{x_i}{x_b} \sim 100$. Fig. 5.14 comes same even if the 3rd term in the numerator of equation(5.16) is not considered because from Fig. 5.17, $\frac{M_c}{M}$ is of the order of 10^{-6} .

5.11 Behaviour in relatively higher values of s

From equation (5.34), for a fixed value of Q and γ , the extent of the medium increases with s and from Fig. 5.17, one can intuitively argue that $\frac{M_c}{M}$ has a tendency to have very small value for large value of s. Fig. 5.16 shows a monotonically increasing behaviour of $\frac{\Psi_{med}}{\Psi_{star}}$ with s and also the slope of each curve corresponding to each γ has monotonically decreasing behaviour with s. Qualitatively, one can say that $\frac{\Psi_{med}}{\Psi_{star}}$ will certainly have higher value for relatively large s but the increment of $\frac{\Psi_{med}}{\Psi_{star}}$ will be very small in that range. Fig. 5.8, Fig. 5.9 and Fig. 5.10 also indicate same kind of behaviour in the changes of the critical parameters. The following table shows relatively large s behaviour. The following table gives some quantitative ideas about this fact.

Critical parameter g is greater than the other parameters. In the section 5.19 this issue is discussed in details. f comes smaller than the calculated value (from equation (5.30)), i.e; f varies slowly with s at the range of relatively large values of s. The parameters corresponding

s	γ	f	g	h	$\frac{M_c}{M}$	$\frac{\Psi_{med}}{\Psi_{star}}$	$\frac{x_i}{x_\infty}$	$\frac{x_b}{x_\infty}$	$\frac{x_i}{x_b}$
55	1.33	2.866	9.212	4.550	1.4875×10^{-8}	0.0219	0.262	0.000273	960.761
	1.41	2.8658	7.349	2.768	4.512×10^{-9}	0.0134	0.262	0.0001676	1566.192
	1.5	2.8656	5.987	1.464	1.086×10^{-9}	0.00716	0.262	1.66×10^{-5}	2942.03
100	1.33	2.888	9.286	4.586	4.613×10^{-9}	0.022	0.215	0.0001515	1420.325
	1.41	2.8878	7.4088	2.7898	1.3992×10^{-9}	0.013556	0.215	9.2972×10^{-5}	2315.161
	1.5	2.8877	6.0356	1.4759	3.36729×10^{-10}	0.007219	0.215	4.95×10^{-5}	4348.675
300	1.33	2.906	9.348	4.616	5.2318×10^{-10}	0.0222	0.1493	5.084×10^{-5}	2936.422
	1.41	2.906	7.4579	2.80796	1.58667×10^{-10}	0.0136	0.1493	3.1197×10^{-5}	4785.944
	1.5	2.9059	6.07548	1.485	3.818×10^{-11}	0.00726	0.1493	1.66×10^{-5}	8988.9839
500	1.33	2.9097	9.3607	4.6224	1.891×10^{-10}	0.02226	0.12593	3.05×10^{-5}	4122.938
	1.41	2.9096	7.46777	2.8116	5.735×10^{-11}	0.01366	0.12594	1.874×10^{-5}	6719.59
	1.5	2.9096	6.0835	1.487	1.38×10^{-11}	0.00727	0.12595	9.98×10^{-6}	12620.49
1000	1.33	2.912	9.37	4.6269	4.7427×10^{-11}	0.0223	0.09996	1.52877×10^{-5}	6539.18
	1.41	2.912	7.475	2.814	1.4382×10^{-11}	0.01367	0.09997	9.38086×10^{-6}	10657.31
	1.5	2.912	6.0896	1.4888	3.461×10^{-12}	0.00728	0.09998	4.995×10^{-6}	20015.73

Table 5.1: Variation with s.

to the validity of iteration method comes good, i.e; the method of iteration is also valid for relatively large s. $\frac{x_i}{x_\infty}$ decreases with s, i.e; we've less insight about the dynamics of the whole medium at large s. With increasing s although the total mass of the medium is increased but the medium is still lightly dense because of the increase in r_∞ and decrease in ρ_∞ with s. That's why the method of iteration is still valid at large s and also f, g and h do not attain large values at this range. Close observation at the table reflects the fact that not only f but also the other critical parameters varies slowly at relatively values of s or in other words the curves corresponding to f, g and h flatten at large s. f, g and h approach value 2.91, 7.48 and 2.814 respectively for $\gamma = 1.41$. For smaller γ these values are bigger and for higher γ these values are smaller. $\frac{\Psi_{med}}{\Psi_{star}}$ shows similar behaviour with s. The curves corresponding to $\frac{\Psi_{med}}{\Psi_{star}}$ also become flat at large s giving the possibility of the method of iteration to be valid even at larger s (> 1000). $\frac{\Psi_{med}}{\Psi_{star}}$ approaches value, 0.014 for $\gamma = 1.41$ and smaller values correspond to γ greater than 1.41 and larger for γ less than 1.41. The above figure shows that $\frac{\Psi_{med}}{\Psi_{star}}$ varies linearly and also most of the variation occurs for small s. This figure depicts the fact that the critical parameter, f converges to a finite value with increasing s and also method of iteration is valid even at large s because with increasing s, $\frac{\Psi_{med}}{\Psi_{star}}$ does not attain arbitrarily large value rather it tends to converge to a value smaller than 1. g and h also show similar behaviour. That's why observing large changes in critical parameters in the frame work of the method of iteration is not possible.

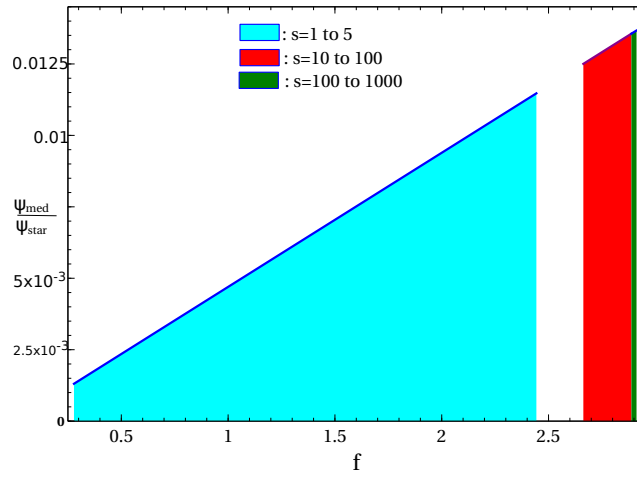


Figure 5.21: $\frac{\Psi_{\text{med}}}{\Psi_{\text{star}}}$ is plotted against f for $\gamma=1.41$. The areas under the discrete lines are shaded to distinguish the behaviour in several ranges of s .

5.12 Isothermal Flow

5.12.1 About isothermal flow

The case where the medium maintains uniform temperature in throughout the whole region of space. The barotropic equation for isothermal fluid is

$$p = K\rho \quad (5.35)$$

where K is a constant.

$$K = \frac{k_B N_A T}{M_A} \quad (5.36)$$

where k_B is Boltzmann constant, N_A is Avogadro number (6.023×10^{23}), T is the constant temperature of the single component fluid (we assume the fluid to be of single component for simplicity. In principle, one can consider multi-component fluid. Since we are not considering the thermal effect in the accreting medium in the model (just like Bondi did [9]), i.e. thermal ionization governed by Saha equation [113] is not taken into the model. We assume one component medium which is a good approximation in predicting the dynamics of the flow [9] within reasonable precision. Putting $\gamma = 1$ in the previous sections do not give full results. The isothermal case is thermodynamically a quite different process from the adiabatic one. Irrespective of

this fact, we will see substantial differences between adiabatic case and isothermal case in the following discussions.) and M_A is molar weight of the fluid. Sound speed is given by

$$c_0^2 = \left(\frac{\partial p}{\partial \rho} \right)_T = K \quad (5.37)$$

The above equation implies that the sound speed is constant along the flow.

the Bernoulli's constant (derived from Euler's momentum conservation equation and assuming steady flow), b is given by

$$b = \frac{v^2}{2} + c_0^2 \ln(\rho) + \psi(r) \quad (5.38)$$

where,

$$\psi(r) = -\frac{GM}{r} - \frac{4\pi G}{r} \int_{R_*}^r \rho r^2 dr - 4\pi G \int_r^\infty \rho(r) r dr$$

At a large distance from the star the potential energy terms are negligibly small, one can write

$$\frac{v^2}{2} + c_0^2 \ln(\rho) + \psi(r) = c_0^2 \ln(\rho_\infty) \quad (5.39)$$

The second term in the above expression (the term corresponding to the integral $\int \frac{dp}{\rho}$) makes isothermal case to hugely differ from the adiabatic one. Some dimensionless quantities are defined as below

$$x = \frac{r}{\frac{GM}{c_0^2}}, y = \frac{v}{c_0}, z = \frac{\rho}{\rho_\infty}$$

Equation (5.39) can be written in terms of dimensionless variables,

$$\frac{y^2}{2} + \ln(z) - \frac{1}{x} - \alpha \left(\frac{I_1}{x} + I_2 \right) = 0 \quad (5.40)$$

where $\alpha = 4\pi\rho_\infty G^3 M^2 c_0^{-6}$, $I_1 = \int_{x^*}^x z x^2 dx$ and $I_2 = \int_x^\infty z x dx$ with $x^* = \frac{R_*}{(\frac{GM}{c_0^2})}$

The mass accretion rate is obtained by integrating the continuity equation,

$$\dot{M} = 4\pi r^2 \rho u = 4\pi (GM)^2 c_0^{-3} \rho_\infty x^2 y z$$

Dimensionless mass accretion rate,

$$\lambda = x^2 y z \quad (5.41)$$

Equation (5.40) can now be written as

$$\frac{\lambda^2}{2x^4 z^2} + \ln(z) - \frac{1}{x} - \alpha \left(\frac{I_1}{x} + I_2 \right) = 0 \quad (5.42)$$

5.12.2 Critical Parameters

The critical points are calculated similarly by optimizing accretion rate (described earlier in section 5.3). Similarly it can be shown that at the critical point Mach number is unity. The critical points are

$$\frac{x_c}{x_b} = (1 + \alpha I_{1c}) \quad (5.43)$$

$$\frac{z_c}{z_b} = \exp(-2) \exp \left(\frac{2}{1 + \alpha I_{1c}} + \alpha \left(\frac{I_{1c}}{x_c} + I_{2c} \right) \right) \quad (5.44)$$

$$\frac{\lambda_c}{\lambda_b} = \left(\frac{x_c}{x_b} \right)^2 \frac{z_c}{z_b} \quad (5.45)$$

The meaning of the notations are same as before. It is also worth mentioning that putting $\gamma = 2$ in equation (5.12), does not give equation (5.44).

Radius of transonic surface increases.

The critical points corresponding to Bondi accretion are

$$x_b = 0.5$$

$$z_b = \exp(1.5)$$

$$\lambda_b = 0.25 \exp(1.5)$$

Similarly it can be shown that Mach number at the critical point, y_c is unity.

5.12.3 Equation of Motion

It can be derived in the same way as discussed in the section 5.4 that

$$\frac{dv}{dr} = \frac{\left(\frac{2c_0^2}{r} - \frac{GM}{r^2} - \frac{4\pi G}{r^2} \int_{R_*}^r \rho r^2 dr\right)}{\left(v - \frac{c_0^2}{v}\right)} \quad (5.46)$$

The equation takes 0/0 form at $r=r_c$ where r_c is the radius of the transonic surface. Applying L'Hospital rule at the critical point

$$\left.\frac{dv}{dr}\right|_{\text{criticalpoint}} = \pm \sqrt{-\frac{c_0^2}{r_c^2} + \frac{GM}{r_c^3} + 4\pi G \frac{I_{1c}}{r_c^3} - 2\pi G \rho_c}. \quad (5.47)$$

I_{1c} and I_{2c} in the expressions can now be evaluated by using method of iteration as discussed before.

5.12.4 The limits of the integrals

The radius of the star appears in I_{1c} and I_{2c} as lower limit and upper limit respectively. This issue is discussed in details in section 5.6. x_∞ appears as upper limit in the integral I_{2c} . The dimensionless potential energy terms appearing in the equation (5.40) is negligible at $x=x_\infty$. We choose a small quantity, Q as negative potential energy at $x=x_\infty$. $Q=Q_1+Q_2$, where

$$Q_1 = \frac{1}{x_\infty} \quad (5.48)$$

and

$$Q_2 = \alpha \left(\frac{I_{1\infty}}{x_\infty}\right) \quad (5.49)$$

where

$$I_{1\infty} = \int_{x_*}^{x_\infty} zx^2 dx$$

Q_1 has to be chosen in such a way that the dimensionless kinetic energy of the fluid $\frac{v^2}{2}$ is

negligible there. The third term in the potential energy does not appear due to obvious reasons. One can find x_∞ from equation (5.48) and density of the fluid at infinity can be found from equation (5.49).

$$\rho_\infty = \frac{Q2x_\infty c_0^6}{4\pi G^3 M^2 I_{1\infty}} \quad (5.50)$$

We define a dimensionless quantity, s as

$$s = \frac{Q2}{Q1} \quad (5.51)$$

s gives the mass ratio of the medium and the accretor. The mass of the medium is calculated using density profile in Bondi accretion.

5.12.5 Changes in Critical parameters

The inputs of the problem are temperature (T) of the fluid, mass ratio of the medium and the accretor (s) and (Q). It is observed that the changes in the critical parameters don't depend on the temperature of the fluid. We set Q to be 0.02 and temperature of the medium, T to be 300°K (any temperature can be chosen as there is no temperature dependence of the shift in critical parameters). Figure 5.22 shows the variation of percentage change in radius of the transonic

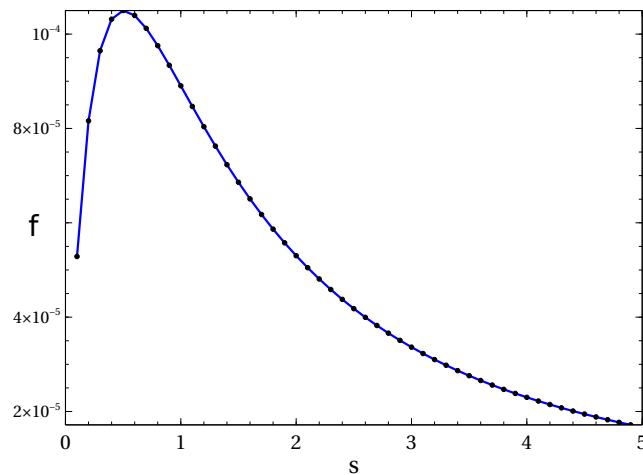


Figure 5.22: Percentage change in radius of transonic surface,
 $f = \frac{x_c - x_b}{x_b} \times 100$

surface with s . The increment in radius of transonic surface is extremely small. One can safely ignore the change in x_b . Inclusion of fluid mass does nothing to the radius of transonic surface. This is a difference from the previously considered adiabatic case.

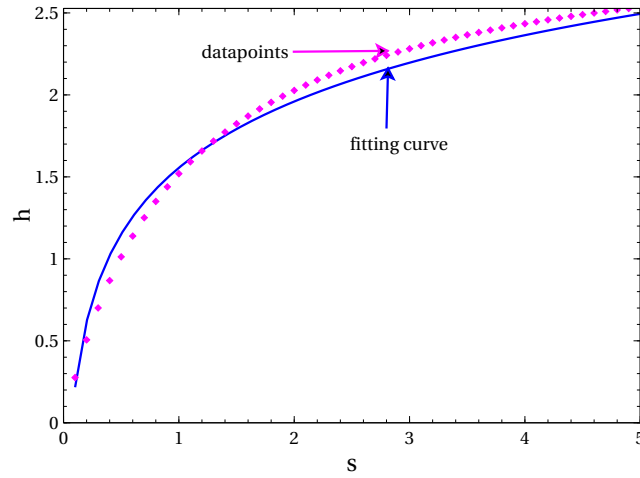


Figure 5.23: Percentage change in accretion rate, $h = \frac{\lambda_c - \lambda_b}{\lambda_b} \times 100$ is fitted with a curve.

In the figure 5.23, the data points corresponding to the changes in mass accretion rate with s is fitted with a curve fitted up to a upper bound in s which is 5. The equation of the fitting curve is

$$h = a + b \ln(s) \tag{5.52}$$

where $a=1.5553$ and $b=0.583462$. $h=0$ for $s=0.0695$. The h values of the figure 5.23 does not match quite well according to the figure 5.10 because of the aforementioned differences between isothermal case and adiabatic case. We don't have to consider inclusion of fluid mass if $s \leq 0.06955$. Percentage change in z_b is same as percentage change in λ_b because x_b does not change. It is clear from equation (5.45). Another mentionable point is that f is same as the mass ratio of the medium (extending from the surface of the star to the transonic surface) and the star. Figure 5.22 simply shows that at the transonic surface the gravitational field due to the medium is negligible compared to the gravity due to the accretor.

The method is still valid for large values of s . The variations become small at the range of relatively larger values of s .

h converges to 3.04 and $\frac{\psi_{med}}{\psi_{star}}$ converges to 0.015 at the range of relatively larger s . This is large s behaviour, it does not match with equation (5.22) and figure 5.23.

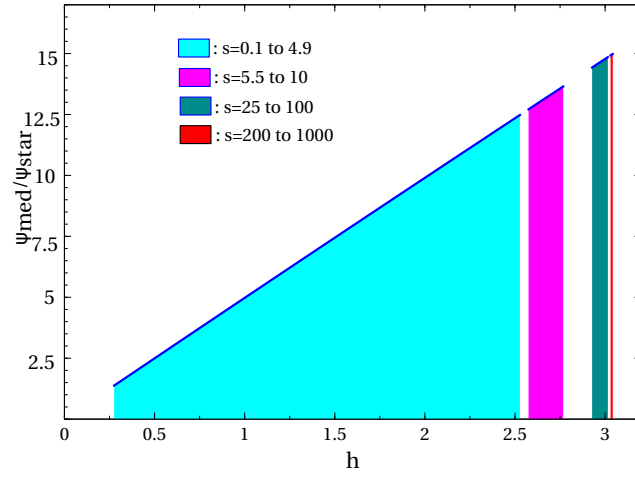


Figure 5.24: Variations of $\frac{\psi_{\text{med}}}{\psi_{\text{star}}} \times 10^3$ and h in different ranges of s . The areas under the discrete lines are shaded to distinguish the behaviour in several ranges of s .

As the percentage increment in the radius of transonic surface is negligible, the Mach number vs radial distance profile isn't shown for brevity.

5.13 Role of self-gravity

In course of time, fluid is deposited on the star and thus the mass of the star is changed. The main problem has actually explicit dependence on time. The whole analysis here is done assuming steady state dynamics. Mass accretion rate for adiabatic flow (calculated from section 5.3 and section 5.2) is given by

$$\begin{aligned} \dot{M}_\gamma &= 4\pi(GM)^2 c_{s\infty}^{-3} \rho_\infty x_b^2 y_b z_b (1 + 0.01h) \\ &= 4\pi(GM)^2 c_{s\infty}^{-3} \rho_\infty z_b^{\frac{\gamma+1}{2}} x_b^2 (1 + 0.01h) \end{aligned} \quad (5.53)$$

The last term in the product corresponds to the effect of inclusion of fluid mass. Taking M to be 1 solar mass, density of the medium at infinity to be $5.45153 \times 10^{-20} \text{ kg/m}^3$ (one can definitely work with less precision), E (in c^2 unit) to be 1×10^{-11} , γ to be 1.41 and $s=3$ (These are the values taken to plot the Mach Number profile), \dot{M}_γ comes to be $3351.465 \times 10^{10} \text{ kg/s}$.

Mass accretion rate for isothermal flow (section 5.13)

$$\dot{M}_{\text{isothermal}} = 4\pi(GM)^2 c_0^{-3} \rho_\infty x_b^2 z_b (1 + 0.01h) \quad (5.54)$$

Taking mass of the star to be 1 solar mass, density of fluid at infinity $1.22 \times 10^{-18} \text{kg/m}^3$, $s=3$ and the temperature of the fluid 300°K , the mass accretion rate for isothermal flow is $7855.104 \times 10^{10} \text{kg/s}$.

The Sun's mass loss per second due to radiation is $0.427 \times 10^{10} \text{kg/s}$ [115] which is negligible compared to the mass gain due to accretion process.

As radius of the transonic surface is proportional to the mass of the star, 1 percent change in mass of the star changes it by 1 percent. 1 percent change in radius of the transonic surface due to accretion rate is comparable to the decrease in radius of transonic surface due to inclusion of fluid mass effect in case of adiabatic flow.

Equation (5.54) shows that

$$\frac{\Delta \dot{M}_{\text{isothermal}}}{\dot{M}_{\text{isothermal}}} = 2 \frac{\Delta M}{M}$$

1 percent change in the mass of the star changes the accretion rate by 2 percent which is comparable to the change in accretion rate due to inclusion of fluid mass in the picture.

Self gravity becomes as significant as inclusion of fluid mass effect in the picture if the observation time is such that within that time interval 1 percent change in mass of the star occurs due to accretion process. 1 percent change in mass of the star occur within the time interval τ .

$$\tau \sim \frac{0.01M}{\dot{M}} \quad (5.55)$$

τ comes to be 0.188 billion years for adiabatic flow and 0.08 billion years for isothermal flow. τ gives the upper bound in time after which one needs to consider the change in mass of the star to compute sonic point. One has to reset the mass of the star to $(M + 0.01M)$ after time τ . The age of our universe is 13.6 billion years [116] and the age of most of the stars vary from 1 billion

years to 10 billion years. The age of the Sun is 4.6 billion years [117]. If the observation time is of the order of age of the star then self-gravity effect has to be considered but still 188 million or 80 million is a large time span.

5.14 Relation between f, g, h

For adiabatic flow the changes in the critical parameters are found to be small in the frame of method of iteration. Mathematically

$$\frac{\delta x_b}{x_b} \ll 1, \frac{\delta \lambda_b}{\lambda_b} \ll 1, \frac{\delta z_b}{z_b} \ll 1$$

Now using expression $\lambda_b^2 = z_b^{(\gamma+1)} x^4$ in section(5.3),

$$2 \frac{\delta \lambda_b}{\lambda_b} = (\gamma + 1) \frac{\delta z_b}{z_b} + 4 \frac{\delta x_b}{x_b} \quad (5.56)$$

Multiplying the above expression by 100,

$$2h = (\gamma + 1)g - 4f \quad (5.57)$$

This the relation among the percentage change in critical parameters. Rearranging,

$$g = \frac{2}{(\gamma + 1)}(h + 2f) \quad (5.58)$$

In the range of γ (1.33 to 1.66), g is always greater than f. Numerical results show that g is also greater than h. Numerical results show that f does not depend on γ and h decreases with γ and from the above expressions, g decreases with γ .

Similarly for isothermal flow using $\lambda_b = x_b^2 z_b$,

$$h = 2f + g \quad (5.59)$$

Our previous analysis shows that f is negligibly small, so

$$h \approx g \tag{5.60}$$

5.15 Summary and Conclusions

We have studied the effect of inclusion of fluid mass in non relativistic spherically symmetric accretion. We haven't considered the growth of the accretor during the process of accretion. We have considered steady flow of infalling fluid and the accretor to be a candidate of Main-sequence stars. One can do the same analysis by considering any type of stars if general relativistic features don't play significant role.

We have designed a methodology to find the changes in spherically symmetric accretion when fluid mass is taken into account. We have set Q , i.e; the precision of the problem and then we have considered several accreting systems by choosing the input parameters. We may have in general several inputs as: mass M of the accretor, γ of the fluid, energy E or constant temperature T (for isothermal flow) of the fluid, density of the fluid at infinity ρ_∞ , the mass ratio of the medium and the accretor and the extent of the medium r_∞ etc. Now according to our methodology after fixing Q when we take s into account that in return fixes the extent of the medium r_∞ according to the input energy E . ρ_∞ is then fixed in accordance with γ ($4/3$ to $5/3$ for adiabatic flow and 1 can be taken for convenience in the case of isothermal flow), E (for adiabatic flow) or T (for isothermal flow) of the fluid. In a summary, when the five input parameters M , Q , s , γ and E or T of the problem are given r_∞ and ρ_∞ are eventually fixed. r_∞ and ρ_∞ are no longer independent input parameters. This five input parameters contain the informations about ρ_∞ and r_∞ . One can start in other way round like by taking input parameters, r_∞ and ρ_∞ first and then setting Q of the problem. In that case, our 5 independent parameters would be M , Q , γ , r_∞ and ρ_∞ . Then one can find the changes in the critical parameters by varying r_∞ and ρ_∞ . That will be another way of looking at the same problem. Similarly, one can have other several ways of looking at the same problem.

Now if an arbitrary accreting system is given in such a way that some input parameters are known then at first we have to check that the known input parameters are sufficient to find any

solution or not and if the given input parameters are sufficient to analyse the system then we have to find the precision Q and if Q is close to 1 (the potential energy terms are not negligible at the boundary of the medium) then the system is outside of our formalism. Otherwise, s of the problem has to be found. If s of the problem is too small (s lies within the range where test fluid approximation is valid) then one can safely proceed without including fluid mass effect otherwise one has to proceed by following the procedure discussed in the above sections.

Using this methodology, we have compared the results with the usual spherically symmetric Bondi flow and we have found that inclusion of fluid mass changes the nature of flow of the infalling fluid. Mass accretion rate is increased for adiabatic flow as well as for isothermal flow and radius of the transonic surface is decreased for adiabatic flow when fluid mass comes into the picture.

This methodology deals with small changes in critical parameters due to inclusion of fluid mass effect to get at least a little insight into a more realistic problem where the mass of the medium plays important role. In the next chapter, we will see that when we consider the effect of gravity of the medium in the spherically symmetric accretion under Newtonian gravity, we find instabilities, and the medium becomes dispersive in nature under linear perturbation. Therefore, considering a more realistic situation, we find that the very assumption about the nondispersive nature of the medium breaks down. To consider the full scheme, we need to consider the back reaction, i.e. the growth of the accretor over time. In that case, there will be no steady state solution of the fluid equations.

Therefore, due to the gravity of the medium, the radius where speed of the medium exceeds the speed of sound is decreased. *In the next chapter, we will be considering linear perturbation over the steady state solution of this model.*

Chapter 6

Instabilities in nonrelativistic spherically symmetric self-gravitating accretion

Most of the contents of this chapter are taken from our work on instabilities in Bondi flow with self-gravity [121]. There are existing works [111], [120] on the correction over the steady state solutions of Bondi accretion [9] due to the effect of gravity of the accreting medium. We linearise density, velocity of the flow to analyse the stability of such steady state solutions. Transonic accretion for inviscid irrotational accretion models are natural systems where analogous blackhole horizon like effect, i.e. acoustic ‘dumbhole’ appears to be an emergent phenomena through linear perturbations in certain quantities like mass accretion rate, the Bernoulli’s constant etc [68], [78], [119],[122]-[124]. So far such works are done for non-self gravitating models of accretion, here we study the changes if the effect of the gravity of the accreting medium is considered. On the other hand, linear perturbations are introduced in such system to analyse the stability of the existing steady state solutions [78], [119], we study the stability of such accretion models, and we find that there are some changes due to the effect of inclusion of the gravity of the medium.

6.1 Spherically symmetric self-gravitating accretion model

For steady flow in the system considered in the previous chapter, the conserved quantity arising from the continuity equation is mass accretion rate, given by

$$\dot{M} = 4\pi r^2 \rho v. \quad (6.1)$$

The steady state solution of this model is considered details in the articles [111], [120].

6.2 Linear perturbation in the system

From now on, we denote the steady state velocity, density, pressure in the medium as $v_0(r)$, $\rho_0(r)$, $p_0(r)$ respectively.

Introducing linear perturbation in the flow, as

$$v(r,t) = v_0(r) + v(r,t)', \quad (6.2)$$

$$\rho(r,t) = \rho_0(r) + \rho(r,t)'. \quad (6.3)$$

As pressure, p is a function of density only, p is also perturbed in linear order. Writing the full continuity and Euler equation as

$$\frac{\partial \rho}{\partial t} + \frac{1}{r^2} \frac{\partial}{\partial r} (\rho v r^2) = 0, \quad (6.4)$$

$$\frac{\partial v}{\partial t} + v \frac{\partial v}{\partial r} = -\frac{1}{\rho} \frac{\partial p}{\partial r} - \frac{GM}{r^2} - \frac{4\pi G}{r^2} \int_{R_*}^r \rho r^2 dr. \quad (6.5)$$

Defining a quantity, proportional to the mass accretion rate (we introduce this quantity for simplicity, one can in principle work with \dot{M} as well) as

$$\mathcal{F} = \frac{\dot{M}}{4\pi} = \rho v r^2. \quad (6.6)$$

In the steady state, \mathcal{F} is a conserved quantity, $\mathcal{F}_0 = \rho_0 v_0 r^2$, under linear perturbation,

$$\mathcal{F} = \mathcal{F}_0 + r^2(\rho_0 v' + v_0 \rho') = \mathcal{F}_0(r) + \mathcal{F}'(r, t). \quad (6.7)$$

Therefore, in the continuity equation, equating the terms in the first order of smallness, we have

$$\frac{\partial \rho'}{\partial t} = -\frac{1}{r^2} \frac{\partial \mathcal{F}'}{\partial r}. \quad (6.8)$$

Unlike the non self-gravitating case, after linearising the Euler equation, we have terms from the gravitational field because the last term in equation (6.5) of the gravitational force, i.e. the gravitational force due to the medium, involves density. Now using the Euler equation in linear order and the above equation, we have a wave equation for \mathcal{F}' , given below

$$\partial_\mu (f^{\mu\nu}(r) \partial_\nu) \mathcal{F}'(r, t) + \frac{4\pi G}{r^2} \mathcal{F}'(r, t) = 0, \quad (6.9)$$

where

$$f^{\mu\nu}(r) = \frac{v_0}{\mathcal{F}_0} \begin{bmatrix} -1 & -v_0 \\ -v_0 & c_{s0}^2 - v_0^2 \end{bmatrix}. \quad (6.10)$$

$f^{\mu\nu}(r)$ can be related to the acoustic metric [78], [119], [122] as emergent phenomena in the system. The timelike killing vector (as the acoustic metric is time independent), becomes spacelike as $v_0 > c_{s0}$, i.e. after crossing the critical point or sonic point (in the case of transonic accretion solution) from subsonic region to supersonic region. Therefore, the radius at which $v_0 = c_{s0}$ for transonic accretion, can be identified as 'dumbhole' horizon [5]. The paper [120] shows that the sonic point is shifted towards the accretor due to the inclusion of the gravity of the accreting medium, therefore the dumbhole horizon has smaller radius than that of in non-self gravitating transonic Bondi accretion solution. The second term in the wave equation is arising due to the inclusion of self-gravity; therefore, it can be considered as an interaction term between the perturbation in the medium with the gravity of the medium. The inverse square nature in the second term is due to the Newtonian inverse square gravity. The presence of this new term modifies the

dispersion relation, using Eikanol approximation [2], [5], we find

$$\omega = \sqrt{c_{s0}^2 k^2 - 4\pi G \rho_0} \pm v_0 k. \quad (6.11)$$

The above dispersion relation (in a reference frame which is moving with the medium) $\omega - k$ is a hyperbolic curve. In this connection we refer to Fig. 1 of our work [142] (not included in the thesis). The only difference is that here the dispersion relation is locally valid around each point in the moving frame, *and about 'locally', the issue is discussed in details in chapter 7.* Therefore, for the stability of such high momentum wave propagation,

$$k \geq \frac{\sqrt{4\pi G \rho_0}}{c_{s0}} \quad \forall r \text{ in the flow.} \quad (6.12)$$

This criteria is very similar to the Jeans instability criteria [40], except for the fact that ρ_0 is a function of r . The stability criteria is also compatible with the Eikanol approximation of high momentum wave. To find the minimum possible k , k_{min} for which the solution is stable, one has to investigate the function $\frac{\sqrt{4\pi G \rho_0}}{c_{s0}}$. For isothermal flow, c_{s0} is constant and from the background solution of the accretion flow [120], [9] (*discussed in the previous chapter*), ρ_0 is maximum at the surface of the star, ρ_{0*} . Therefore, for isothermal flow, for stability at all radii in the flow,

$$k_{min} = \frac{\sqrt{4\pi G \rho_{0*}}}{c_{s0}}. \quad (6.13)$$

This is the stability condition at all radii; for wave number less than k_{min} , the flow becomes unstable near the surface of the star. The corresponding value of maximum possible value of λ , λ_{max} for stability,

$$\lambda_{max} = \sqrt{\frac{\pi c_{s0}^2}{G \rho_{0*}}}. \quad (6.14)$$

For adiabatic flow, $p = F(\rho) = k\rho^\gamma$, where k is a constant related to the specific entropy [42], γ is the specific heat ratio; $\frac{4}{3} < \gamma < \frac{5}{3}$. From the expression of sound speed, we get, the maximum possible value of λ for all r ,

$$\lambda_{max} = \sqrt{\frac{\pi \gamma k}{G \rho_{0*}^{2-\gamma}}}. \quad (6.15)$$

For instability, λ_{max} has to be small enough so that the Eikonal approximation is also true. Therefore, in both the cases instability arises from the medium near the surface of the accretor for waves having wavelength above certain limit.

The expression of the group velocity from the dispersion relation,

$$v_g = \frac{\partial \omega}{\partial k} = \frac{c_{s0}^2 k}{\sqrt{c_{s0}^2 k^2 - 4\pi G \rho_0}} \pm v_0. \quad (6.16)$$

Therefore, relative to the moving medium, the group velocity of such wave is

$$v_g|_{medium} = \frac{c_{s0}^2 k}{\sqrt{c_{s0}^2 k^2 - 4\pi G \rho_0}}. \quad (6.17)$$

Therefore, the dispersion relation is superluminal [5], i.e. the propagation speed (the group velocity) of linear perturbation is greater than the thermodynamic speed of sound. For relatively high momentum wave, v'_g is closer to the thermodynamic sound speed. Shorter wavelength perturbation has less speed. Therefore, the acoustic horizon is not absolute in the model, rather it depends on the wavelength of perturbation. The frequency dependence of the position of the acoustic horizon is also there in the quantum model of Bose-Einstein Condensate [5]. Therefore, this is a classical analogue model of gravity where such thing is observed.

6.3 Linear Stability Analysis of stationary solution

In the previous chapter, we discussed about steady state solution. We found the changes due to the inclusion of gravity of the medium. Here we consider whether the steady state solution considered in the previous chapter is stable under linear perturbation or not (*as we did in chapter 4*). We consider a trial solution of the form [78], [110] $\mathcal{F}^l(r,t) = \mathcal{F}_\omega(r)e^{i\omega t}$. We have from the equation (6.9),

$$\begin{aligned} \omega^2 \mathcal{F}_\omega f^{tt} - i\omega[\partial_r(\mathcal{F}_\omega(r)f^{rt}) + f^{tr}\partial_r\mathcal{F}_\omega(r)] \\ - \partial_r f^{rr} \partial_r \mathcal{F}_\omega(r) - \frac{4\pi G}{r^2} \mathcal{F}_\omega(r) = 0. \end{aligned} \quad (6.18)$$

6.3.1 Standing Wave

A standing wave has vanishing amplitude of perturbation at two different radii, r_1 and r_2 ($r_1 < r_2$), i.e. $\mathcal{F}_\omega(r_1) = \mathcal{F}_\omega(r_2) = 0$. Therefore, we have by integration

$$A\omega^2 + C = 0, \quad (6.19)$$

where

$$A = \int_{r_1}^{r_2} \mathcal{F}_\omega^2(r) f^{tt}(r) dr, \quad (6.20)$$

$$C = \int_{r_1}^{r_2} (\partial_r \mathcal{F}_\omega(r))^2 f^{rr}(r) dr - 4\pi G \int_{r_1}^{r_2} \frac{\mathcal{F}_\omega(r)^2}{r^2} dr. \quad (6.21)$$

The expression of frequency is given by

$$\omega^2 = -\frac{C}{A}. \quad (6.22)$$

The above equation gives the frequency of such standing wave solution, i.e. the frequency depends on r_1 , r_2 and the standing wave profile. Hence

$$\omega^2 = \frac{1}{\int_{r_1}^{r_2} \frac{\mathcal{F}_\omega^2(r)}{\rho_0 r^2} dr} \left[\int_{r_1}^{r_2} (\partial_r \mathcal{F}_\omega(r))^2 \frac{(c_{s0}^2 - v_0^2)}{\rho_0 r^2} dr \right] - \frac{4\pi G}{\int_{r_1}^{r_2} \frac{\mathcal{F}_\omega^2(r)}{\rho_0 r^2} dr} \left[\int_{r_1}^{r_2} \frac{\mathcal{F}_\omega(r)^2}{r^2} dr \right]. \quad (6.23)$$

The above expression implies that, if both the nodes (at r_1 and r_2) of such wave lie within the supersonic region of flow (the region where $v_0 > c_{s0}$), the stationary flow is unstable (instability implies $\omega^2 < 0$) under such perturbation which is also seen in the non self-gravitating case [78], [110]. In the supersonic region, it is not possible to spatially constraint the perturbation such that at two different radii, it vanishes at all time. In the subsonic region stability depends on the two competing terms of the above equation.

For stability, $\omega^2 > 0$

$$\int_{r_1}^{r_2} (\partial_r \mathcal{F}_\omega(r))^2 \frac{(c_{s0}^2 - v_0^2)}{\rho_r^2} dr \geq 4\pi G \int_{r_1}^{r_2} \frac{\mathcal{F}_\omega(r)^2}{r^2} dr. \quad (6.24)$$

The magnitude of $\mathcal{F}_\omega(r)$ has to be such that the assumption about the linearity of perturbation is valid. As r increases, $|\partial_r(\mathcal{F}_\omega(r))|$ decreases due to stretching because we assume that between two radii, there is not a single point where, $\mathcal{F}_\omega(r)$ vanishes. Therefore, assuming that the two nodes are separated by a long distance, in the bulk region (region around the middle of the two nodes), $\partial_r(\mathcal{F}_\omega(r))$ is practically zero, making the integrand in the left hand side to zero. Assuming the integrals are finite at all points, if the separation between the two nodes increases, the left hand side of the above equation does not increase much as compared to the right hand side of the above equation. Therefore, after a certain limit (depending on $\mathcal{F}_\omega(r)$) of distance between the two nodes, stability would not be maintained. Hence, the stationary solution becomes unstable under such standing wave having wavelength greater than a certain length. Therefore, due to inclusion of self-gravity in the system, it is not possible to maintain standing wave with vanishing amplitude at large separation.

6.3.2 Radially Travelling Wave

The background stationary solution is smooth and continuous at all radii. The background quantities appearing in the linear wave equation, equation (6.18) are smoothly varying, hence we make use of WKB (Wentzel-Kramers-Brillouin) method [113] to find solution for $\mathcal{F}_\omega(r)$. We seek solution of the form,

$$\mathcal{F}_\omega(r) = A(r)e^{i\theta(r)}, \quad (6.25)$$

where $A(r)$, the amplitude, is a slowly varying function of r , i.e. it varies slowly compared to $\theta(r)$ [113]. Therefore, the solution gives more accuracy for short wavelength, i.e. in the high frequency limit.

Plugging such solution in equation (6.18), the real part and the imaginary part gives respectively

$$\begin{aligned} \omega^2 A f^{tt} + 2A\omega f^{rt} \theta' - f^{rr}(A'' - A\theta'^2) \\ - A' \partial_r(f^{rr}) - \frac{4\pi G A}{r^2} = 0, \end{aligned} \quad (6.26)$$

$$\begin{aligned} \omega A \partial_r(f^{rt}) + 2\omega f^{rt} A' + f^{rr}(2A'\theta' + A\theta'') \\ + A\theta' \partial_r(f^{rr}) = 0, \end{aligned} \quad (6.27)$$

where $A' = \frac{dA}{dr}$, $\theta' = \frac{d\theta}{dr}$, $A'' = \frac{d^2 A}{dr^2}$, $\theta'' = \frac{d^2 \theta}{dr^2}$. From equation (6.27), we find

$$A^2(\omega f^{rt} + \theta' f^{rr}) = \text{constant}. \quad (6.28)$$

Neglecting the term A'' , $A' \partial_r(f^{rr})$ in the equation (6.26) ($\because A(r)$ is slowly varying and the background quantities are slowly varying with r in comparison to $\theta(r)$), we find

$$\theta' = \frac{-\omega f^{rt} \pm \omega \sqrt{(f^{rt})^2 - f^{tt} f^{rr} + \frac{4\pi G f^{rr}}{\omega^2 r^2}}}{f^{rr}}. \quad (6.29)$$

Therefore,

$$A(r) = \frac{C}{\left(\omega \sqrt{(f^{rt})^2 - f^{tt} f^{rr} + \frac{4\pi G f^{rr}}{\omega^2 r^2}} \right)^{\frac{1}{2}}}, \quad (6.30)$$

where C is a constant depending on the initial condition on $\mathcal{F}_\omega(r)$. Putting the values, we get

$$\theta'_\pm = \frac{\omega v_0 \pm \omega \sqrt{c_{s0}^2 + \frac{4\pi G \rho_0 (c_{s0}^2 - v_0^2)}{\omega^2}}}{c_{s0}^2 - v_0^2} \quad (6.31)$$

and

$$A(r) = C \left(\frac{\rho_0 r^2}{\omega \sqrt{c_{s0}^2 + \frac{4\pi G \rho_0 (c_{s0}^2 - v_0^2)}{\omega^2}}} \right)^{\frac{1}{2}}. \quad (6.32)$$

Therefore, the complete solution can be written as

$$\mathcal{F}'(r, t) = \left(\frac{\rho_0 r^2}{\omega \sqrt{c_{s0}^2 + \frac{4\pi G \rho_0 (c_{s0}^2 - v_0^2)}{\omega^2}}} \right)^{\frac{1}{2}} e^{i\omega t} \times \left[C_+ e^{i \int^r \theta'_+(r) dr} + C_- e^{i \int^r \theta'_-(r) dr} \right], \quad (6.33)$$

where C_+ is the amplitude corresponding to the travelling wave, propagating radially outward and C_- is the amplitude corresponding to the travelling wave, propagating radially inward. One can easily see this by dropping the term due to the self-gravity in the above equations. Interestingly, the amplitude of such wave is same as the amplitude of the travelling wave for non-self gravitating case at $v_0 = c_{s0}$. The expression of θ'_\pm is same as k (in terms of ω and the background stationary quantities) in the equation (5.11). Therefore, the solution is stable for certain limit in θ'_\pm . This is because, we are assuming high frequency wave; by WKB method, we get the expression of the amplitude in addition. If we look at the frequency spectrum, we see that the amplitude decreases with the increase in wavenumber.

Alternatively, one can solve the equation (6.18) in high frequency limit by taking a trial solution of the form, given below

$$\mathcal{F}_\omega(r) = \exp \left[\sum_{n=-1}^{n=\infty} \frac{K_n(r)}{\omega^n} \right]. \quad (6.34)$$

This standard method of travelling wave analysis used in several literature [68], [78] and [110], [119] would also give same solution found above. This is basically another way of implementing WKB method.

Therefore in summary, we have investigated the time dependent problem in perturbative approach in the non-relativistic spherically symmetric accretion model in Newtonian gravity. We find that the linear perturbation in mass accretion rate satisfies a wave equation with an interaction term with gravity due to the inclusion of gravity of the infalling medium. From the wave equation, we find the acoustic metric and we find that the interaction term with gravity in the wave equation, modifies the dispersion relation. Unlike the non-self gravitating case, the dispersion relation is superluminal, and as a result of this the acoustic dumbhole horizon is not absolute in our case, rather it's frequency dependent. This is a classical analogue model of gravity where

such thing is observed. The inclusion of the gravity of the medium, gives rise to instabilities which are absent if the gravity of the medium is switched off.

Chapter 7

Lagrangian description for accreting astrophysical systems

7.1 Introduction

In the chapter 2, we discussed about the dependence between two conditions, i.e., irrotationality condition and barotropic condition. *In the introduction chapter*, we derived the massless scalar field equation of linear perturbation in velocity potential, and we drew the analogy between the massless scalar field equation in curved spacetime. *In chapter 4*, we discussed about linear perturbation of other astrophysically significant quantities. *In chapter 2*, we also wrote about the emergent gravity phenomena from the coordinate system of an observer moving with the background velocity of the medium. We concluded that if the wavelength of the linear perturbations is very short (the Eikonal limit [36], [42]), the moving observer in the sufficient near vicinity of them, will perceive the disturbance as sound wave propagating in a uniform medium; hence in the near vicinity of that observer in motion, the emergent spacetime is flat, i.e, acoustic Minkowski spacetime. Therefore, this reference frame is similar to the local inertial frame in general Theory of relativity. In this chapter, we consider the astrophysical accretion models to work with some realistic examples and we introduce a procedure to find a rough estimate about the wavelength of Eikonal waves originated at different positions, such that moving (with the background flow) observers at those positions in the medium, observe the wave to propagate just

like waves in a uniform static medium (in the neighbourhood of those observers). The contents of this chapter is taken our work on LPT in the context of emergent spacetime [118].

7.2 Astrophysical accretion model

In *chapter 3*, we have discussed about steady state solutions in conical accretion disk model for barotropic flow under pseudo-Schwarzschild potential and under pseudo-Kerr potential. In the *chapter 4*, we have discussed about emergent gravity in accretion models through linear perturbation. We have shown that the linear perturbation of more astrophysical significant scalar quantity, the Bernoulli's constant, also satisfies the massless scalar field equation from which one derives the acoustic metric. We have concluded in the *chapter 4* that linear perturbation of the conserved quantities (conserved in steady state flow), i.e, mass accretion rate, \mathcal{F} (arising from continuity equation) and the Bernoulli's constant, ζ (arising from Euler equation), gives rise to emergent gravity in the time dependent case. In reference to *the chapter 2*, we can introduce Lagrangian description of perturbation of these quantities, as

$$\Delta\zeta = \zeta' + \delta \cdot \nabla \zeta_0 = \zeta' \quad (\because \text{the background flow is steady, } \zeta_0 \text{ is constant}) \quad (7.1)$$

$$\Delta\mathcal{F} = \mathcal{F}' + \delta \cdot \nabla \mathcal{F}_0 = \mathcal{F}' \quad (7.2)$$

Therefore, the

$$\begin{aligned} \partial_\mu (f^{\mu\nu}(\mathbf{x}) \partial_\nu) \zeta'(\mathbf{x}, t) &= 0 \\ \Rightarrow \partial_\mu (f^{\mu\nu}(\mathbf{x}) \partial_\nu) \Delta\zeta(\mathbf{x}, t) &= 0 \quad (\because \nabla \zeta_0 = 0) \end{aligned} \quad (7.3)$$

Similar equation holds for the mass accretion rate too. Therefore, the linear perturbation of the conserved quantities in Lagrangian Perturbation Theory in the time dependent case, gives rise to emergent gravity too.

7.3 Estimation of the wavelength of the perturbation

As we have already discussed in *chapter 2* that eikonal wave does not see the conformal factor in the acoustic metric, therefore, we have in the frame of the observer moving with the background speed of the medium; the metric (equation 2.31),

$$ds^2|_{\text{geometric}} = \tilde{g}_{\mu\nu}(\mathbf{x}', t') dx'^{\mu} dx'^{\nu} = \left(- (c_{s0}^2 - (\mathbf{v}_0 - \mathbf{V})^2) dt'^2 - 2(\mathbf{v}_0 - \mathbf{V}) dt' \cdot d\mathbf{x}' + d\mathbf{x}'^2 \right) \quad (7.4)$$

In the near vicinity of the observer $\mathbf{v}_0 \sim \mathbf{V}$, therefore, we can set a very small quantity;

$$|\mathbf{v}_0 - \mathbf{V}| = \varepsilon \mathcal{V}, \quad (7.5)$$

where ε is a small dimensionless number ($\ll 1$) and \mathcal{V} is a quantity having dimension of speed, we choose this quantity according to the speed scale of the problem. We estimate the measure of the length around the observer over which the background speed of the medium differ by $\varepsilon \mathcal{V}$, this length l gives the measure of the wavelength of the eikonal wave. Therefore, in the near vicinity of the observer, the acoustic metric of the emergent spacetime is effectively flat for waves having such short wavelength ($\leq l$). In other word, the speed of sound is same in all direction within this length l , and to realize such effect the wavelength of the linear disturbance has to be $\leq l$.

7.4 Conical Adiabatic Flow

The conical disk model is preferred than other models [73], [75] because it is more realistic than constant height disk accretion model and simpler than vertical equilibrium model. Therefore, we choose to work with this model only. In connection to *chapter 4*, we can write the acoustic metric in geometric limit, as

$$ds^2|_{\text{geometric}} = \left(-(c_{s0}^2 - v_0^2) dt^2 + 2v_0(r) dt dr + dr^2 \right), \quad (7.6)$$

where r is cylindrical polar coordinate. The technique of finding, $v_0 = v_0(r)$ and $c_{s0} = c_{s0}(r)$ under Pseudo-Schwarzschild and Pseudo-Kerr potential, is discussed in *chapter 3*. Therefore, we can design the acoustic metric in such flow depending on the parameter set: $[\zeta, \gamma, \lambda, a]$. Let us consider an observer, moving along the x - axis towards the accretor sitting at the origin. The observer is moving with the background speed of the medium. Therefore, according to the Galilean transformation given in *chapter 2*:

$$x = x' + R - \int^t V(R, t) dt, \quad (7.7)$$

$$t = t', \quad (7.8)$$

$$y = y', \quad (7.9)$$

As the observer moves towards the accretor, $V(R, t)$ takes the value of the speed of the background medium. The initial distance of the observer is R . After making a coordinate transformation of the acoustic metric 7.6 to the Cartesian coordinate in two dimension (because the radial flow is happening on the disk plane), we have (c_{s0} and v_0 are scalar by definition)

$$\begin{aligned} ds^2|_{\text{geometric}} = & -(c_{s0}^2 - v_0^2)dt^2 + 2v_0dt(\cos\phi dx + \sin\phi dy) \\ & + (\cos^2\phi dx^2 + \sin^2\phi dy^2 + \sin 2\phi dx dy), \end{aligned} \quad (7.10)$$

where

$$\cos\phi = \frac{x}{\sqrt{x^2+y^2}} \quad (7.11)$$

$$\sin\phi = \frac{y}{\sqrt{x^2+y^2}}. \quad (7.12)$$

As the observer is moving along the x - axis, in the near vicinity of the observer, ϕ is roughly zero, and also as we are considering wave which propagates along the radial direction. The observer examines wave propagating on the x - axis, therefore

$$ds^2|_{\text{geometric}} = -(c_{s0}^2 - v_0^2)dt^2 + 2v_0dt dx + dx^2, \quad (7.13)$$

From the observer's reference frame, the above acoustic metric becomes

$$ds^2|_{\text{geometric}} = -(c_{s0}^2 - (v_0 - V)^2)dt'^2 + 2(v_0 - V)dt'dx' + dx'^2 \quad (7.14)$$

In the near vicinity of the observer, along the x - axis $|v_0 - V| = \varepsilon\mathcal{V}$. Therefore, according to the discussion in the previous section,

$$ds^2|_{\text{geometric}} = -(c_{s0}^2 - \varepsilon^2\mathcal{V}^2)dt'^2 + 2\varepsilon\mathcal{V}dt'dx' + dx'^2. \quad (7.15)$$

Hence, considering the leading terms in the acoustic metric in the near neighbourhood of the observer,

$$ds^2|_{\text{geometric}} = -c_{s0}^2 dt'^2 + dx'^2. \quad (7.16)$$

As we have shown in the *Chapter 1, Introduction*, that Eikonal wave follows null geodesic, hence it propagates with same speed c_{s0} along positive x axis and negative x axis in the close vicinity of the observer. Therefore, in the near vicinity of the observer, the emergent spacetime is flat because the short wavelength of perturbation is measured in the accelerated reference frame. Owing to the axial symmetry of the problem, any observer moving radially towards the accretor, will have same conclusion while studying radially propagating wave. Now we estimate the lengthscale l over which the speed of the background medium varies by $\varepsilon\mathcal{V}$ to get an idea about the wavelength of Eikonal wave at different radii to produce such effect. Therefore, it all depends on how $v_0(r)$ varies with r . As we have shown in the *chapter 2* that $\nabla = \nabla'$, we only try to find the variation in the reference frame fixed with respect to the accretor at the origin. The faster the variation of v_0 with r , smaller the length, l is. In the next section we numerically compute l by considering suitable $\varepsilon\mathcal{V}$.

7.5 Numerical Estimation of the wavelength

As we choose $\varepsilon\mathcal{V}$ small enough, therefore we can relate the length l with step size (step length to numerically solve the problem) of the problem h by the following manner;

$$l = \frac{h\varepsilon\mathcal{V}}{\Delta v}, \quad (7.17)$$

where Δv is the magnitude of change in background speed for the change of radial distance by h . We work with magnitudes of change to get an idea about l . $l = lc$ at the critical point (critical point and sonic point are same in the case of conical flow (see *chapter 3*). We compute the variation of $\log(l/lc)$ with radial distance. We present the variation in the following figures. We denote the critical point by C in red in the following figures. We also show the speed variation of the background medium with the radial distance to get an idea about how speed variation influences l . In velocity profile, if there is/are a turning point/s, we choose the minimum value of variation (taking into account variation of speed from both the increasing side and decreasing side of r around the turning point/s) in background speed around the turning point to set $\varepsilon\mathcal{V}$. If there is no turning point in the background velocity profile, we simply set $\varepsilon\mathcal{V} = 0.001 \times v_c$, where v_c the speed of the background medium at the sonic point. It is quite evident that one would get a good idea about the variation of l with r by choosing this methodology. We denote the turning points in the figure as $T1$, $T2$.. We then vary the parameters of the problem ζ and λ to see the variation in l at different regions of the parameter space (see figure 3.1 of *chapter 3*). First we work with pseudo-Schwarzschild potential (potential 2 of *chapter 3*) and then we consider Pseudo-Kerr potential (potential 5 in the *chapter 3*).

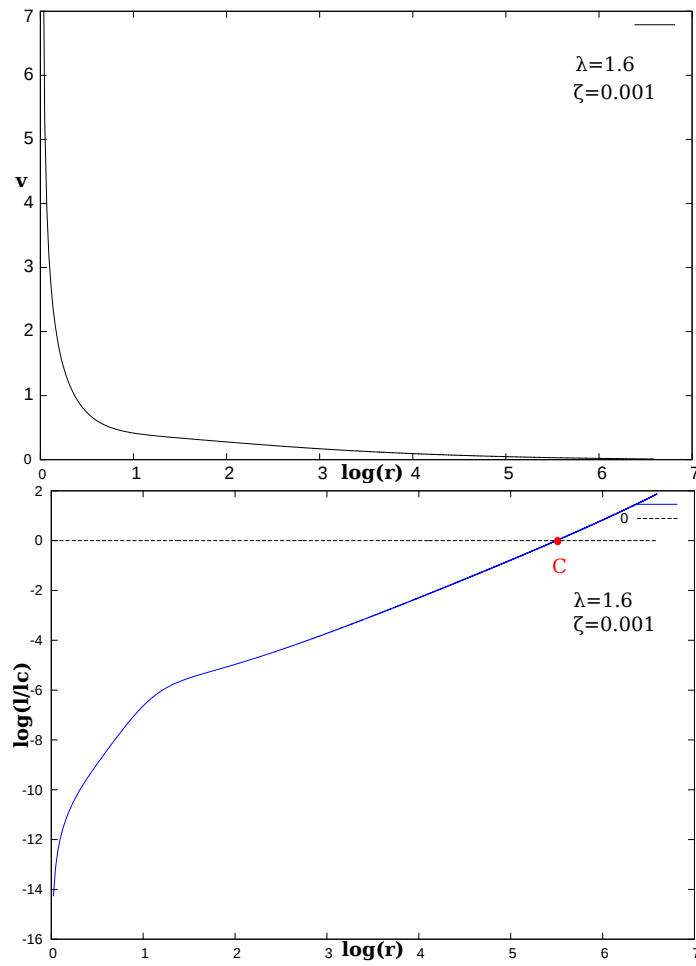


Figure 7.1: Background speed variation (top) and variation in l (bottom). Region in the parameter space: region with single critical point relatively away from the accretor.

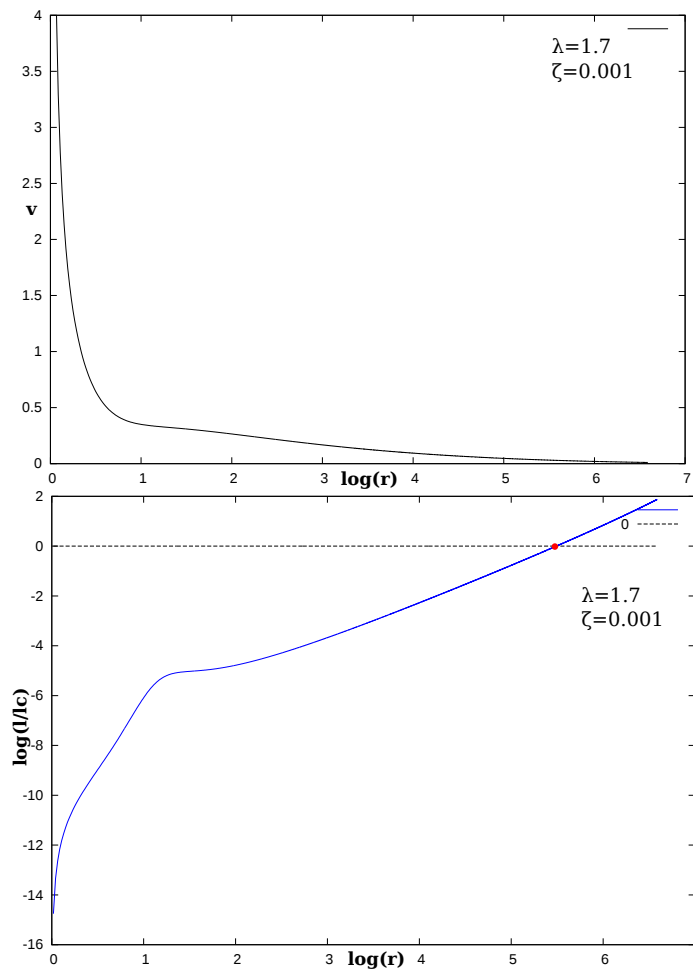


Figure 7.2: Background speed variation (top) and variation in l (bottom). Region in the parameter space: region with single critical point situated relatively away from the accretor.

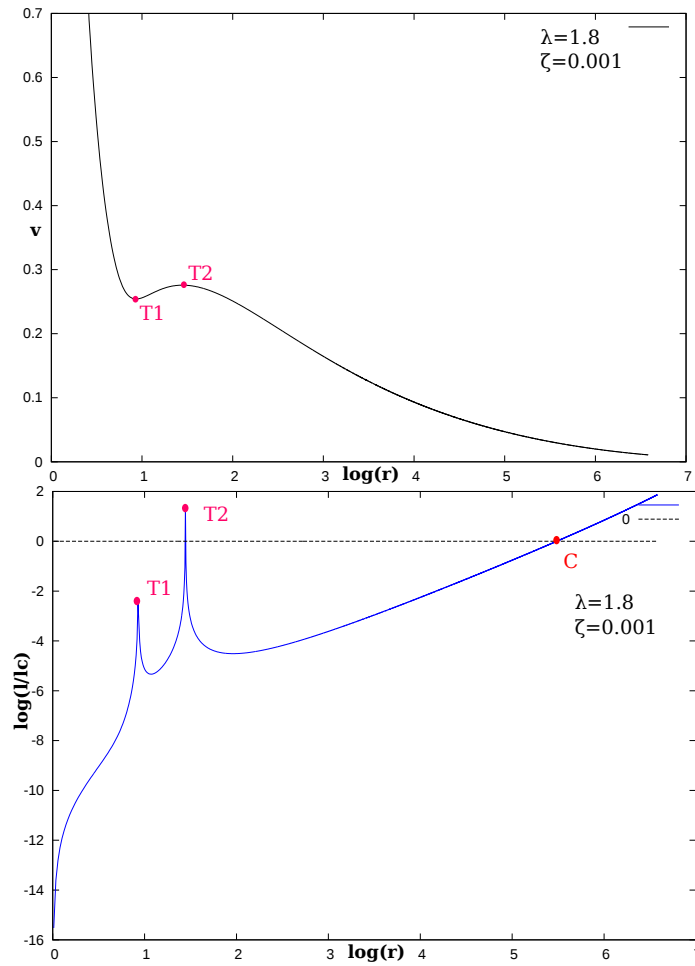


Figure 7.3: Background speed variation (top) and variation in l (bottom). Region in the parameter space: region with three critical points, transonic accretion curve passing through the farthest (from the accretor) critical point. Formation of sharp peaks at the turning points in the figure of $l - r$ variation.

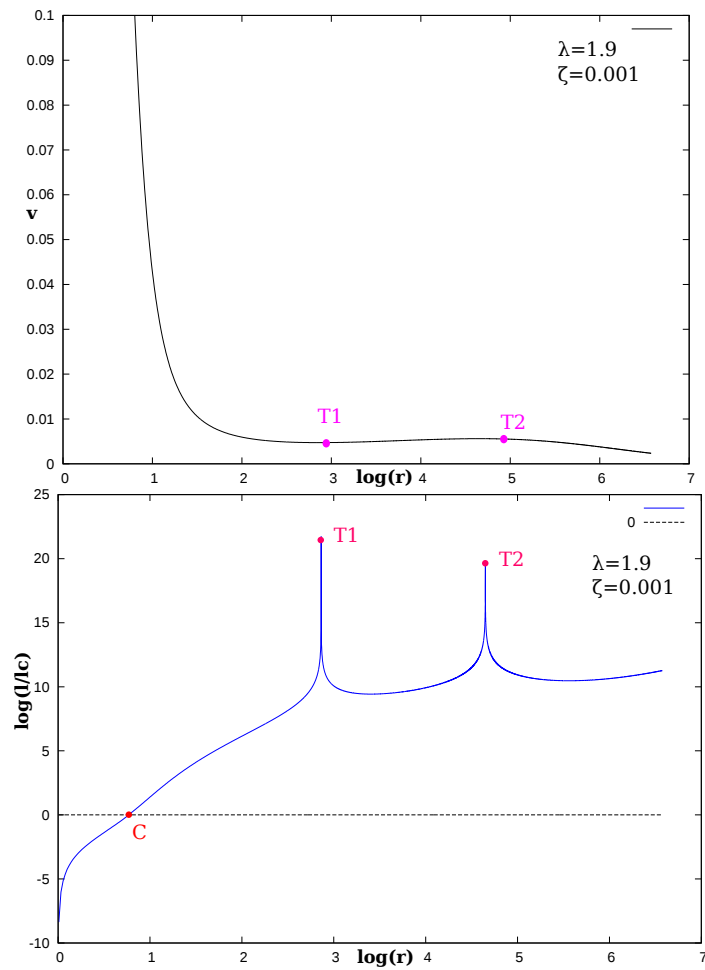


Figure 7.4: Background speed variation (top) and variation in l (bottom). Region in the parameter space: region with three critical points, transonic accretion curve passing through the nearest (from the accretor) critical point. Formation of sharp peaks at the turning points in the figure of $l - r$ variation.

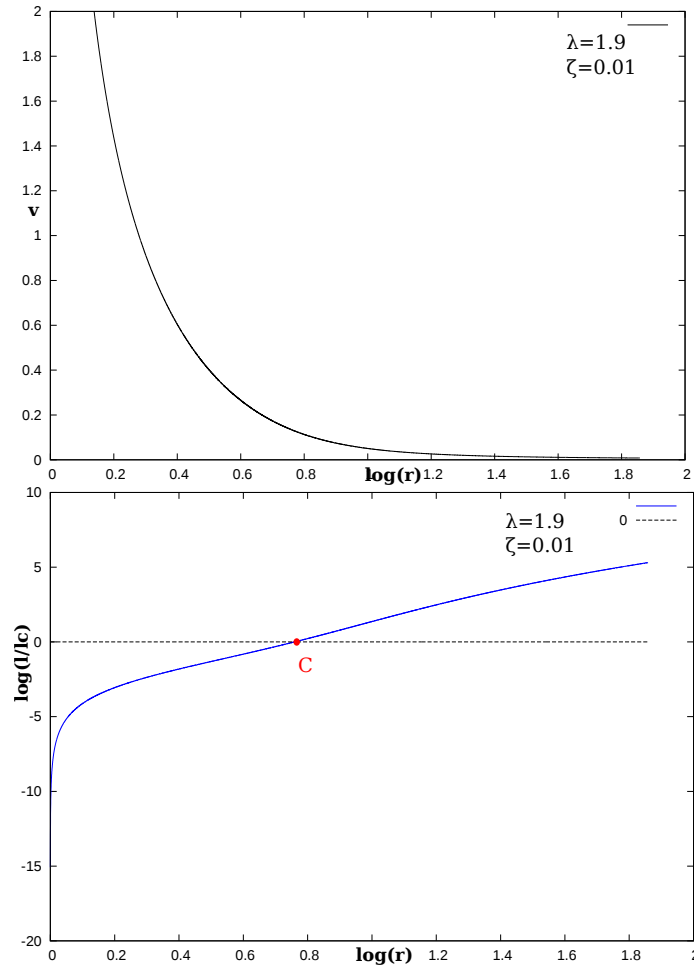


Figure 7.5: Background speed variation (top) and variation in l (bottom). Region in the parameter space: region with single critical point situated near the accretor.

Thus we cover each single region of the parameter space. The peaks form at the turning points because the variation of the background speed becomes increasingly slow around the turning points, thus resulting into sharp increase in the length l . We can categorise the event in two divisions. The transonic accretion curve passing through the critical point situated away from the accretor, belongs to one class, and the transonic accretion curve passing through the critical point near the accretor belongs to the other one. This is in reference to figure 3.1. In the above figures, we choose different $\varepsilon^{\mathcal{V}}$ for different set of parameter values (The way of setting $\varepsilon^{\mathcal{V}}$ is described earlier). Now we try to figure out the dependence of l on parameter values. Now we look at how the length lc depends on the parameter values by keeping $\varepsilon^{\mathcal{V}}$ fixed. From equation 7.17,

$$lc = \frac{\varepsilon^{\mathcal{V}}}{|q|}, \quad (7.18)$$

where q is the slope of velocity with respect to r at the critical point (see *chapter 3*). As $\varepsilon^{\mathcal{V}}$ is chosen to be constant, $l \propto \frac{1}{|q|}$. We find the variation in $\frac{1}{|q|}$ with the parameter values. The figures

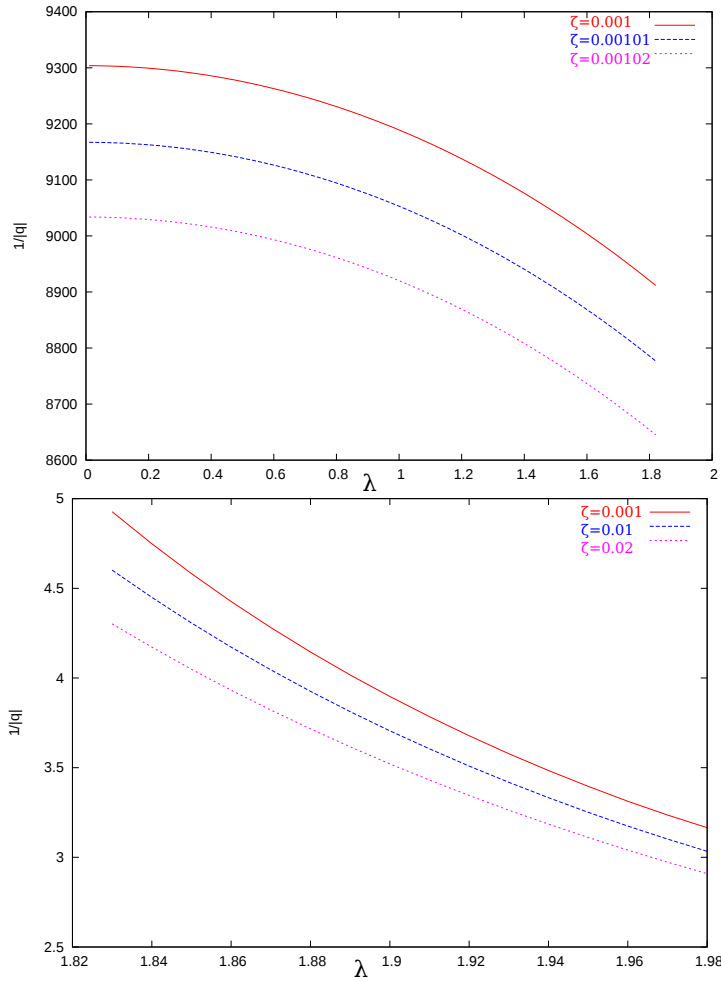


Figure 7.6: $\frac{1}{|q|}$ vs λ , region: accretion curve passing through the critical point situated away from the accretor (top) and $\frac{1}{|q|}$ vs λ , region: accretion curve passing through the critical point situated near the accretor (bottom).

clearly show that the length l decreases with the increase of specific angular momentum and it increases with the decrease in the Bernoulli's constant.

7.5.1 Variation with the spin parameter of the pseudo-Newtonian potential

As the velocity profile [52] (considering Pseudo-Kerr potential) looks qualitatively similar to the Pseudo-Schwarzschild case, we do not show the the variation of $\log(l/lc)$ with r , rather we look at how blackhole spin influences lc in the following figures. Variation of lc with ζ is similar

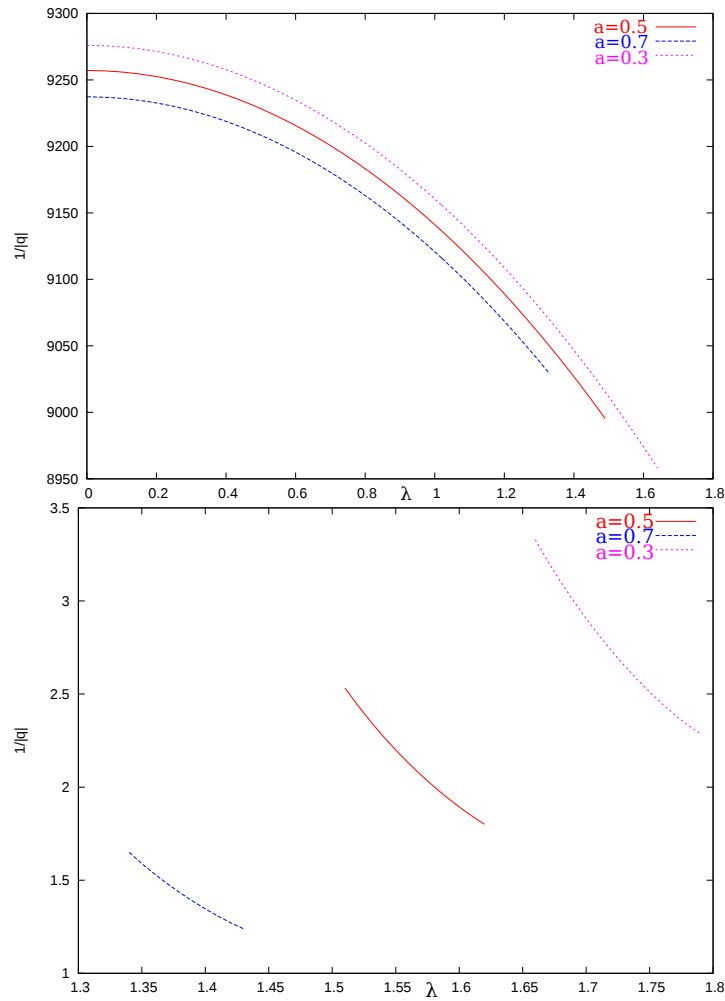


Figure 7.7: $\frac{1}{|q|}$ vs λ , region: accretion curve passing through the critical point situated away from the accretor; the curves corresponding to different values of a stop at different λ because that's the end of this kind of region in the parameter space (top) and $\frac{1}{|q|}$ vs λ , region: accretion curve passing through the critical point situated near the accretor; the curves corresponding to different values of a start at different λ because that's the beginning of this kind of region (which is again the end of the mentioned region in the top figure) in the parameter space (bottom).

to as before. The figures indicate that lc increases with the decreasing value of spin parameter, a .

If the observer moving with the background flow perturbs the medium at his locations at different instants of time, and if the wavelength of such perturbations are small enough, within very short time within very short distance from that observer the wave propagates with same speed (the speed of sound in the static medium) along the possible directions. By 'possible direction', we mean radially outward (from the accretor) and radially inward (towards the accretor) in the Astrophysical models of accreting blackhole. Our aim has been to find the wavelength of such

wave at different positions. We estimate a lengthscale ($= l$) such that wave having wavelength less than or equal to l , propagates with same speed along the available directions. Therefore, within a short time τ ($= \frac{l}{v_0}$, the time needed for that observer to cross that distance l . Within l , v_0 and c_{s0} does not vary much), the observer can see the Eikonal wave propagating uniformly with speed $c_{s0}(r)$ within that distance, l . Our main aim in the chapter has been to find the length l to have an idea about the maximum wavelength of the Eikonal wave. Therefore, in the observer's reference frame, the Eikonal wave corresponding to this maximum wavelength, has time period, $T = \frac{l}{c_{s0}}$ (as evident from the dispersion relation 1.34). Hence, $\frac{T}{\tau} = m$ with m being Mach number at that point. Hence, $\frac{1}{m}$ represents the number of full cycles, to be measured by the observer such that within the period of time τ . Waves having wavelength less than or equal to l has time period less than or equal to T . $\frac{1}{m}$ is the lower bound of number of cycles ($= \mathcal{N}$) to be observed by the moving observer to realize such effect. At the 'dumbhole' horizon, $\mathcal{N} = 1$. Thus even if the arbitrary choice of $\varepsilon^{\mathcal{V}}$ (depending on the choice of precision of the observer on the sensitivity of the background quantities with distance) makes l arbitrary, we have found a concrete number which represents the minimum number of cycles of such Eikonal wave to realise such effect (the event of observing uniformly propagating sound along the relevant directions, as viewed by the observer moving with the background flow). The variation of m with radial distance is discussed in details in several works [28]-[30], [35], [52]. From this chapter, we can also have some general qualitative beforehand idea (before doing any numerics) about how to find the variation of l with r from a given velocity profile in general. For example, in the spherically symmetric accretion (Bondi accretion), the speed of the background medium monotonically decreases with r along the transonic accretion curve [9] with asymptotically decreasing slope. Therefore, l will monotonically increase becoming more steeper with r . Again, if there is a extrema in a velocity profile, in the figure of $l - r$, around that maxima or minima, there will be sharp peaks. For relativistic treatment, one needs to write down the fluid equations in covariant form and one needs to consider the general relativistic LPT.

Chapter 8

Further scopes and Discussions

We have considered astrophysical accretion models to produce the emergent spacetime geometry. So far, we have only discussed about the geometrical aspects regarding this phenomena. We have not focused on the analogous Hawking radiation event from the analogue blackhole in the astrophysical accretion models. As the emergent gravity models, represent the kinematic aspects of the general theory of relativity, there will be analogous phenomena Hawking radiation. In the accreting astrophysical system, analogue of Hawking radiation is studied in the literature [33]. The main focus of our thesis, have been to study the geometrical aspects of the analogue black hole spacetime with application in the models of accreting astrophysical system.

The introduction of Lagrangian Perturbation Theory (LPT), gives additional features in the work. Considering, the eikonal wave in the geometrical limit of acoustics, has given us a different perspective to look at the subject. Our analysis of LPT in the context of emergent gravity is so far restricted to non-relativistic cases, general relativistic treatment can be done in principle. For example, in the chapter-4, we introduced general relativistic accretion models and we studied linear perturbation of Bernoulli's constant, $h\nu_t$ over existing steady state solutions. The second piece of the puzzle lies on the formulating the expressions for Lagrangian perturbations which we introduced in the chapter-2. Basically, we have to redefine the relevant fluid quantities in a suitable general relativistic fashion. In that case, we can even include astrophysical accretion onto blackhole in the formalism of pure general relativistic treatment.

Inclusion of gravitational effect of the background medium, has added more realistic features in the problem. As we have shown that due to the inclusion of gravity of the medium, makes it

dispersive. This might make the problem little more intriguing, if Hawking radiation from such dispersive medium is studied just like in [143].

One can also work with nonlinear perturbations. In one of our work [125] (not included in the thesis), it is shown that weakly nonlinear wave in static fluid medium, produces emergent spacetime which has some similarities with gravitational wave propagating in a Minkowski spacetime. There are also some works in the literature where nonlinear perturbation is studied in the models of accreting astrophysical system [126]-[129].

We have not considered shocked accretion. Shocked flow in such models of Astrophysical accretion rise to multi-transonic accretion which produce coexisting analogue blackhole-whitehole spacetime [33],[123][124]. There are also analogues of rotating blackhole [130][144], we can also try to find such geometry in the astrophysical accretion models. The challenge of dealing with rotational fluid is that the vorticity free (locally)-assumption gets modified. I have plans to work with rotational fluid and to employ such methodology in the context of accretion models as well.

Astrophysical accretion is a natural phenomena, the theme of our thesis has been to study emergent gravity effect in some models of accretion. In a black hole accretion, there is an event horizon corresponding to the background spacetime; as the surrounding medium is falling onto the black hole, it also creates an emergent analogous black hole space time horizon of larger radii. The physical nature of this acoustic spacetime metric (having the acoustic horizon), depends on the velocity profile, density profile of the barotropic medium. The dynamics of the medium again depends on the black hole space time. Thus the emergent spacetime has dependence on the real space time too. We highlight certain features in the context of analogue gravity in astrophysical accretion models. The accretion models, an example of a classical fluid systems, have been the subject of our thesis.

There are several works in the literature where analogue gravity effect is studied in quantum fluids. For example in Bose-Einstein Condensate, a quantum fluid system, is a widely studied candidate system to produce such emergent phenomena [131], [132]. BEC is by definition inviscid which is an advantage over water like fluids in experiments. Low momentum excitations over a condensate stationary state in dilute gases with strongly repulsive atomic interaction

between two atoms, satisfying Thomas-Fermi (T-F) approximation of Gross-Pitaevskii equation [133], give rise to emergent gravity. The recent exciting observation of detecting analogue of thermal Hawking radiation and its temperature in BEC [134] from an one dimensional flow producing a black hole horizon shows the practical possibility of experimental verifications of some works in the field of emergent gravity in BEC.

In closing, we summarise by stating that accretion models not only describe a natural system to study emergent gravity but also it produces the geometrical aspects of emergent spacetime having ‘dumbhole’ horizon in an elegant fashion. It is a rich system from the perspective of dynamical systems theory. For example, existence of multiple critical points, existence of turning points in velocity, makes the system interesting and worth studying in the context of the subject, emergent gravity.

Bibliography

- [1] W. G. Unruh., *Phys. Rev. Lett.* 46, 1351 (1981).
- [2] M. Visser., *Class. Quant. Grav.* 15, 1767 (1998).
- [3] T. A. Jacobson and G. E. Volovik., *Phys. Rev. D* 58, 064021 (1998).
- [4] N.D. Birrell, P.C.W. Davies., ‘Quantum Fields in Curved Space’, Cambridge, UK: Cambridge Univ. Press (1984-02-23).
- [5] B. Carlos, et al, *living Rev. Relativity*, 8 (2005).
- [6] Novello, M., Visser, M., Volovik, G. E., *Artificial black holes*, 1st Edition. World Scientific Publishing Company (2002).
- [7] John L. Friedman and Bernard F. Schutz., *The Astrophysical Journal*, 221:937-957 (1978).
- [8] Sharvari Nadkarni-Ghosh¹ and Jayanta K. Bhattacharjee., *Front. Phys.* (2018).
- [9] Bondi, H., *mnras* , 112 (1952).
- [10] E. Liang and K. Thompson, ‘Transonic disk accretion onto black holes’, *The Astrophysical Journal*, vol. 240, pp. 271-274 (1980).
- [11] T. K. Das and B. Czerny, ‘Hysteresis effects and diagnostics of the shock formation in low angular momentum axisymmetric accretion in the kerr metric’, *New Astronomy*, vol. 17, no. 3, pp. 254-271, (2012).
- [12] M. A. Abramowicz and W. H. Zurek, ‘Rotation-induced bistability of transonic accretion onto a black hole’, *The Astrophysical Journal*, vol. 246, pp. 314-320 (1981).

- [13] B. Muchotrzeb and B. Paczynski, 'Transonic accretion flow in a thin disk around a black hole', *Acta Astronomica*, vol. 32, pp. 1-11 (1982).
- [14] B. Muchotrzeb, 'Transonic accretion flow in a thin disk around a black hole. II', *Acta Astronomica*, vol. 33, pp. 79-87 (1983).
- [15] J. Fukue, 'Shock propagations in a geometrically thin accretion disk', *Publications of the Astronomical Society of Japan*, vol. 35, pp. 355-364 (1983).
- [16] J. Fukue, 'Transonic disk accretion revisited', *PASJ*, vol. 39, pp. 309-327 (1987).
- [17] J. F. Lu, 'Non-uniqueness of transonic solution for accretion onto a Schwarzschild black hole', *Astronomy and Astrophysics*, vol. 148, pp. 176-178 (1985).
- [18] J. F. Lu *Gen. Rel. Grav.*, vol. 18 (1986).
- [19] B. Muchotrzeb and C. B. *Acta Astronomica*, vol. 36 (1986).
- [20] M. A. Abramowicz and S. Kato, 'Constraints for transonic black hole accretion', *Astrophysical Journal*, vol. 336, pp. 304-312 (1989).
- [21] M. A. Abramowicz and S. K. Chakrabarti, 'Standing shocks in adiabatic black hole accretion of rotating matter', *Astrophysical Journal*, vol. 350, pp. 281-287 (1990).
- [22] S. K. Chakrabarti, 'Accretion processes on a black hole', *Physics Reports*, vol. 266, no. 5, pp. 229-390 (1996).
- [23] M. Kafatos and R. X. Yang, 'Transonic Inviscid Disc Flows in the Schwarzschild Metric- Part One', *Monthly Notices of the Royal Astronomical Society*, vol. 268, p. 925 (1994).
- [24] R. Yang and M. Kafatos, 'Shock study in fully relativistic isothermal flows, 2', *Astronomy and Astrophysics*, vol. 295, pp. 238-244 (1995).
- [25] V. I. Pariev, 'Hydrodynamic accretion on to a rapidly rotating kerr black hole', *Monthly Notices of the Royal Astronomical Society*, vol. 283, no. 4, pp. 1264-1280 (1996).
- [26] J. Peitz and S. Appl, 'Viscous accretion discs around rotating black holes', *Monthly Notices of the Royal Astronomical Society*, vol. 286, pp. 681-695 (1997).

-
- [27] D. M. Caditz and S. Tsuruta, ‘Adiabatic shocks in accretion flows’, *The Astrophysical Journal*, vol. 501, no. 1, p. 242 (1998).
- [28] T. K. Das, ‘Generalized shock solutions for hydrodynamic black hole accretion’, *The Astrophysical Journal*, vol. 577, no. 2, p. 880 (2002).
- [29] T. K. Das, J. K. Pendharkar, and S. Mitra, ‘Multitransonic black hole accretion disks with isothermal standing shocks’, *The Astrophysical Journal*, vol. 592, no. 2, p. 1078 (2003).
- [30] P. Barai, T. K. Das, and P. J. Wiita, ‘The dependence of general relativistic accretion on black hole spin’, *The Astrophysical Journal Letters*, vol. 613, no. 1, p. L49 (2004).
- [31] J. Fukue, ‘Sound Speed and the Pseudo-Newtonian Potential’, *Publications of the Astronomical Society of Japan*, vol. 56, pp. 959-963 (2004).
- [32] J. Fukue, ‘Sound speed and the pseudo-newtonian potential’, *Publications of the Astronomical Society of Japan*, vol. 56, no. 6, pp. 959-963 (2004).
- [33] H. Abraham, N. Bilic, and T. K. Das, ‘Acoustic horizons in axially symmetric relativistic accretion’, *Classical and Quantum Gravity*, vol. 23, no. 7, p. 2371 (2006).
- [34] T. K. Das, N. Bilic, and S. Dasgupta, ‘A black-hole accretion disc as an analogue gravity model’, *Journal of Cosmology and Astroparticle Physics*, vol. 2007, no. 06, p. 009 (2007).
- [35] Nag, S., Acharya, S., Ray, A. K., Das, T. K., ‘The role of flow geometry in influencing the stability criteria for low angular momentum axisymmetric black hole accretion’, *New Astronomy* 17 (3), 285-295 (2012).
- [36] Born, Max., Wolf, Emil. , ‘Principles of Optics’, Cambridge University Press, 7th ed (1999).
- [37] S. Weinberg, ‘Gravitation and Cosmology Principles and Applications of the General Theory of Relativity’, John Wiley and Sons, New York (2013).
- [38] Sean M. Carroll, ‘Spacetime and Geometry: An Introduction to general relativity’, Pearson Education, Limited (2017).
-

- [39] Valery P. Frolov and Igor D. Novikov, 'Back Hole Physics: Basic Concepts and New Developments', Kluwer Academic Publishers, The Netherlands (1998).
- [40] Clarke, C. J. and Carswell, R. F., 'Principle of Astrophysical Fluid Dynamics', Cambridge University Press (2007).
- [41] Isaac Newton., 'The Principia: Mathematical Principles of Natural Philosophy', Snowball Publishing (2010).
- [42] Landau and Lifshitz, 'Course of Theoretical Physics', Vol 6, 2nd ed, Reed Educational and Professional Publishing Ltd (1987).
- [43] Robert Resnick., 'Introduction to Special Relativity', Wiley Eastern Private Ltd, First Edition (1958).
- [44] H. Lamers and J. Cassinelli, 'Introduction to Stellar Winds', Cambridge University Press (1999).
- [45] J. Frank, A. King, and D. Raine, 'Accretion Power in Astrophysics', Cambridge astrophysics series, Cambridge University Press (1985).
- [46] S. Kato, J. Fukue, and S. Mineshige, 'Black-Hole Accretion Disks: Towards a New Paradigm', Kyoto University Press (2008).
- [47] T. Okuda, V. Teresi, E. Toscano, and D. Molteni, 'Radiative shocks in rotating accretion flows around black holes', Publications of the Astronomical Society of Japan, vol. 56, no. 3, pp. 547-552 (2004).
- [48] T. Okuda, V. Teresi, and D. Molteni, 'Shock oscillation model for quasi-periodic oscillations in stellar mass and supermassive black holes', Monthly Notices of the Royal Astronomical Society, vol. 377, pp. 1431-1438, June (2007).
- [49] P. Suková and A. Janiuk, 'Shocks in the low angular momentum accretion flow', Journal of Physics: Conference Series, vol. 600, no. 1, p. 012012 (2015).

-
- [50] P. Suková and A. Janiuk, ‘Oscillating shocks in the low angular momentum flows as a source of variability of accreting black holes’, *Monthly Notices of the Royal Astronomical Society*, vol. 447, no. 2, pp. 1565-1579 (2015).
- [51] P. Suková, Charzyński, and A. Janiuk, ‘Shocks in the relativistic transonic accretion with low angular momentum’, *Monthly Notices of the Royal Astronomical Society*, vol. 472, no. 4, pp. 4327-4342 (2017).
- [52] T. K. Das, S. Nag, S. Hegde, S. Bhattacharya, I. Maity, B. Czerny, P. Barai, P. J. Wiita, V. Karas, and T. Naskar, ‘Black hole spin dependence of general relativistic multi-transonic accretion close to the horizon’, *New Astronomy*, vol. 37, pp. 81-104 (2015).
- [53] M. Mocibrodzka, T. K. Das, and B. Czerny, ‘The pattern of accretion flow on to sgr a*’, *Monthly Notices of the Royal Astronomical Society*, vol. 370, no. 1, p. 219 (2006).
- [54] G. Rousseaux, C. Mathis, P. Massa, T. G. Philbin, and U. Leonhardt, ‘Observation of negative- frequency waves in a water tank: a classical analogue to the hawking effect?’, *New Journal of Physics*, vol. 10, no. 5, p. 053015 (2008).
- [55] G. Rousseaux, P. Massa, C. Mathis, P. Couillet, T. G. Philbin, and U. Leonhardt, ‘Horizon effects with surface waves on moving water’, *New Journal of Physics*, vol. 12, no. 9, p. 095018 (2010).
- [56] G. Jannes, R. Piquet, P. Maïssa, C. Mathis, and G. Rousseaux, ‘Experimental demonstration of the supersonic-subsonic bifurcation in the circular jump: A hydrodynamic white hole’, *Phys. Rev. E*, vol. 83, p. 056312 (2011).
- [57] S. Weinfurtner, E. W. Tedford, M. C. J. Penrice, W. G. Unruh, and G. A. Lawrence, ‘Measurement of stimulated hawking emission in an analogue system’, *Phys. Rev. Lett.*, vol. 106, p. 021302 (2011).
- [58] U. Leonhardt and S. Robertson, ‘Analytical theory of hawking radiation in dispersive media’, *New Journal of Physics*, vol. 14, no. 5, p. 053003 (2012).
-

- [59] S. J. Robertson, 'The theory of hawking radiation in laboratory analogues', *Journal of Physics B: Atomic, Molecular and Optical Physics*, vol. 45, no. 16, p. 163001 (2012).
- [60] Illarionov A., Sunyaev R. A., *A and A*, 39, 205 (1975).
- [61] Liang E. P. T., Nolan P. L., *Space. Sci. Rev.*, 38, 353 (1984).
- [62] Bisikalo A. A., Boyarchuk V. M., Chechetkin V. M., Kuznetsov O. A., Molteni D., *MNRAS*, 300, 39 (1984).
- [63] Illarionov A. F., *Soviet Astron.*, 31, 618 (1988).
- [64] Ho L. C., *Observational Evidence For Black Holes in the Universe*. Dordrecht: Kluwer, p. 153 (1999).
- [65] Igumenshchev I. V., Abramowicz M. A., *MNRAS*, 303, 309 (1999).
- [66] S. K. Chakrabarti and S. Das, 'Model dependence of transonic properties of accretion flows around black holes', *Monthly Notices of the Royal Astronomical Society*, vol. 327, no. 3, pp. 808-812 (2001).
- [67] B. Paczynski and B. Muchotrzeb *Acta Actron.*, vol. 32, no. 1 (1982).
- [68] S. Chaudhury, A. K. Ray, and T. K. Das, 'Critical properties and stability of stationary solutions in multitransonic pseudo-schwarzschild accretion', *Monthly Notices of the Royal Astronomical Society*, vol. 373, no. 1, pp. 146-156 (2006).
- [69] Paczyński, B., and Wiita, P. J., *A and A*, 88, 23 (1980).
- [70] Nowak, A. M., and Wagoner, R. V., *ApJ*, 378, 656 (1991).
- [71] Artemova, I. V., Björnsson, G., and Novikov, I. D., *ApJ*, 461, 565 (1996).
- [72] Wang Y., Wu X., *Chin. Phys. B*, 21, 050504 (2012).
- [73] Saha S., Sen S., Nag S., Raychowdhury S., Das T. K., *New Astron.*, 43, 10 (2016).
- [74] Tapas K. Das., *The Astrophysical Journal*, 577:880-892 (2002).

-
- [75] Neven Bilic et al., *Class. Quantum Grav.* 31 035002 (2014).
- [76] N. Bilic., *Classical and Quantum Gravity*, vol. 16, no. 12, p. 3953, (1999).
- [77] D. B. Ananda, S. Bhattacharya, and T. K. Das., *General Relativity and Gravitation*, vol. 47, no. 9, p. 96, (2015).
- [78] D. A. Bollimpalli, S. Bhattacharya, and T. K. Das., *New Astronomy*, vol. 51, pp. 153-160, (2017).
- [79] J. F. Hawley, L. L. Smarr, and J. R. Wilson., *The Astrophysical Journal*, vol. 277, pp. 296-311, Feb. (1984).
- [80] J. F. Hawley, L. L. Smarr, and J. R. Wilson., *The Astrophysical Journal*, vol. 55, pp. 211-246, June (1984).
- [81] A. Kheyfets, W. A. Miller, and W. H. Zurek., *Physical Review D*, vol. 41, pp. 451-454, Jan. (1990).
- [82] J. F. Hawley., *The Astrophysical Journal*, vol. 381, pp. 496-507, Nov. (1991).
- [83] M. Yokosawa., *Publications of the Astronomical Society of Japan*, vol. 47, pp. 605-615, Oct. (1995).
- [84] I. V. Igumenshchev and A. M. Beloborodov., *Monthly Notices of the Royal Astronomical Society*, vol. 284, no. 3, p. 767, (1997).
- [85] I. V. Igumenshchev and A. M. Beloborodov., *Monthly Notices of the Royal Astronomical Society*, vol. 284, no. 3, p. 767, (1997).
- [86] K. Nobuta and T. Hanawa., *The Astrophysical Journal*, vol. 510, pp. 614-630, Jan. (1999).
- [87] D. Molteni, G. Tóth, and O. A. Kuznetsov., *The Astrophysical Journal*, vol. 516, pp. 411-419, May (1999).
- [88] J. M. Stone, J. E. Pringle, and M. C. Begelman., *Monthly Notices of the Royal Astronomical Society*, vol. 310, pp. 1002-1016, Dec. (1999).
-

- [89] S. E. Caunt and M. J. Korpi., *Astronomy and Astrophysics*, vol. 369, pp. 706-728, Apr. (2001).
- [90] J. P. De Villiers and J. F. Hawley., *The Astrophysical Journal*, vol. 577, pp. 866-879, Oct. (2002).
- [91] D. Proga and M. C. Begelman., *The Astrophysical Journal*, vol. 582, no. 1, p. 69, (2003).
- [92] G. Gerardi, D. Molteni, and V. Teresi, *ArXiv Astrophysics e-prints astro-ph/0501549*, Jan. (2005).
- [93] M. Moscibrodzka and D. Proga., *The Astrophysical Journal*, vol. 679, pp. 626-638, May (2008).
- [94] H. Nagakura and S. Yamada., *The Astrophysical Journal*, vol. 689, no. 1, pp. 391-406, (2008).
- [95] H. Nagakura and S. Yamada., *The Astrophysical Journal*, vol. 696, no. 2, pp. 2026-2035, (2009).
- [96] A. Janiuk, M. Sznajder, M. Mocibrodzka, and D. Proga., *The Astrophysical Journal*, vol. 705, no. 2, pp. 1503-1521, (2009).
- [97] C. Bambi and N. Yoshida., *Physical Review D*, vol. 82, p. 064002, Sept. (2010).
- [98] C. Bambi and N. Yoshida., *Physical Review D*, vol. 82, p. 124037, Dec. (2010).
- [99] P. Barai, D. Proga, and K. Nagamine., *Monthly Notices of the Royal Astronomical Society*, vol. 418, pp. 591-611, Nov. (2011).
- [100] P. Barai, D. Proga, and K. Nagamine., *Monthly Notices of the Royal Astronomical Society*, vol. 424, pp. 728-746, July (2012).
- [101] Y. Zhu, R. Narayan, A. Sadowski, and D. Psaltis, *Monthly Notices of the Royal Astronomical Society*, vol. 451, pp. 1661-1681, Aug. (2015).
- [102] R. Narayan, Y. Zhu, D. Psaltis, and A. Sadowski, *Monthly Notices of the Royal Astronomical Society*, vol. 457, pp. 608-628, Mar. (2016).

-
- [103] M. Mościbrodzka, H. Falcke, and H. Shiokawa., *Astronomy and Astrophysics*, vol. 586, p. A38, Feb. (2016).
- [104] A. Sądowski, M. Wielgus, R. Narayan, D. Abarca, J. C. McKinney, and A. Chael., *Monthly Notices of the Royal Astronomical Society*, vol. 466, pp. 705-725, Apr. (2017).
- [105] P. Mach, M. Piróg, and J. A. Font., *ArXiv e-prints gr-qc:1803.04032*, Mar. (2018).
- [106] J. Karkowski, W. Kulczycki, P. Mach, E. Malec, A. Odrzywolek, and M. Pirog, *ArXiv e-prints gr-qc:1802.02848*, Feb. (2018).
- [107] K. Inayoshi, J. P. Ostriker, Z. Haiman, and R. Kuiper., *Monthly Notices of the Royal Astronomical Society*, vol. 476, pp. 1412-1426, May (2018).
- [108] P. C. Fragile, S. M. Etheridge, P. Anninos, B. Mishra, and W. Kluzniak., *ArXiv e-prints astro-ph.HE: 1803.06423*, Mar. (2018).
- [109] M. A. Abramowicz, A. Lanza, and M. J. Percival., *The Astrophysical Journal*, vol. 479, no. 1, p. 179, (1997).
- [110] Jacobus A. Petterson, Joseph Silk, J. P. Ostriker., *Mnras* (1980).
- [111] Chia, T. T., *Mon. Not. R. Astron. Soc.*, 185 (1978).
- [112] Demircan, O. and Kahraman, G., *Astrophys. Space Sci.*, 181 (1991).
- [113] Griffiths, David. J., 'Introduction to Quantum Mechanics (2nd Edition)', Pearson Education, Inc.: page no. 356 (2004).
- [114] Hartle, James. B., 'Gravity An Introduction to Einstein's general Relativity', Pearson Education, Inc (2013).
- [115] Mullan, Dermott. J., 'Physics of the Sun A First Course', page no. 5, CRC press Taylor and Francis Group Boze Raton London Newyork (2010).
- [116] Spitzer, L. Jr., 'Physical Processes in the Interstellar Medium', WILEY-VCH Verlag GmbH and Co. KGaA, Weinheim (2004).
-

- [117] Stix, Michael., 'The Sun An Introduction', page no. 16, Springer-Verlag, Berlin Heidelberg Newyork, corrected second print (1991).
- [118] Datta, S and Tapas K. Das., arXiv:1910.06768 [gr-qc] (2019).
- [119] Datta, S. et al., New Astronomy, Vol 63 (2018).
- [120] Datta, S., Astrophysics and Space Science (2016).
- [121] Datta, S., arXiv:1902.00359 [astro-ph.HE] (2019).
- [122] Naskar, T et al., Phys. Rev. D 76, 123002 (2007).
- [123] Md. A. Shaikh, et al., Classical and Quantum Gravity, Volume 34, Number 15 (2017).
- [124] Md. A. Shaikh., Classical and Quantum Gravity, Volume 35, Number 5 (2018).
- [125] Satadal Datta., Phys. Rev. D 98, 064049 (2018).
- [126] Sourav Sen and Arnab K. Ray., Phys. Rev. D 89, 063004 (2014).
- [127] Soumyajit Bose et al., Phys. Rev. D 89, 103011 (2014).
- [128] Nandan Roy et al., arXiv:1803.05312 (2018).
- [129] Md. A. Shaikh., arXiv:1805.09672 [gr-qc] (2018).
- [130] Matt Visser and Silke Weinfurtner., Class. Quantum Grav. 22 2493 (2005).
- [131] L. J. Garay et al., Phys.Rev.Lett. 85 4643-4647 (2000).
- [132] L. J. Garay et al., Phys.Rev.A. 63 023611 (2001).
- [133] Franco Dalfovo et al., Rev. Mod. Phys., Vol. 71, No. 3, (1999).
- [134] Juan Ramón Muñoz de Nova1 et al., Nature, Vol-569 (2019).
- [135] Matt Visser and Silke Weinfurtner., Class. Quantum Grav. 22 2493 (2005).
- [136] T. Jacobson., "Black Hole Evaporation and Ultrashort Distances", Phys. Rev. D44, 1731 (1991).

- [137] W.G. Unruh., "Sonic Analogue of Black Holes and the Effects of High Frequencies on Black Hole Evaporation", Phys. Rev. D51, 2827 (1995).
- [138] S. Corley, T. Jacobson., Phys. Rev. D54, 1568 (1996).
- [139] S. Corley., "Computing the spectrum of black hole radiation in the presence of high frequency dispersion: An analytical approach", Phys. Rev. D57, 6280 (1998)
- [140] W.G. Unruh and R. Schützhold., "On the universality of the Hawking effect", Phys. Rev. D71, 024028 (2005).
- [141] Scott James Robertson., arXiv:1106.1805 (2011).
- [142] Datta, S., arXiv:1707.03284v1 [gr-qc] (2017).
- [143] Scott James Robertson., arXiv:1106.1805v1 (2011).
- [144] Maurício Richartz, Angus Prain, Stefano Liberati, and Silke Weinfurtner., Phys. Rev. D 91, 124018 (2015).
- [145] Juhan Frank, Andrew King and Derek Rain., 'Accretion Power in Astrophysics', Cambridge University Press (2002).
- [146] Pratik Tarafdar and Tapas K. Das., International Journal of Modern Physics D Vol. 24, No. 14 (2015).
- [147] Hung-Yi Pu et al., Classical and Quantum Gravity, Volume 29, Number 24 (2012).
- [148] Pratik Tarafdar and Tapas K. Das., International Journal of Modern Physics D Vol. 27, No. 3 (2018).